

INFORMATION TO USERS

This manuscript has been reproduced from the microfilm master. UMI films the text directly from the original or copy submitted. Thus, some thesis and dissertation copies are in typewriter face, while others may be from any type of computer printer.

The quality of this reproduction is dependent upon the quality of the copy submitted. Broken or indistinct print, colored or poor quality illustrations and photographs, print bleedthrough, substandard margins, and improper alignment can adversely affect reproduction.

In the unlikely event that the author did not send UMI a complete manuscript and there are missing pages, these will be noted. Also, if unauthorized copyright material had to be removed, a note will indicate the deletion.

Oversize materials (e.g., maps, drawings, charts) are reproduced by sectioning the original, beginning at the upper left-hand corner and continuing from left to right in equal sections with small overlaps.

ProQuest Information and Learning
300 North Zeeb Road, Ann Arbor, MI 48106-1346 USA
800-521-0600

UMI[®]

University of Alberta

Modulation of Quantal Size of Catecholamine-Containing Granules
in Rat Adrenal Chromaffin Cells

by

Kim San Tang



A thesis submitted to the Faculty of Graduate Studies and Research in partial
fulfillment of the requirements for the degree of Doctor of Philosophy

Department of Pharmacology

Edmonton, Alberta

Fall 2005



Library and
Archives Canada

Bibliothèque et
Archives Canada

Published Heritage
Branch

Direction du
Patrimoine de l'édition

0-494-08743-9

395 Wellington Street
Ottawa ON K1A 0N4
Canada

395, rue Wellington
Ottawa ON K1A 0N4
Canada

Your file *Votre référence*

ISBN:

Our file *Notre référence*

ISBN:

NOTICE:

The author has granted a non-exclusive license allowing Library and Archives Canada to reproduce, publish, archive, preserve, conserve, communicate to the public by telecommunication or on the Internet; loan, distribute and sell theses worldwide, for commercial or non-commercial purposes, in microform, paper, electronic and/or any other formats.

The author retains copyright ownership and moral rights in this thesis. Neither the thesis nor substantial extracts from it may be printed or otherwise reproduced without the author's permission.

AVIS:

L'auteur a accordé une licence non exclusive permettant à la Bibliothèque et Archives Canada de reproduire, publier, archiver, sauvegarder, conserver, transmettre au public par télécommunication ou par l'Internet, prêter, distribuer et vendre des thèses partout dans le monde, à des fins commerciales ou autres, sur support microforme, papier, électronique et/ou autres formats.

L'auteur conserve la propriété du droit d'auteur et des droits moraux qui protègent cette thèse. Ni la thèse ni des extraits substantiels de celle-ci ne doivent être imprimés ou autrement reproduits sans son autorisation.

In compliance with the Canadian Privacy Act some supporting forms may have been removed from this thesis.

Conformément à la loi canadienne sur la protection de la vie privée, quelques formulaires secondaires ont été enlevés de cette thèse.

While these forms may be included in the document page count, their removal does not represent any loss of content from the thesis.

Bien que ces formulaires aient inclus dans la pagination, il n'y aura aucun contenu manquant.

Canada

**“It’s misleading to suppose there’s any basic difference
between education and entertainment.”**

– *Herbert Marshall McLuhan (1911 - 1980)*

***The author dedicates this dissertation
to the memory of his grandma***

Loh Ah May (1908 - 1987)

Abstract

The amount of releasable catecholamines from individual granules (i.e. quantal size; Q) in isolated single rat chromaffin cells was investigated using carbon fiber amperometry. The distribution of $Q^{1/3}$ of amperometric events could be reasonably described by the summation of at least three Gaussian distributions, which reflects multiple populations of granules with different modal Q . A rundown in mean cellular Q by ~15 - 40% after 3 days of culture was largely due to a shift in the proportional release of large Q granules to medium Q granules. The synthetic glucocorticoid dexamethasone was able to prevent the rundown of mean cellular Q and the shift in the proportional release of different populations of granules after 3 days of culture. In contrast, elevation of cAMP for 3 days increased the mean cellular Q by ~35% (relative to time-matched controls) and was associated with a uniform increase of Q of every granule. Q is also known to affect the kinetics of release. Therefore, the natural variation in Q among rat chromaffin granules was exploited to examine the influence of Q on release kinetics. The percentage of events with a foot and the duration of foot signals were found to increase with Q . Among the events without a foot, the kinetics of the main amperometric spikes (estimated from the half-width duration) slowed down as Q increased. A similar slowing was also observed in the events with a foot, but only at $Q^{1/3} < 0.6 \text{ pC}^{1/3}$. At larger Q , the increase in half-width reached a plateau, indicating that an additional mechanism accelerates the rapid phase of release from large Q events with a foot. The major effect of cAMP was

on the events with $Q^{1/3} \geq 0.6 \text{ pC}^{1/3}$, where the duration of foot signals and the fractional release during the foot signal were reduced. The overall findings suggest that distinct populations of granules in rat chromaffin cells can be differentially regulated by culture duration, glucocorticoids, and cAMP, and the release from large Q granules can be accelerated by a cAMP-dependent mechanism that involves interactions among matrix dissolution, expansion, and fusion pore dilation.

Acknowledgements

The author would like to express his appreciation to his advisors, Drs. Amy and Fred Tse, for their guidance, support, and criticisms throughout the dissertation process. The author appreciated their enthusiasm for good research. Many thanks also go to the author's supervisory committee members, Drs. William F. Dryden and Marek Duszyk, for their helpful suggestions and directions in carrying out the research. Profound debt is also extended to the external reader, Dr. Robert H. Chow, for his insightful comments on the author's work.

Heartfelt appreciation is extended to Dr. Glen B. Baker for his time in correcting this manuscript and for his permission in using the NRU's research facilities. The author would also like to thank Ms. Gail Rauw for her assistantships in obtaining the HPLC data. Sincere thanks go to Dr. Alexander S. Clanachan for his assistantships in the statistical analysis. The author also wishes to acknowledge with thanks to Dr. Elena Posse de Chaves, who was very kind in showing the author the procedures for protein analysis.

The author is indebted to Drs. Jianhua Xu and Andy K. Lee for their invaluable time and priceless guidance in analyzing and discussing the results of this study. Profound gratitude is also extended to Cecilia Shiu for her constant support and technical assistance. The author would like to offer his appreciation to Fenglian Xu, Elizabeth Hughes, and Valerie Yeung for their friendship and help with laboratory work.

Financial support from the following institutions is gratefully acknowledged: the Canadian Institutes for Health Research (F.W.T. operating grant); the Department of Pharmacology, the Faculty of Graduate Studies and Research, and the Student Financial Aid and Information Center of the University of Alberta; and the Universiti Putra Malaysia.

Finally, the author is forever indebted to his mother, Wong A Mooi for her patience, love, and understanding. Without her encouragement, this endeavour would not have been possible.

“Terima kasih” to all of you!

Table of Contents

CHAPTER 1

General Introduction	1
1.1 Chromaffin cells	2
1.1.1 Embryonic origin	2
1.1.2 Multiple phenotypes of chromaffin cells	3
1.1.3 Paracrine effects of glucocorticoids	6
1.1.4 Stimulus-secretion coupling	7
1.1.5 Chromaffin granules	10
1.2 Catecholamines	12
1.2.1 Physiological, pharmacological, and pathological relevance	13
1.2.2 Biosynthesis	14
1.2.3 Cytoplasmic and intracellular concentrations	17
1.2.4 Granular transport and storage	18
1.2.5 Release	20
1.3 Research objectives	23
1.3.1 The presence of multiple populations of granules with different quantal size in rat chromaffin cells	23
1.3.2 Paracrine and autocrine regulation of quantal size	24
1.3.3 Regulation of the kinetics of catecholamine release from individual granules	25
References	29

CHAPTER 2

Materials and Methods	50
2.1 Chemicals	51
2.2 Cell preparation and culture	51
2.3 Solutions	52
2.4 Electrochemical detection of catecholamine release	52
2.5 Data analysis	55
2.6 Measurement of cellular catecholamine content	56
References	63

CHAPTER 3

Differential Regulation of Multiple Populations of Granules by Culture

Duration, Cyclic AMP, and Glucocorticoids	65
3.1 Introduction	66
3.2 Results	68
3.2.1 Time-dependent rundown of mean cellular quantal size and the effect of dBcAMP	68
3.2.2 The presence of multiple populations of granules with different modal quantal size	70
3.2.3 Differential regulation of multiple populations of granules by culture duration and cAMP	77
3.2.4 The changes in quantal size were not always correlated to changes in cellular catecholamine content	83

3.2.5	Dexamethasone prevented the rundown in mean cellular quantal size after 3 days of culture	85
3.2.6	Dexamethasone prevented the shift in proportional release of different populations of granules	89
3.2.7	The prevention of mean quantal size rundown by dexamethasone could not be mimicked by an inhibitor of nitric oxide synthase	91
3.2.8	Dexamethasone also prevented the rundown in cellular catecholamine content during short-term culture	92
3.3	Discussion	93
3.3.1	Presence of multiple populations of granules	93
3.3.2	Time-dependent rundown of mean cellular quantal size and its prevention by glucocorticoids	97
3.3.3	Regulation of quantal size by cAMP	99
	References	119

CHAPTER 4

	Changes in the Kinetics of Quantal Catecholamine Release with Quantal Size and Elevation of Cyclic AMP	128
4.1	Introduction	129
4.2	Results	131
4.2.1	Influence of quantal size and cAMP on the foot signals	131

4.2.2	Influence of quantal size and cAMP on the main amperometric spikes	137
4.3	Discussion	139
4.3.1	Correlation between the release kinetics and quantal size	139
4.3.2	Modulation of quantal release kinetics by cAMP	145
	References	160
 CHAPTER 5		
	General Discussion	166
5.1	Summary	167
5.1.1	Chapter 3	167
5.1.2	Chapter 4	169
5.2	Interpretation of multiple populations of granules with different quantal size	171
5.3	Implications of multiple populations of granules with different quantal size on the kinetics of quantal catecholamine release	174
5.4	Significance	176
	References	182

List of Tables

Table 1-1	Summary of the drugs that can counteract the effect of catecholamines	28
-----------	---	----

List of Figures

Figure 1-1	The catecholamine biosynthetic pathway	27
Figure 2-1	Carbon fiber amperometry	58
Figure 2-2	Determination of carbon fiber electrode sensitivity	59
Figure 2-3	[Ca ²⁺] _i transient and amperometric events triggered by bath application of a high [K ⁺] solution (50 mM)	60
Figure 2-4	An example of amperometric event	61
Figure 2-5	Examples of events that were rejected by the selection criteria	62
Figure 3-1	The distribution of Q generated by pooling individual amperometric events collected from cells in four treatment groups	104
Figure 3-2	Changes in the mean cellular quantal size with duration of culture and cAMP	105
Figure 3-3	Two different ways of generating the distribution of Q ^{1/3}	106
Figure 3-4	Presence of more than one population of granules	107
Figure 3-5	Presence of more than two populations of granules	108
Figure 3-6	Presence of at least three populations of granules	109
Figure 3-7	Wide range of distribution of the mean of cellular quantal size	110
Figure 3-8	Multiple populations of granules were released in the majority of cells	111
Figure 3-9	Differential regulations of the multiple populations of granules	112

Figure 3-10	The rundown in quantal size during cell culture was not due to a uniform percentage decrease in the quantal size of every granule	113
Figure 3-11	The quantal size of every granule was uniformly increased (by ~35%) with 3 days of cAMP treatment	114
Figure 3-12	Changes in the cellular catecholamine content and the proportion of different catecholamines with culture duration and cAMP	115
Figure 3-13	The distribution of $Q^{1/3}$ of individual amperometric events deviated significantly from a single Gaussian distribution but not for the distribution of cellular mean $Q^{1/3}$	116
Figure 3-14	Dexamethasone prevented the shift in the proportional release of the granules during rundown	117
Figure 3-15	Dexamethasone prevented the time-dependent rundown in the cellular catecholamine content without affecting the proportion of the different catecholamines	118
Figure 4-1	A wide variety of amperometric events could be detected in rat chromaffin cells	150
Figure 4-2	Influence of quantal size and cAMP on the frequency of amperometric events with a foot signal	151
Figure 4-3	Influence of quantal size and cAMP on the duration of foot signals	152

Figure 4-4	Distributions of foot duration from events selected from five different ranges of quantal size	153
Figure 4-5	Influence of quantal size and cAMP on the fractional release during the foot signal	154
Figure 4-6	Distributions of fractional release during the foot signal from events selected from five different ranges of quantal size	155
Figure 4-7	Influence of quantal size and cAMP on the half-width of the main amperometric spikes	156
Figure 4-8	Distributions of half-width from events with or without a foot signal selected from different ranges of quantal size	157
Figure 4-9	Distributions of half-width from events with a foot signal selected from different ranges of quantal size	158
Figure 4-10	Distributions of half-width from events without a foot signal selected from different ranges of quantal size	159
Figure 5-1	Diagram illustrating the differential regulation of multiple populations of granules with different quantal size by culture duration and dexamethasone	178
Figure 5-2	Diagram illustrating the differential regulation of multiple populations of granules with different quantal size by culture duration and cAMP	179
Figure 5-3	The release of catecholamines by free diffusion	180
Figure 5-4	Expansion of granule matrix	181

List of Abbreviations

τ	time constant
χ^2	chi-square
$[Ca^{2+}]_i$	intracellular Ca^{2+} concentration
ATP	adenosine 5'-triphosphate
cAMP	cyclic adenosine 3',5'-monophosphate
DA	dopamine
dBcAMP	dibutyryl cyclic-AMP
dex	dexamethasone
d_{max}	maximum vertical difference
DMEM	Dulbecco's modified Eagle's medium
E	epinephrine
EDTA	ethylenediaminetetraacetic acid
HPLC	high-performance liquid chromatography
K-S test	Kolmogorov-Smirnov test
L-DOPA	3,4-dihydroxy-L-phenylalanine
L-NMMA	N^G -monomethyl-L-arginine
MEM	minimal essential medium
NE	norepinephrine
NO	nitric oxide
NOS	nitric oxide synthase
NPY	neuropeptide Y

PC12	rat pheochromocytoma 12
PNMT	phenylethanolamine N-methyltransferase
Q	quantal size
$Q^{1/3}$	cube-root of quantal size
rms	root-mean-square
v-ATPase	vacuolar-type ATPase
VGCC	voltage-gated Ca^{2+} channel
VMAT	vesicular monoamine transporter

CHAPTER 1

General Introduction

This thesis has three foci. The first is the distribution in the amount of catecholamine released from individual granules (i.e. the quantal size, Q) of the rat adrenal chromaffin cells (Chapter 3). The second is the change in the distribution of quantal size associated with cell culture duration, and the pharmacological manipulations of cyclic AMP (cAMP) and glucocorticoids (Chapter 3). The third is the modulation of the kinetics of quantal release, which is either dependent or independent on the changes in quantal size (Chapter 4). Therefore, in this introductory chapter, a review of the following aspects is included as a background information of this thesis.

This chapter is a review of two topics. The first part focuses on the anatomical and physiological characteristics of chromaffin cells, and biochemical properties of chromaffin granules. The second part focuses on the catecholamine synthesis and packaging, and its release by exocytosis. There are several excellent reviews on the above topics (Johnson 1988; Van der Kloot 1991; Aunis 1998; Henry *et al.* 1998; Flatmark 2000; Sulzer and Pothos 2000). Some of the information from the above reviews is summarized here to provide a historical context for the specific issues addressed in this thesis.

1.1 Chromaffin cells

1.1.1 Embryonic origin

Chromaffin cells are the parenchymal cells of the adrenal medullary tissue. These cells stain readily with various reagents that oxidize

catecholamines to green or brown products and thus were given the name "chromaffin" (Rang *et al.* 1995). Chromaffin cells are derived from the neural crest ectoderm (Kobayashi 1977). At an early stage of embryonic life, the precursor of chromaffin cells (chromoblasts) migrates from the neural crest and accumulates in the adrenal cortical primordium, forming the extra-adrenal blastema before infiltrating into this tissue (Coupland, 1989). The chromaffin cells are innervated by the preganglionic sympathetic fibers of the splanchnic nerve (Holets and Elde 1982), which originate from the intermediolateral cell column of the thoracic segment of spinal cord (Appel and Elde 1988). The main neurotransmitter released from the splanchnic nerve is acetylcholine.

1.1.2 Multiple phenotypes of chromaffin cells

Early electron microscopic studies have suggested that there are two phenotypes of chromaffin cells: norepinephrine (NE)- and epinephrine (E)-containing cells (Coupland 1965). NE-containing cells can be distinguished from E-containing cells based on the ultrastructural features of their granules after glutaraldehyde fixation (Coupland *et al.* 1964). Glutaraldehyde reacts with the primary amine group of NE and forms a Schiff base (Glavinovic *et al.* 1998). In contrast, E possesses a secondary amine group and therefore cannot react with glutaraldehyde. The NE-glutaraldehyde complex is insoluble and remains within chromaffin granule (Coupland and Hopwood 1966). Since E does not form a complex with glutaraldehyde, it remains soluble and diffuses out of the granule. Therefore, NE-containing granules are highly electron dense, larger in diameter

and volume than E-containing granules (Coupland 1965; Glavinovic *et al.* 1998). A clear halo is also observed around the dense core of NE-containing granules (Nordmann 1984; Glavinovic *et al.* 1998). This is an artifact due to osmotic swelling of the granule produced by the presence of the NE-glutaraldehyde complex.

Immunohistochemical and biochemical studies have shown that three phases of chromaffin cell development can be distinguished in rats (Verhofstad *et al.* 1989). First, chromaffin cells synthesize and store only NE up to the 18th day of gestation. Second, individual chromaffin cells contain both NE- and E-storing granules from the 18th day of gestation to 2 or 3 days after birth. Distinct NE- and E-containing cells were first identified in 2-, 3-, or 4-day old rats (Coupland and Tomlinson 1989; Verhofstad *et al.* 1989; Hodel 2001). In the rat, the number of E- and NE-containing cells is 80% and 20%, respectively (Nordmann 1984; Verhofstad *et al.* 1989). In the bovine adrenal medulla, ~75% of the chromaffin cells are E-containing and the rest are NE-containing cells (Koval *et al.* 2000). In the porcine adrenal medulla, NE-containing cells comprise about half of the total number of chromaffin cells (Verhofstad *et al.* 1989). The percentages of the two cell types are very similar to those of the cellular E and NE content in the different animal species, suggesting that the two types of granules have similar concentrations of catecholamines (Nordmann 1984; Verhofstad *et al.* 1985).

The localization of the two types of chromaffin cells in the adrenal medulla also varies with animal species. For example, in the rat, clusters of NE-containing

cells are randomly distributed in the adrenal medulla (Verhofstad *et al.* 1989). In contrast, NE-containing cells in porcine adrenal medulla form spherical clusters which are surrounded by rims of E-containing cells (Verhofstad *et al.* 1989). In the bovine adrenal medulla, E-containing cells are located in the periphery region, and the NE-containing cells are located in the central region of the medulla (Bunn *et al.* 1988).

It is generally believed that each chromaffin cell secretes either NE or E, but not a mixture of both. This is because the enzyme phenylethanolamine N-methyltransferase (PNMT), which converts NE into E, is found only in some cells. Chromaffin cells which do not contain PNMT secrete NE, while those that contain the enzyme in their cytoplasm secrete E. The two-cell-type theory presented above is based mainly on histochemical studies. However, both HPLC and cyclic voltammetric studies on single bovine chromaffin cells have suggested that this traditional model is incorrect because both NE and E can be released from the same cell (Cooper *et al.* 1992; Pihel *et al.* 1994). Although most of the chromaffin cells release either NE or E, ~11 - 17% of the cells secrete mixtures of both. In these cells, each secretory granule appears to contain predominantly either NE or E. The above review suggests that there are at least three types of chromaffin cells: NE-, E-, or NE and E-secreting. On the other hand, there are two main types of granules: NE- or E-containing, located either in different or same cells.

However, an electron microscopic study has shown that bovine chromaffin cells can be divided into four morphologically different subtypes based on the electron density of the cytoplasm and granules (Koval *et al.* 2000). In addition,

based on the shape, size, and electron density of granules after fixation, Koval *et al.* (2001) demonstrated that the chromaffin granules in the same cell can have different morphology. They found that there are five different types of electron-dense granules in these cells. The review above suggests that there may be multiple types of chromaffin cells, and multiple types of granules may be released from single chromaffin cells.

1.1.3 *Paracrine effects of glucocorticoids*

The adrenal medulla is encapsulated by the adrenal cortex. The venous blood from the adrenal cortex drains through the adrenal medulla before entering the general circulation. The cortical cells in the adrenal cortex secrete glucocorticoids into the bloodstream. This vascular system subjects the chromaffin cells of the adrenal medulla to extremely high concentrations (~two orders of magnitude higher than those in the peripheral circulation) of glucocorticoids (Jones *et al.* 1977). Glucocorticoids are known to have important regulatory actions on the morphology of neonatal rat chromaffin cells (Unsicker *et al.* 1978). Glucocorticoids prevent the induction of neurite growth in neonatal chromaffin cells by nerve growth factor (Doupe *et al.* 1985). Glucocorticoids were also reported to enhance the activity and gene expression of tyrosine hydroxylase (Tischler *et al.* 1982; Tank *et al.* 1986; Lewis *et al.* 1987) and PNMT (Kelner and Pollard 1985; Carroll *et al.* 1991). In the absence of glucocorticoids, the activity of tyrosine hydroxylase (Tank *et al.* 1986; Tischler *et al.* 1982) and PNMT (Kelner and Pollard 1985; Betito *et al.* 1992) was decreased in serum-free

cell culture. Glucocorticoids in micromolar concentrations were able to maintain characteristics of chromaffin cells such as the presence of PNMT, synthesis of E, and large chromaffin granules (Doupe *et al.* 1985). The phenotype of chromaffin cells is also determined mainly by the glucocorticoids. For example, in the porcine adrenal medulla, an intact hypophyseal-adrenocortical system was shown to be a prerequisite for the maintenance of the number of E-containing cell as well as the amount of cellular E (Verhofstad *et al.* 1989). On the other hand, fetal hypophysectomy did not affect the number of NE-containing cells or the cellular level of NE. These findings indicate important paracrine actions of glucocorticoids on chromaffin cells.

1.1.4 Stimulus-secretion coupling

Chromaffin cells synthesize, store, and release catecholamines in response to stress. Under physiological conditions, acetylcholine released by the splanchnic nerve activates nicotinic receptors on the surface of chromaffin cells, leading to the opening of the nicotinic channels (Wada *et al.* 1985). This results in an influx of Na^+ , and to a lesser extent Ca^{2+} , and causes depolarization (Douglas *et al.* 1967a; 1967b). Depolarization in turn activates voltage-gated Na^+ channels (Cena *et al.* 1983) and voltage-gated Ca^{2+} channels (VGCC) (Garcia *et al.* 1984). The entry of extracellular Ca^{2+} via VGCC causes a transient rise in intracellular Ca^{2+} concentration ($[\text{Ca}^{2+}]_i$), which is the primary trigger for exocytosis of chromaffin granules (Cheek and Barry 1993).

In most species, chromaffin cells are known to express both nicotinic and muscarinic receptors. Unlike ionotropic nicotinic receptors, muscarinic receptors (i.e. M₁, M₂, and M₃) are metabotropic receptors and are coupled to phospholipase C. Activation of muscarinic receptors induces inositol-1,4,5-triphosphate (IP₃) production, which in turn releases Ca²⁺ from intracellular stores (Ohta *et al.* 2002; Inoue *et al.* 2003). Although both receptors are present on bovine chromaffin cells, nicotinic receptors play a dominant role in the control of catecholamine release (Cheek and Burgoyne 1985). In chick chromaffin cells, however, catecholamine secretion could be triggered only by muscarinic receptors (Knight and Baker 1986). On the other hand, in guinea pig (Role and Perlman 1983), rat (Wakade and Wakade 1983; Chowdhury *et al.* 1994), porcine chromaffin cells (Nassar-Gentina *et al.* 1997), both nicotinic and muscarinic receptors can trigger catecholamine secretion. In rat chromaffin cells, a combination of hexamethonium (nicotinic receptor antagonist) and atropine (muscarinic receptor antagonist) was required to abolish the catecholamine secretion evoked by exogenous acetylcholine, but neither hexamethonium nor atropine alone was sufficient to abolish the catecholamine secretion (Wakade and Wakade 1983). In contrast, secretion evoked by endogenous acetylcholine via splanchnic nerve stimulation was largely reduced (75%) by hexamethonium alone. This suggests a dormant presence of nicotinic receptors in the synaptic zones, whereas extrasynaptic regions contain a mixture of both receptors. A differential expression of nicotinic and muscarinic receptors in E- and NE-

containing chromaffin cells has been reported in both bovine and rat chromaffin cells (Michelena *et al.* 1991; Zaika *et al.* 2004).

In addition to acetylcholine, chromaffin cells can respond to a large variety of peptides and neurotransmitters [e.g. adenosine 5'-triphosphate (ATP), γ -aminobutyric acid (GABA), glycine, pituitary adenylate cyclase-activating polypeptide (PACAP), vasointestinal peptide (VIP), neuropeptide Y (NPY), neurokinins, somatostatin, opioid peptides, atrial natriuretic peptides (ANP), angiotensin II, histamine, and bradykinin] (Aunis 1998). Autoreceptors (i.e. D_2 , α_2 , and β receptors) are also present on chromaffin cells (Greenberg and Zinder 1982; Bigornia *et al.* 1990). They are called "autoreceptors" because these receptors are activated by catecholamines that are released from the same or neighboring cells. D_2 -dopaminergic and α_2 -adrenergic receptors are known to couple to G_i -proteins, which in turn inhibits adenylate cyclase and cAMP production (Vallar and Meldolesi 1989; Angleson *et al.* 1999; Tsuda *et al.* 2003). They are inhibitory autoreceptors, such that the stimulation of these receptors reduces the subsequent release of catecholamines through a negative feedback mechanism via inhibition of cAMP production. There are two types of β -adrenergic receptors on rat chromaffin cells: β_1 - and β_2 -adrenergic receptors. β_1 -adrenergic receptors act via G_s -proteins that are coupled to adenylyl cyclase and cAMP production, whereas β_2 -adrenergic receptors are coupled to either G_s - or G_i -proteins (Bean *et al.* 1984; Xiao *et al.* 1995; Daaka *et al.* 1997; Kilts *et al.* 2000). Activation of β -adrenergic receptors has been shown to increase the basal release of catecholamines (Parramon *et al.* 1995) and to potentiate (Carbone *et al.* 2001) or

inhibit (Hernandez-Guijo *et al.* 1999) L-type Ca^{2+} channel activity in chromaffin cells. The presence of multiple receptors on chromaffin cells indicates that catecholamine secretion from chromaffin cells can be modulated via a variety of mechanisms.

1.1.5 Chromaffin granules

Each chromaffin cell contains ~30 000 granules (Phillips *et al.* 1983). The average diameter of chromaffin granules is ~180 nm in rat (Doupe *et al.* 1985; Coupland and Tomlinson 1989; Ales *et al.* 1999) and ~350 nm in bovine chromaffin cells (Coupland 1968; Plattner *et al.* 1997). Since the first description of chromaffin granules by Coupland (1965) 40 years ago, extensive biochemical work has been carried out on the structural aspect and composition of these granules in chromaffin cells. Phillips (1974a; 1974b) introduced the preparation of chromaffin granule "ghosts" that were obtained by osmotic lysis. Although these preparations were very useful to study granular catecholamine uptake, the probability of getting the fraction of right-side out sealed vesicles is rare. According to Gasnier *et al.* (1987), only 10% of the membranes obtained by an osmotic shock can reseal correctly. Furthermore, the information obtained from the use of the isolated granules has its obvious drawbacks since it does not involve interaction with the plasma membrane, a critical point in the exocytotic process.

Since chromaffin granules can be isolated from the adrenal medulla with good yield and purity, it has been possible to estimate the numbers of

catecholamine molecules present in each granule. The number of catecholamine molecules in a single rat chromaffin granule is ~3 million in NE-containing granules and ~2 million in E-containing granules (Tomlinson *et al.* 1987). Similar values have been obtained for bovine chromaffin granules (Winkler and Carmichael 1982). This is equivalent to an amine concentration of 0.6 M within the core of granule.

Analysis of dried catecholamine-storing bovine chromaffin granules revealed a composition (by weight) of 20% catecholamine, 35% protein, 22% lipid, and 15% ATP (Coupland and Hopwood 1966). Catecholamines are stored with ATP (150 mM), guanosine 5'-triphosphate (GTP) (17 mM), ascorbic acid (25 mM), Ca²⁺ (40 mM), Mg²⁺ (5.5 mM), and a number of intragranular proteins and peptides (Aunis 1998). The main proteins in the granules are dopamine β-hydroxylase and chromogranins (Helle 1966; Winkler and Fischer-Colbrie 1992). Three types of chromogranins are present in chromaffin cells, namely chromogranin A, chromogranin B, and chromogranin C (secretogranin II). Bovine E-containing cells contained a lot more chromogranin A, but slightly less chromogranin C than NE-containing cells (Weiss *et al.* 1996). The peptides in the granules include NPY, proenkephalins, and enkephalins (Schultzberg *et al.* 1978).

The membrane of the chromaffin granules also possesses multiple proteins involved in the uptake and storage of catecholamines. The proteins that contribute to the uptake of catecholamines are the transporters for amines and the vacuolar type ATPase (v-ATPase) that serves as a proton pump (Henry *et al.*

1998). ATP is hydrolysed by v-ATPase located on the granule membrane, which generates a proton electrochemical gradient. Catecholamine uptake from the cytoplasm into chromaffin granules is driven by the proton electrochemical potential generated by the v-ATPase (Pollard *et al.* 1976; Johnson 1988). This property, together with the proton impermeability of the granule membrane, enables the granules to maintain a low internal pH of ~5.6. The magnitude of the pH gradient is limited by the membrane conductance to counterions. The increase in the membrane conductance to anions compensates for the influx of positively charged protons (Schneider 1981). It has been shown that the anion Cl⁻ stimulates the activity of the v-ATPase in isolated chromaffin granules (Pazoles *et al.* 1980; Johnson 1988). Thus, the v-ATPase activity and the regulation of the pH gradient across the membrane are controlled by the granule membrane potential together with the anion Cl⁻. Catecholamine loading of chromaffin granules is mediated by specific transporters that are driven by an pH gradient across the granule membrane (Henry *et al.* 1998). The types of transporter involved in the packaging of catecholamines will be reviewed in Section 1.2.4 of this chapter.

1.2 Catecholamines

The term “catecholamines” refers to any organic compound with a catechol nucleus (i.e. a benzene ring with two adjacent hydroxyl groups) and an amine-containing group (Rang *et al.* 1995). Biogenic catecholamines are

hormones and/or neurotransmitters in the central and peripheral nervous systems (Weiner and Molinoff 1994). The major physiological catecholamines include dopamine (DA), NE, and E. DA is the metabolic precursor of NE and E, and it also serves as a neurotransmitter in its own right within the central nervous system. NE is the principal postganglionic sympathetic neurotransmitter released by noradrenergic neurons. E is released along with NE from the adrenal chromaffin cells. E is also found in small quantities in the brainstem.

1.2.1 Physiological, pharmacological, and pathological relevance

During the fight or flight response, catecholamines are released from the chromaffin cells as hormones and from the sympathetic nervous system as neurotransmitters. This response affects diverse systems in the body, including the respiratory, cardiovascular, and metabolic systems. E or NE at 1 μ M plasma concentration has been reported to cause pulmonary edema, hypertension-linked coma, or heart failure (Aunis and Langley 1999). Excessive dopaminergic activity in the brain has been implicated in schizophrenia (Rang *et al.* 1995). Therefore, catecholamine secretion must be strictly regulated to avoid excessive stress response. Many drugs are available to counteract the effect of catecholamines. These drugs can affect catecholamine synthesis (e.g. carbidopa, α -methyltyrosine), transport (e.g. reserpine), or release (e.g. guanethidine), or can serve as adrenergic receptor antagonists (e.g. propranolol, practolol, phenoxybenzamine, prazosin). The main target of action and the function(s) for each drug are summarized in Table 1-1. On the other hand, catecholamines also

have therapeutic value. For example, E has been used to treat asthma (emergency treatment), anaphylactic shock, and cardiac arrest (Rang *et al.* 1995). A selective loss of dopaminergic neurons originating from the substantia nigra in the midbrain is known to be the major cause of Parkinson's disease. Over the years, several therapeutic approaches have been developed to counteract or compensate for the DA deficiency that underlies Parkinson's disease (Rosenthal 1998). The most prevalent choice among these is the oral administration of 3,4-dihydroxy-L-phenylalanine (L-DOPA), which is the precursor for DA (Rang *et al.* 1995). L-DOPA crosses the blood-brain barrier and is most likely taken up by the remaining dopaminergic neurons. Unfortunately, L-DOPA treatment is no longer effective after several years, possibly because of the continuous loss of dopaminergic neurons. Transplantation of catecholamine-containing cells such as fetal dopaminergic neurons, glomus cells of carotid body, and chromaffin cells of adrenal medulla has been considered as a potential treatment for Parkinson's disease and has been tested on rats and humans (Rosenthal 1998). However, the major disadvantage of this treatment is that most of the cells do not survive after the transplant, possibly due to the lack of survival factors.

1.2.2 Biosynthesis

The biosynthetic pathway of catecholamines has been studied in great detail. Catecholamines are synthesized from the essential amino acid L-tyrosine

in a sequence of enzymatic steps (reviewed in detail by Flatmark 2000). The following section is a brief summary of the synthesis pathway (Figure 1-1).

The first cytoplasmic step is the conversion of L-tyrosine to L-DOPA by tyrosine hydroxylase (Nagatsu *et al.* 1964). This enzyme is a mixed function oxidase that uses L-tyrosine as substrate, tetrahydrobiopterin (BH₄) as cofactor, dioxygen, and Fe²⁺ to generate L-DOPA, dihydrobiopterin, and H₂O (Kumer and Vrana 1996). Tyrosine hydroxylase has a molecular weight of ~60 kDa and is a homotetramer. It catalyses the addition of hydroxyl group to L-tyrosine. In the adrenal medulla, this enzyme exists in two distinct physical forms, a soluble form in cytoplasm and a membrane-bound form that is associated with chromaffin granules (Kuhn *et al.* 1990). Granule contents are free of the enzyme. In most tissues, the activity of tyrosine hydroxylase is much lower than that of dopa decarboxylase or dopamine β-hydroxylase. Under optimal conditions, dopa decarboxylase and dopamine β-hydroxylase activities in adrenal medulla slices are greater than 10,000 nmoles/g/hr, whereas catalytic activity of tyrosine hydroxylase ranges from 4-20 nmoles/g/hr (Nagatsu *et al.* 1964). Therefore, it is generally accepted that tyrosine hydroxylase catalyzes the rate-limiting step in the synthesis of catecholamines (Levitt *et al.* 1965). Tyrosine hydroxylase has a K_m ~10 μM for tyrosine and the endogenous concentration of tyrosine is ~100 μM (Nagatsu *et al.* 1964). Due to the high tissue concentration of tyrosine, it is unlikely that the rate of amine synthesis is limited by the availability of tyrosine. Besides tyrosine, the tyrosine hydroxylase reaction also requires an adequate supply of BH₄ as a cofactor, which in turn depends on three enzymes for its

biosynthesis and one for its continuous regeneration to the catalytically active form (Flatmark 2000). The endogenous concentration of BH₄ is subsaturating (~20 μM) and K_m is ~100 μM. Thus, the availability of BH₄ may limit the rate of catecholamine synthesis.

L-DOPA is converted to DA by dopa decarboxylase. Dopa decarboxylase is the first catecholamine biosynthetic enzyme to be discovered (Flatmark 2000). Dopa decarboxylase is also called L-aromatic amino acid decarboxylase because it catalyses the decarboxylation of all aromatic L-amino acids (Flatmark 2000). It is a homodimeric cytoplasmic enzyme and has a low K_m for L-DOPA (Weiner and Molinoff 1994). As a result, endogenous L-DOPA is efficiently converted to DA. This is the reason why it has been difficult to detect endogenous L-DOPA in the tissue.

DA is then converted to NE by dopamine β-hydroxylase. Dopamine β-hydroxylase is a homotetrameric glycoprotein and mixed function oxidase (Flatmark 2000). This enzyme requires one atom of copper per subunit for catalytic activity (Abudu *et al.* 1998), utilizes dioxygen and requires ascorbate as a single electron donor to form the hydroxyl group (Terland and Flatmark 1975). The hydroxyl group is then added to the β-carbon on the side chain of DA (Craine *et al.* 1973). Dopamine β-hydroxylase is found within the catecholamine storage granules, mainly as a membrane-bound form, but some is soluble (Bjerrum *et al.* 1979; Skotland and Flatmark 1979). The free soluble form of enzyme is released along with catecholamines during exocytosis and is found in plasma (Weiner and Molinoff 1994).

In the adrenal medulla and some neurons in mammalian brainstem, NE is N-methylated by enzyme PNMT to form E (Flatmark 2000). PNMT is a cytoplasmic enzyme and requires the methyl donor S-adenosylmethionine for methylation to occur. This enzyme transfers a methyl group from S-adenosylmethionine to the nitrogen of NE, forming a secondary amine, E (Connett and Kirshner 1970).

1.2.3 Cytoplasmic and intragranular concentrations

The conversion of L-tyrosine to L-DOPA, and L-DOPA to DA occurs in the cytoplasm. The DA in cytoplasm is then taken up into the catecholamine storage granules by vesicular monoamine transporter (VMAT; reviewed in Section 1.2.4). In NE-containing granules, the final β -hydroxylation of DA by dopamine β -hydroxylase occurs within the granules. In E-containing granules, NE diffuses back into the cytoplasm where it is N-methylated by PNMT (Mosharov *et al.* 2003). E is then transported back from cytoplasm into chromaffin granules for storage.

Most of the catecholamines in chromaffin cells are contained in granules; only a little is free in the cytoplasm under normal circumstances. The cytoplasmic catecholamine concentration has been proposed to be 10 μ M whereas the intragranular concentration is estimated to be 550 mM (Phillips 1982). However, recent work from cell-attached patch amperometry suggest that the intragranular catecholamine concentration is much higher (\sim 1 M) and remarkably uniform in each bovine chromaffin cell (Gong *et al.* 2003). Using intracellular patch

electrochemistry in cyclic voltammetric mode, the cytoplasmic catecholamine concentrations in cultured rat chromaffin cells were found to range from 2 - 50 μM (Mosharov *et al.* 2003). To date, this provides the only available data on the concentrations of catecholamines in the cytoplasm of mammalian cells. Negative feedback regulation of tyrosine hydroxylase by catecholamines and other catechol derivatives, and degradation of catecholamines by the mitochondrial monoamine oxidase, are the two major mechanisms that maintain low levels of catecholamine concentrations in the cytoplasm (Mosharov *et al.* 2003; Weiner and Molinoff 1994).

1.2.4 Granular transport and storage

VMAT is involved in the transportation of catecholamine into the chromaffin granules (Henry *et al.* 1998). This protein has 12 transmembrane domains and is homologous with a family of bacterial drug resistance transporters. Since the intragranular concentration of catecholamines is very high, packaging requires active transport (Johnson 1988). The mechanism that concentrates catecholamines within the chromaffin granules requires a pH gradient as its driving force. The action of VMAT dissipates the pH gradient because the transport involves the exchange of two luminal protons for one cytoplasmic monoamine molecule (Knoth *et al.* 1981). The pH gradient is maintained by a proton pump. This action of the proton pump is an ATP-dependent process. This pump creates a pH gradient, maintaining an

intragranular pH of ~5.5 that corresponds to the isoelectric point of chromogranin A (Yoo and Albanesi 1990).

It has been proposed that chromogranin A, the major water-soluble protein in chromaffin granules, plays an important role in forming a complex with soluble products (Helle *et al.* 1985; Winkler and Fischer-Colbrie 1992), leading to formation of a “hydrogel-like” structure known as the gel matrix (Aunis 1998). Chromogranin A undergoes pH-induced conformational changes. It exists as a tetramer at pH 5.5, which dissociates to a dimer at pH 7.4, a change that is accompanied by a decrease in catecholamine binding (Yoo and Lewis 1992). Acidification of the intragranular environment could increase the affinity of chromogranin A for catecholamines, hence reducing the free catecholamine present within granule. Therefore the bound catecholamine would decrease the transmembrane gradient and favor catecholamine intragranular accumulation.

The estimated turnover rate of VMAT is about two molecules of catecholamine per sec (Gasnier *et al.* 1987) and each chromaffin granule contains ~20 VMAT molecules (Henry *et al.* 1998). Therefore, an influx of 40 molecules of catecholamine per sec is achieved for each chromaffin granule. VMAT has a high affinity for reserpine, which blocks vesicular catecholamine uptake *in vitro* and *in vivo* (Liu *et al.* 1992). Reserpine is a highly lipophilic, specific, irreversible inhibitor of the VMAT which terminates the ability of the chromaffin granules to concentrate catecholamines. Treatment with reserpine causes depletion of catecholamines in the granules of bovine chromaffin cells (Gong *et al.* 2003) and rat pheochromocytoma (PC12) cells (Colliver *et al.* 2000).

Two pharmacologically distinct monoamine transporters, VMAT₁ and VMAT₂ (Liu *et al.* 1992; 1994), are responsible for transporting catecholamines, serotonin, and histamine. VMAT₂ can be distinguished from VMAT₁ by its ability to use submillimolar concentrations of histamine as substrate and by its 10-fold higher sensitivity to tetrabenazine (Peter *et al.* 1994). Human VMAT₁ is almost insensitive to tetrabenazine (Erickson *et al.* 1996). In addition to pharmacological differences, VMAT₁ and VMAT₂ differ in their tissue distribution. In rats, VMAT₁ was found to be expressed in the adrenal medulla and VMAT₂ in the central nervous system (Liu *et al.* 1992). On the other hand, VMAT₂ is the major isoform expressed in the bovine adrenal medulla (Henry *et al.* 1994). In humans, both VMAT₁ and VMAT₂ are equally present in adrenal medulla.

Catecholamines are stored in chromaffin granules together with chromogranin, ATP, and dopamine β -hydroxylase, all of which are released by exocytosis (Lang *et al.* 1997; Aunis 1998). It is generally assumed that a reversible complex is formed between catecholamines, ATP, and chromogranin within the granule. This would serve to reduce the osmolarity of granular catecholamine content and also to reduce the tendency of the catecholamines to leak out of the chromaffin granules.

1.2.5 Release

Secretion of catecholamines from chromaffin cells occurs via Ca²⁺-dependent exocytosis. The release by exocytosis has been inferred from the demonstration that high-molecular weight proteins such as dopamine β -

hydroxylase stored in the granule were released together with the catecholamines whereas proteins localized to the cytoplasm were not released. The release of the entire granule (i.e. matrix and membrane) can be excluded because lipid constituents of the granule membrane are not found in the perfusate (Aunis 1998). In regulated exocytosis, secretory granules are synthesized in the Golgi apparatus and then translocated to the cell membrane. The inhibitory regulators (e.g. cortical F-actin cytoskeleton, synapsin, synaptotagmin) exist to prevent uncontrolled, spontaneous membrane fusion (Martin 1997; Bajjalieh 1999). A fusion event involves many coordinated steps. Before fusion, granules are transported and docked to the specific site on the plasma membrane (Pfeffer 1999). This step involves assembly of soluble N-ethylmaleimide-sensitive fusion attachment protein receptor (SNARE) complex (Chen and Scheller 2001). The granule then goes through several "priming" steps to prepare it for release (Klenchin and Martin 2000). These "priming" steps are ATP-dependent (Aunis 1998). The final step of exocytosis is membrane fusion, which is Ca^{2+} -dependent (Augustine 2001). This step leads to formation of fusion pore (Chen and Scheller 2001), which exposes the granule matrix to the extracellular environment.

Upon release, the granule matrix is exposed to the lower Ca^{2+} concentration (~2 mM) and the higher pH (~7.4) of the extracellular medium. It has been demonstrated in bovine chromaffin cells that a severe reduction in the time course of catecholamine release at a low extracellular pH (pH of 5.5) (Jankowski *et al.* 1993). Those findings support the idea that release of

catecholamines requires dissolution of the granule matrix and the rate of dissolution can be altered. The change in pH and Ca^{2+} concentration of granule matrix when exposed to extracellular medium modifies the structure of chromogranin A, which in turn causes swelling of the granule matrix. These changes reduce the catecholamine-binding capacity of the granule matrix. Catecholamines and other soluble granular components (e.g. dopamine β -hydroxylase, chromogranin, and NPY) are released into the extracellular space upon stimulation (Lang *et al.* 1997). Some granules fuse transiently with the plasma membrane and release their contents through a partially open fusion pore without merging of granule and plasma membrane (Ales *et al.* 1999). This phenomenon is known as “kiss-and-run” exocytosis. In the case of “kiss and run” exocytosis, the high molecular-weight components stay inside the granule (Albillos *et al.* 1997).

For the last two decades, the development of tools such as capacitance measurements (Neher and Marty 1982) and amperometry has permitted the assay of exocytosis in single cells. Amperometry is the first approach to provide a direct measurement of the amount of releasable catecholamine (quantal size) and kinetics of release of individual granules. More recently, the introduction of patch amperometry (combination of capacitance measurement and amperometric detection of catecholamines in the cell-attached configuration) has allowed the simultaneous determination of exocytosis, fusion pore dilation, and catecholamine release of single chromaffin granules (Albillos *et al.* 1997). Many amperometric events were preceded by a foot signal (which reflects the leakage

of catecholamines from initial opening of fusion pores), followed by a main amperometric spike (which reflects the rapid release of catecholamines from the granule matrix via fully dilated fusion pores) (Chow and von Ruden 1995). The shape of the main amperometric spike can be characterized by a fast rising phase, a peak (the maximum current amplitude), and a slow falling phase. The kinetics of the main amperometric spike can be characterized by the rise-time (the duration of the signal when it rises to its maximum current amplitude), half-width (the duration of the signal when it stays above 50% of its maximum current amplitude), and decay time constant (τ) (duration of the signal when it falls to 37% of its maximum current amplitude). Previous amperometric studies have also demonstrated the existence of stand-alone signals, which represent openings of fusion pores that never dilate but flicker before closing (i.e. "kiss-and-run" exocytosis) (Bruns and Jahn 1995; Chow and von Ruden 1995; Zhou *et al.* 1996; Ales *et al.* 1999; Wang *et al.* 2003). Under normal conditions, the stand-alone signals are rarely observed (< 1%) in rat chromaffin cells (Xu and Tse 1999).

1.3 Research objectives

1.3.1 The presence of multiple populations of granules with different quantal size in rat chromaffin cells

The review in Section 1.1.2 suggested that the old model of two subtypes of chromaffin cells, each containing only E or NE granules, may no longer be

valid. In a recent study of bovine chromaffin cells, the presence of up to four populations of cells with different granule diameters and morphology has been reported (Koval *et al.* 2000). Since the concentration of catecholamines is uniform among granules (Gong *et al.* 2003), the differences in granule diameter raise the possibility that the amount of catecholamines (quantal size) released from different populations of granules might be different. With the development of the amperometric technique, it is possible to measure accurately the quantal size of individual granules released from chromaffin cells. Therefore, the first objective of this thesis is to determine: (a) whether there are distinct populations of granules with different quantal size; and (b) whether there are subtypes of chromaffin cells that preferentially release certain populations of granules (with specific quantal size). In all the experiments, single rat chromaffin cells (cultured for 1 or 3 days) will be employed and the quantal size of individual granules will be estimated from the time integral of individual amperometric events.

1.3.2 Paracrine and autocrine regulation of quantal size

The quantal size of chromaffin granules can be regulated by multiple factors, including catecholamine synthesis, transport, and storage. As reviewed in Section 1.2.2, the major rate-limiting enzyme of catecholamine synthesis is tyrosine hydroxylase. The activity of tyrosine hydroxylase is known to be down-regulated during long-term culture of chromaffin cells (Doupe *et al.* 1985; Hodel 2001). Interestingly, the activity and gene expression of tyrosine hydroxylase can be enhanced by glucocorticoids (Tischler *et al.* 1982; Tank *et al.* 1986; Lewis *et*

al. 1987) as well as by cAMP (Lewis *et al.* 1987; Hwang *et al.* 1994). In addition, glucocorticoids were also reported to increase the activity of the enzyme PNMT, which converts NE to E (Kelner and Pollard 1985; Betito *et al.* 1992). The gene expression of PNMT has also been reported to be regulated by glucocorticoids (Carrol *et al.*, 1991) and by cAMP (Stachowiak *et al.* 1990; Carroll *et al.* 1991; Hwang *et al.* 1994). On the other hand, the activity and gene expression of VMAT, the transporter that is responsible for catecholamine uptake into granules (reviewed in Section 1.2.4), has also been reported to be regulated by cAMP (Desnos *et al.* 1992; Nakanishi *et al.* 1995; Ribeiro *et al.* 2002). The expression of chromogranin A, a major component of the granule matrix (reviewed in Sections 1.1.5 and 1.2.4), has also been reported to be regulated by glucocorticoids (Rozansky *et al.* 1994) and cAMP (Wu *et al.* 1995; Canaff *et al.* 1998; Mahapatra *et al.* 2003). This raises the possibility that glucocorticoids or elevation of intracellular cAMP may affect catecholamine synthesis, transport, or storage, and thus in turn modulates the quantal size. Therefore, the second objective of this thesis is to determine whether the quantal size of different populations of granules in rat chromaffin cells can be modulated by (a) culture duration; (b) glucocorticoids; and (c) elevation of intracellular cAMP.

1.3.3 Regulation of the kinetics of catecholamine release from individual granules

The kinetics of catecholamine release from individual granules can be influenced by multiple factors, including quantal size, the kinetics of the fusion

pore opening, dilation, or closure, and dissolution of the granule matrix. Previous amperometric studies (Alvarez de Toledo *et al.* 1993; Bruns and Jahn 1995) have shown that granules with large quantal size were accompanied by longer foot signals and longer half-width of the main amperometric signals, but smaller fractional release during the foot signal. However, most of these early studies involve comparisons among different cell types (e.g. mast cells, bovine chromaffin cells, and Retzius cells of the leech). In bovine chromaffin cells, elevation of intracellular cAMP has been shown to cause slowing of the kinetics of amperometric events (Machado *et al.* 2001). It is not clear whether the effect of cAMP on the kinetics of catecholamine release is due solely to changes in quantal size or involves other mechanisms (e.g. slower rate of fusion pore dilation or dense core matrix dissolution). The presence of multiple populations of granules in rat chromaffin cells may offer a unique opportunity to examine the influence of quantal size on the kinetics of release. Therefore, the third objective of this thesis is to examine the regulation of the kinetics of amperometric events by (a) quantal size; and (b) elevation of intracellular cAMP.

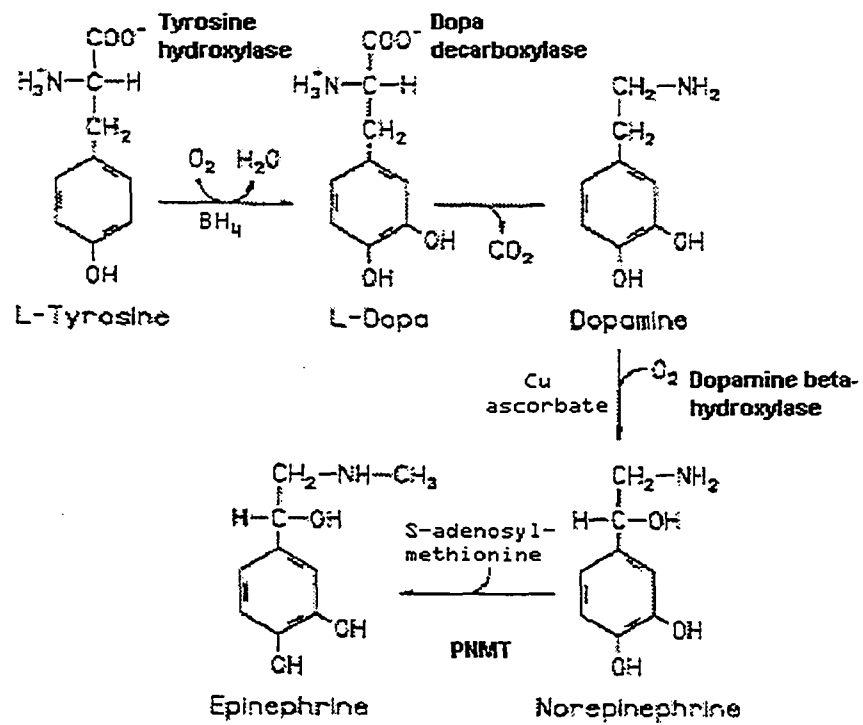


Figure 1-1 The catecholamine biosynthetic pathway (modified from Flatmark, 2000).

Type	Drug	Main action	Uses/function
Drugs affecting catecholamine synthesis	Carbidopa	Inhibits dopa decarboxylase	Used as adjunct to L-DOPA, to prevent peripheral side effects
	α -Methyltyrosine	Inhibits tyrosine hydroxylase	Pheochromocytoma
Drugs affecting catecholamine uptake	Reserpine	Irreversible inhibitors of VMAT, thus inhibit uptake of catecholamines into granules	Hypertension
Drugs affecting catecholamine release	Guanethidine	Some local anesthetic activity	Hypertension
Adrenergic receptor antagonists	Propranolol	β -antagonist (non-selective)	Angina, hypertension, cardiac arrhythmias
	Practolol	β_1 -antagonist	Hypertension, angina, cardiac arrhythmias
	Phenoxybenzamine	α -antagonist (non-selective, irreversible)	Peripheral vasospasm, pheochromocytoma
	Prazosin	α_2 -antagonist	Hypertension

Table 1-1 Summary of the drugs that can counteract the effect of catecholamines (modified from Rang *et al.*, 1995).

References

- Abudu N., Banjaw M. Y., and Ljones T. (1998) Kinetic studies on the activation of dopamine beta-monooxygenase by copper and vanadium ions. *European Journal of Biochemistry* **257**, 622-629.
- Albillos A., Dernick G., Horstmann H., Almers W., Alvarez de Toledo G., and Lindau M. (1997) The exocytotic event in chromaffin cells revealed by patch amperometry. *Nature* **389**, 509-512.
- Ales E., Tabares L., Poyato J. M., Valero V., Lindau M., and Alvarez de Toledo G. (1999) High calcium concentrations shift the mode of exocytosis to the kiss-and-run mechanism. *Nature Cell Biology* **1**, 40-44.
- Alvarez de Toledo G., Fernandez-Chacon R., and Fernandez J. M. (1993) Release of secretory products during transient vesicle fusion. *Nature* **363**, 554-558.
- Angleson J. K., Cochilla A. J., Kilic G., Nussinovitch I., and Betz W. J. (1999) Regulation of dense core release from neuroendocrine cells revealed by imaging single exocytic events. *Nature Neuroscience* **2**, 440-446.
- Appel N. M. and Elde R. P. (1988) The intermediolateral cell column of the thoracic spinal cord is comprised of target-specific subnuclei: evidence from retrograde transport studies and immunohistochemistry. *Journal of Neuroscience* **8**, 1767-1775.

- Augustine G. J. (2001) How does calcium trigger neurotransmitter release?
Current Opinion in Neurobiology **11**, 320-326.
- Aunis D. (1998) Exocytosis in chromaffin cell of the adrenal medulla.
International Review of Cytology **181**, 213-320.
- Aunis D. and Langley K. (1999) Physiological aspects of exocytosis in chromaffin cells of the adrenal medulla. *Acta Physiologica Scandinavica* **167**, 89-97.
- Bajjalieh S. M. (1999) Synaptic vesicle docking and fusion. *Current Opinion in Neurobiology* **9**, 321-328.
- Bean B. P., Nowycky M. C., and Tsien R. W. (1984) Beta-adrenergic modulation of calcium channels in frog ventricular heart cells. *Nature* **307**, 371-375.
- Betito K., Diorio J., Meaney M. J., and Boksa P. (1992) Adrenal phenylethanolamine N-methyltransferase induction in relation to glucocorticoid receptor dynamics - evidence that acute exposure to high cortisol levels is sufficient to induce the enzyme. *Journal of Neurochemistry* **58**, 1853-1862.
- Bigornia L., Allen C. N., Jan C. R., Lyon R. A., Titeler M., and Schneider A. S. (1990) D₂-dopamine receptors modulate calcium channel currents and catecholamine secretion in bovine adrenal chromaffin cells. *Journal of Pharmacology and Experimental Therapeutics* **252**, 586-592.

- Bjerrum O. J., Helle K. B., and Bock E. (1979) Immunochemically identical hydrophilic and amphiphilic forms of the bovine adrenomedullary dopamine beta-hydroxylase. *Biochemical Journal* **181**, 231-237.
- Bruns D. and Jahn R. (1995) Real-time measurement of transmitter release from single synaptic vesicles. *Nature* **377**, 62-65.
- Bunn S. J., Marley P. D., and Livett B. G. (1988) The distribution of opioid binding subtypes in the bovine adrenal medulla. *Neuroscience* **27**, 1081-1094.
- Canaff L., Bevan S., Wheeler D. G., Moulant A. J., Rehfuss R. P., White J. H., and Hendy G. N. (1998) Analysis of molecular mechanisms controlling neuroendocrine cell specific transcription of the chromogranin A gene. *Endocrinology* **139**, 1184-1196.
- Carbone E., Carabelli V., Cesetti T., Baldelli P., Hernandez-Guijo J. M., and Giusta L. (2001) G-protein- and cAMP-dependent L-channel gating modulation: a manifold system to control calcium entry in neurosecretory cells. *Pflugers Archiv - European Journal of Physiology* **442**, 801-813.
- Carroll J. M., Evinger M. J., Goodman H. M., and Joh T. H. (1991) Differential and coordinate regulation of TH and PNMT mRNAs in chromaffin cell cultures by second messenger system activation and steroid treatment. *Journal of Molecular Neuroscience* **3**, 75-83.

- Cena V., Nicolas G. P., Sanchezgarcia P., Kirpekar S. M., and Garcia A. G. (1983) Pharmacological dissection of receptor-associated and voltage-sensitive ionic channels involved in catecholamine release. *Neuroscience* **10**, 1455-1462.
- Cheek T. R. and Barry V. A. (1993) Stimulus-secretion coupling in excitable cells: a central role for calcium. *Journal of Experimental Biology* **184**, 183-196.
- Cheek T. R. and Burgoyne R. D. (1985) Effect of activation of muscarinic receptors on intracellular free calcium and secretion in bovine adrenal chromaffin cells. *Biochimica et Biophysica Acta* **846**, 167-173.
- Chen Y. A. and Scheller R. H. (2001) SNARE-mediated membrane fusion. *Nature Reviews - Molecular Cell Biology* **2**, 98-106.
- Chow R. H. and von Ruden L. (1995) Electrochemical detection of secretion from single cells, in *Single-Channel Recording* (Sakmann B. and Neher E., eds.), pp. 245-275. Plenum Press, New York.
- Chowdhury P. S., Guo X., Wakade T. D., Przywara D. A., and Wakade A. R. (1994) Exocytosis from a single-rat chromaffin cell by cholinergic and peptidergic neurotransmitters. *Neuroscience* **59**, 1-5.
- Colliver T. L., Pyott S. J., Achalabun M., and Ewing A. G. (2000) VMAT-mediated changes in quantal size and vesicular volume. *Journal of Neuroscience* **20**, 5276-5282.

- Connett R. J. and Kirshner N. (1970) Purification and properties of bovine phenylethanolamine N-methyltransferase. *Journal of Biological Chemistry* **245**, 329-334.
- Cooper B. R., Jankowski J. A., Leszczyszyn D. J., Wightman R. M., and Jorgenson J. W. (1992) Quantitative determination of catecholamines in individual bovine adrenomedullary cells by reversed-phase microcolumn liquid chromatography with electrochemical detection. *Analytical Chemistry* **64**, 691-694.
- Coupland R. E. (1965) Electron microscopic observations on structure of rat adrenal medulla .I. Ultrastructure and organization of chromaffin cells in normal adrenal medulla. *Journal of Anatomy* **99**, 231-254.
- Coupland R. E. (1968) Determining sizes and distribution of sizes of spherical bodies such as chromaffin granules in tissue sections. *Nature* **217**, 384-388.
- Coupland R. E. and Hopwood D. (1966) The mechanism of differential staining reaction for adrenaline- and noradrenaline-storing granules in tissues fixed in glutaraldehyde. *Journal of Anatomy* **100**, 227-243.
- Coupland R. E., Hopwood D., and Pyper A. S. (1964) Method for differentiating between noradrenaline- and adrenaline-storing cells in light and electron microscope. *Nature* **201**, 1240-1242.

- Coupland R. E. and Tomlinson A. (1989) The development and maturation of adrenal medullary chromaffin cells of the rat *in vivo*: a descriptive and quantitative study. *International Journal of Developmental Neuroscience* **7**, 419-438.
- Craine J. E., Daniels G. H., and Kaufman S. (1973) Dopamine-beta-hydroxylase. The subunit structure and anion activation of bovine adrenal enzyme. *Journal of Biological Chemistry* **248**, 7838-7844.
- Daaka Y., Luttrell L. M., and Lefkowitz R. J. (1997) Switching of the coupling of the beta₂-adrenergic receptor to different G proteins by protein kinase A. *Nature* **390**, 88-91.
- Desnos C., Laran M. P., and Scherman D. (1992) Regulation of the chromaffin granule catecholamine transporter in cultured bovine adrenal medullary cells: stimulus-biosynthesis coupling. *Journal of Neurochemistry* **59**, 2105-2112.
- Douglas W. W., Kanno T., and Sampson S. R. (1967a) Effects of acetylcholine and other medullary secretagogues and antagonists on membrane potential of adrenal chromaffin cells: an analysis employing techniques of tissue culture. *Journal of Physiology - London* **188**, 107-120.

- Douglas W. W., Kanno T., and Sampson S. R. (1967b) Influence of ionic environment on membrane potential of adrenal chromaffin cells and on depolarizing effect of acetylcholine. *Journal of Physiology - London* **191**, 107-121.
- Doupe A. J., Landis S. C., and Patterson P. H. (1985) Environmental influences in the development of neural crest derivatives: glucocorticoids, growth-factors, and chromaffin cell plasticity. *Journal of Neuroscience* **5**, 2119-2142.
- Erickson J. D., Schafer M. K. H., Bonner T. I., Eiden L. E., and Weihe E. (1996) Distinct pharmacological properties and distribution in neurons and endocrine cells of two isoforms of the human vesicular monoamine transporter. *Proceedings of the National Academy of Sciences of the United States of America* **93**, 5166-5171.
- Flatmark T. (2000) Catecholamine biosynthesis and physiological regulation in neuroendocrine cells. *Acta Physiologica Scandinavica* **168**, 1-17.
- Garcia A. G., Sala F., Reig J. A., Viniegra S., Frias J., Fonteriz R., and Gandia L. (1984) Dihydropyridine Bay-K-8644 activates chromaffin cell calcium channels. *Nature* **309**, 69-71.
- Gasnier B., Scherman D., and Henry J. P. (1987) Inactivation of the catecholamine transporter during the preparation of chromaffin granule membrane ghosts. *Febs Letters* **222**, 215-219.

- Glavinovic M. I., Vitale M. L., and Trifaro J. M. (1998) Comparison of vesicular volume and quantal size in bovine chromaffin cells. *Neuroscience* **85**, 957-968.
- Gong L. W., Hafez I., de Toledo G. A., and Lindau M. (2003) Secretory vesicles membrane area is regulated in tandem with quantal size in chromaffin cells. *Journal of Neuroscience* **23**, 7917-7921.
- Greenberg A. and Zinder O. (1982) Alpha-receptor and beta-receptor control of catecholamine secretion from isolated adrenal medulla cells. *Cell and Tissue Research* **226**, 655-665.
- Helle K. B. (1966) Some chemical and physical properties of soluble protein fraction of bovine adrenal chromaffin granules. *Molecular Pharmacology* **2**, 298-310.
- Helle K. B., Reed R. K., Pihl K. E., and Serckhanssen G. (1985) Osmotic properties of the chromogranins and relation to osmotic pressure in catecholamine storage granules. *Acta Physiologica Scandinavica* **123**, 21-33.
- Henry J. P., Botton D., Sagne C., Isambert M. F., Desnos C., Blanchard V., Raismanvozari R., Krejci E., Massoulie J., and Gasnier B. (1994) Biochemistry and molecular biology of the vesicular monoamine transporter from chromaffin granules. *Journal of Experimental Biology* **196**, 251-262.

- Henry J. P., Sagne C., Bedet C., and Gasnier B. (1998) The vesicular monoamine transporter: from chromaffin granule to brain. *Neurochemistry International* **32**, 227-246.
- Hernandez-Guijo J. M., Carabelli V., Gandia L., Garcia A. G., and Carbone E. (1999) Voltage-independent autocrine modulation of L-type channels mediated by ATP, opioids and catecholamines in rat chromaffin cells. *European Journal of Neuroscience* **11**, 3574-3584.
- Hodel A. (2001) Effects of glucocorticoids on adrenal chromaffin cells. *Journal of Neuroendocrinology* **13**, 217-221.
- Holets V. and Elde R. (1982) The differential distribution and relationship of serotonergic and peptidergic fibers to sympathoadrenal neurons in the intermediolateral cell column of the rat: a combined retrograde axonal transport and immunofluorescence study. *Neuroscience* **7**, 1155-1174.
- Hwang O., Kim M. L., and Lee J. D. (1994) Differential induction of gene expression of catecholamine biosynthetic enzymes and preferential increase in norepinephrine by forskolin. *Biochemical Pharmacology* **48**, 1927-1934.
- Inoue M., Sakamoto Y., Fujishiro N., Imanaga I., Ozaki S., Prestwich G. D., and Warashina A. (2003) Homogeneous Ca^{2+} stores in rat adrenal chromaffin cells. *Cell Calcium* **33**, 19-26.

- Jankowski J. A., Schroeder T. J., Ciolkowski E. L., and Wightman R. M. (1993) Temporal characteristics of quantal secretion of catecholamines from adrenal medullary cells. *Journal of Biological Chemistry* **268**, 14694-14700.
- Johnson R. G. (1988) Accumulation of biological amines into chromaffin granules: a model for hormone and neurotransmitter transport. *Physiological Reviews* **68**, 232-307.
- Jones M. T., Hillhouse E. W., and Burden J. L. (1977) Dynamics and mechanics of corticosteroid feedback at hypothalamus and anterior pituitary gland. *Journal of Endocrinology* **73**, 405-417.
- Kelner K. L. and Pollard H. B. (1985) Glucocorticoid receptors and regulation of phenylethanolamine-N-methyltransferase activity in cultured chromaffin cells. *Journal of Neuroscience* **5**, 2161-2168.
- Kilts J. D., Gerhardt M. A., Richardson M. D., Sreeram G., Mackensen G. B., Grocott H. P., White W. D., Davis R. D., Newman M. F., Reves J. G., Schwinn D. A., and Kwatra M. M. (2000) Beta₂-adrenergic and several other G protein-coupled receptors in human atrial membranes activate both G_s and G_i. *Circulation Research* **87**, 705-709.
- Klenchin V. A. and Martin T. F. J. (2000) Priming in exocytosis: attaining fusion-competence after vesicle docking. *Biochimie* **82**, 399-407.

- Knight D. E. and Baker P. F. (1986) Observations on the muscarinic activation of catecholamine secretion in the chicken adrenal. *Neuroscience* **19**, 357-366.
- Knoth J., Zallakian M., and Njus D. (1981) Stoichiometry of H⁺-linked dopamine transport in chromaffin granule ghosts. *Biochemistry* **20**, 6625-6629.
- Kobayashi S. (1977) Adrenal medulla: chromaffin cells as paraneurons. *Archivum Histologicum Japonicum* **40**, 61-79.
- Koval L. M., Yavorskaya E. N., and Lukyanetz E. A. (2000) Ultrastructural features of medullary chromaffin cell cultures. *Neuroscience* **96**, 639-649.
- Koval L. M., Yavorskaya E. N., and Lukyanetz E. A. (2001) Electron microscopic evidence for multiple types of secretory vesicles in bovine chromaffin cells. *General and Comparative Endocrinology* **121**, 261-277.
- Kuhn D. M., Arthur R., Yoon H., and Sankaran K. (1990) Tyrosine hydroxylase in secretory granules from bovine adrenal medulla. Evidence for an integral membrane form. *Journal of Biological Chemistry* **265**, 5780-5786.
- Kumer S. C. and Vrana K. E. (1996) Intricate regulation of tyrosine hydroxylase activity and gene expression. *Journal of Neurochemistry* **67**, 443-462.

- Lang T., Wacker I., Steyer J., Kaether C., Wunderlich I., Soldati T., Gerdes H. M., and Almers W. (1997) Ca²⁺-triggered peptide secretion in single cells imaged with green fluorescent protein and evanescent-wave microscopy (vol 18, pg 857, 1997). *Neuron* **19**, U9.
- Levitt M., Spector S., Sjoerdsma A., and Udenfriend S. (1965) Elucidation of rate-limiting step in norepinephrine biosynthesis in perfused guinea-pig heart. *Journal of Pharmacology and Experimental Therapeutics* **148**, 1-7.
- Lewis E. J., Harrington C. A., and Chikaraishi D. M. (1987) Transcriptional regulation of the tyrosine hydroxylase gene by glucocorticoid and cyclic AMP. *Proceedings of the National Academy of Sciences of the United States of America* **84**, 3550-3554.
- Liu Y. J., Peter D., Roghani A., Schuldiner S., Prive G. G., Eisenberg D., Brecha N., and Edwards R. H. (1992) A cDNA that suppresses MPP⁺ toxicity encodes a vesicular amine transporter. *Cell* **70**, 539-551.
- Liu Y. J., Schweitzer E. S., Nirenberg M. J., Pickel V. M., Evans C. J., and Edwards R. H. (1994) Preferential localization of a vesicular monoamine transporter to dense core vesicles in PC12 cells. *Journal of Cell Biology* **127**, 1419-1433.
- Machado J. D., Morales A., Gomez J. F., and Borges R. (2001) cAMP modulates exocytotic kinetics and increases quantal size in chromaffin cells. *Molecular Pharmacology* **60**, 514-520.

- Mahapatra N. R., Mahata M., O'Connor D. T., and Mahata S. K. (2003) Secretin activation of chromogranin A gene transcription. Identification of the signaling pathways in cis and in trans. *Journal of Biological Chemistry* **278**, 19986-19994.
- Martin T. F. J. (1997) Stages of regulated exocytosis. *Trends in Cell Biology* **7**, 271-276.
- Michelena P., Moro M. A., Castillo C. J. F., and Garcia A. G. (1991) Muscarinic receptors in separate populations of noradrenaline-containing and adrenaline-containing chromaffin cells. *Biochemical and Biophysical Research Communications* **177**, 913-919.
- Mosharov E. V., Gong L. W., Khanna B., Sulzer D., and Lindau M. (2003) Intracellular patch electrochemistry: regulation of cytosolic catecholamines in chromaffin cells. *Journal of Neuroscience* **23**, 5835-5845.
- Nagatsu T., Levitt M., and Udenfriend S. (1964) Tyrosine Hydroxylase - Initial Step in Norepinephrine Biosynthesis. *Journal of Biological Chemistry* **239**, 2910-2917.
- Nakanishi N., Onozawa S., Matsumoto R., Hasegawa H., and Yamada S. (1995) Cyclic AMP-dependent modulation of vesicular monoamine transport in pheochromocytoma cells. *Journal of Neurochemistry* **64**, 600-607.

- Nassar-Gentina V., Catalan L., and Luxoro M. (1997) Nicotonic and muscarinic components in acetylcholine stimulation of porcine adrenal medullary cells. *Molecular and Cellular Biochemistry* **169**, 107-113.
- Neher E. and Marty A. (1982) Discrete changes of cell membrane capacitance observed under conditions of enhanced secretion in bovine adrenal chromaffin cells. *Proceedings of the National Academy of Sciences of the United States of America* **79**, 6712-6716.
- Nordmann J. J. (1984) Combined stereological and biochemical analysis of storage and release of catecholamines in the adrenal medulla of the rat. *Journal of Neurochemistry* **42**, 434-437.
- Ohta T., Wakade A. R., Yonekubo K., and Ito S. (2002) Functional relation between caffeine- and muscarine-sensitive Ca^{2+} stores and no Ca^{2+} releasing action of cyclic adenosine diphosphate-ribose in guinea pig adrenal chromaffin cells. *Neuroscience Letters* **326**, 167-170.
- Parramon M., Gonzalez M. P., and Osetgasque M. J. (1995) A reassessment of the modulatory role of cyclic AMP in catecholamine secretion by chromaffin cells. *British Journal of Pharmacology* **114**, 517-523.
- Pazoles C. J., Creutz C. E., Ramu A., and Pollard H. B. (1980) Permeant anion activation of MgATPase activity in chromaffin granules. Evidence for direct coupling of proton and anion transport. *Journal of Biological Chemistry* **255**, 7863-7869.

- Peter D., Jimenez J., Liu Y. J., Kim J., and Edwards R. H. (1994) The chromaffin granule and synaptic vesicle amine transporters differ in substrate recognition and sensitivity to inhibitors. *Journal of Biological Chemistry* **269**, 7231-7237.
- Pfeffer S. R. (1999) Transport-vesicle targeting: tethers before SNAREs. *Nature Cell Biology* **1**, E17-E22.
- Phillips J. H. (1974a) Steady-state kinetics of catecholamine transport by chromaffin granule ghosts. *Biochemical Journal* **144**, 319-325.
- Phillips J. H. (1974b) Transport of catecholamines by resealed chromaffin granule "ghosts". *Biochemical Journal* **144**, 311-8.
- Phillips J. H. (1982) Dynamic aspects of chromaffin granule structure. *Neuroscience* **7**, 1595-1609.
- Phillips J. H., Burridge K., Wilson S. P., and Kirshner N. (1983) Visualization of the exocytosis endocytosis secretory cycle in cultured adrenal chromaffin cells. *Journal of Cell Biology* **97**, 1906-1917.
- Pihel K., Schroeder T. J., and Wightman R. M. (1994) Rapid and selective cyclic voltammetric measurements of epinephrine and norepinephrine as a method to measure secretion from single bovine adrenal medullary cells. *Analytical Chemistry* **66**, 4532-4537.

- Plattner H., Artalejo A. R., and Neher E. (1997) Ultrastructural organization of bovine chromaffin cell cortex - analysis by cryofixation and morphometry of aspects pertinent to exocytosis. *Journal of Cell Biology* **139**, 1709-1717.
- Pollard H. B., Zinder O., Hoffman P. G., and Nikodejevic O. (1976) Regulation of transmembrane potential of isolated chromaffin granules by ATP, ATP analogs, and external pH. *Journal of Biological Chemistry* **251**, 4544-4550.
- Rang H. P., Dale M. M., Ritter J. M., and Gardner P. (1995) *Pharmacology*, Churchill Livingstone, New York.
- Ribeiro L., Azevedo I., and Martel F. (2002) Comparison of the effect of cyclic AMP on the content and release of dopamine and 1-methyl-4-phenylpyridinium (MPP⁺) in PC12 cells. *Autonomic and Autacoid Pharmacology* **22**, 277-289.
- Role L. W. and Perlman R. L. (1983) Both nicotinic and muscarinic receptors mediate catecholamine secretion by isolated guinea-pig chromaffin cells. *Neuroscience* **10**, 979-985.
- Rosenthal A. (1998) Auto transplants for Parkinson's disease? *Neuron* **20**, 169-172.
- Rozansky D. J., Wu H. J., Tang K. C., Parmer R. J., and Oconnor D. T. (1994) Glucocorticoid activation of chromogranin A gene expression. Identification and characterization of a novel glucocorticoid response element. *Journal of Clinical Investigation* **94**, 2357-2368.

- Schneider D. L. (1981) ATP-dependent acidification of intact and disrupted lysosomes. Evidence for an ATP-driven proton pump. *Journal of Biological Chemistry* **256**, 3858-3864.
- Schultzberg M., Lundberg J. M., Hokfelt T., Terenius L., Brandt J., Elde R. P., and Goldstein M. (1978) Enkephalin-like immunoreactivity in gland cells and nerve terminals of adrenal medulla. *Neuroscience* **3**, 1169-1186.
- Skotland T. and Flatmark T. (1979) On the amphiphilic and hydrophilic forms of dopamine beta-mono-oxygenase in bovine adrenal medulla. *Journal of Neurochemistry* **32**, 1861-1863.
- Stachowiak M. K., Hong J. S., and Viveros O. H. (1990) Coordinate and differential regulation of phenylethanolamine N-methyltransferase, tyrosine hydroxylase and proenkephalin mRNAs by neural and hormonal mechanisms in cultured bovine adrenal medullary cells. *Brain Research* **510**, 277-288.
- Sulzer D. and Poos E. N. (2000) Regulation of quantal size by presynaptic mechanisms. *Reviews in the Neurosciences* **11**, 159-212.
- Tank A. W., Ham L., and Curella P. (1986) Induction of tyrosine hydroxylase by cyclic AMP and glucocorticoids in a rat pheochromocytoma cell line: effect of the inducing agents alone or in combination on the enzyme levels and rate of synthesis of tyrosine hydroxylase. *Molecular Pharmacology* **30**, 486-496.

- Terland O. and Flatmark T. (1975) Ascorbate as a natural constituent of chromaffin granules from the bovine adrenal medulla. *Febs Letters* **59**, 52-56.
- Tischler A. S., Perlman R. L., Nunnemacher G., Morse G. M., Delellis R. A., Wolfe H. J., and Sheard B. E. (1982) Long-term effects of dexamethasone and nerve growth factor on adrenal medullary cells cultured from young adult rats. *Cell and Tissue Research* **225**, 525-542.
- Tomlinson A., Durbin J., and Coupland R. E. (1987) A quantitative analysis of rat adrenal chromaffin tissue: morphometric analysis at tissue and cellular-level correlated with catecholamine content. *Neuroscience* **20**, 895-904.
- Tsuda K., Tsuda S., and Nishio I. (2003) Role of alpha₂-adrenergic receptors and cyclic adenosine monophosphate-dependent protein kinase in the regulation of norepinephrine release in the central nervous system of spontaneously hypertensive rats. *Journal of Cardiovascular Pharmacology* **42**, S81-S85.
- Unsicker K., Krisch B., Otten U., and Thoenen H. (1978) Nerve growth factor induced fiber outgrowth from isolated rat adrenal chromaffin cells: impairment by glucocorticoids. *Proceedings of the National Academy of Sciences of the United States of America* **75**, 3498-3502.
- Vallar L. and Meldolesi J. (1989) Mechanisms of signal transduction at the dopamine D₂ receptor. *Trends in Pharmacological Sciences* **10**, 74-77.

- Van der Kloot W. (1991) The regulation of quantal size. *Progress in Neurobiology* **36**, 93-130.
- Verhofstad A. A. J., Coupland R. E., and Colenbrander B. (1989) Immunohistochemical and biochemical analysis of the development of the noradrenaline- and adrenaline-storing cells in the adrenal medulla of the rat and pig. *Archives of Histology and Cytology* **52**, 351-360.
- Verhofstad A. A. J., Coupland R. E., Parker T. R., and Goldstein M. (1985) Immunohistochemical and biochemical study on the development of the noradrenaline and adrenaline-storing cells of the adrenal medulla of the rat. *Cell and Tissue Research* **242**, 233-243.
- Wada A., Takara H., Izumi F., Kobayashi H., and Yanagihara N. (1985) Influx of ^{22}Na through acetylcholine receptor-associated Na channels: relationship between ^{22}Na influx, ^{45}Ca influx and secretion of catecholamines in cultured bovine adrenal medulla cells. *Neuroscience* **15**, 283-292.
- Wakade A. R. and Wakade T. D. (1983) Contribution of nicotinic and muscarinic receptors in the secretion of catecholamines evoked by endogenous and exogenous acetylcholine. *Neuroscience* **10**, 973-978.
- Wang C. T., Lu J. C., Bai J. H., Chang P. Y., Martin T. F. J., Chapman E. R., and Jackson M. B. (2003) Different domains of synaptotagmin control the choice between kiss-and-run and full fusion. *Nature* **424**, 943-947.

- Weiner N. and Molinoff P. B. (1994) Catecholamines, in *Basic Neurochemistry: Molecular, Cellular, and Medical Aspects* (Siegel G. J., Agranoff B. W., Albers R. W., and Molinoff P. B., eds.), pp. 261-281. Raven Press, New York.
- Weiss C., Cahill A. L., Laslop A., Fischer-Colbrie R., Perlman R. L., and Winkler H. (1996) Differences in the composition of chromaffin granules in adrenaline and noradrenaline containing cells of bovine adrenal medulla. *Neuroscience Letters* **211**, 29-32.
- Winkler H. and Carmichael S. W. (1982) The chromaffin granule, in *The Secretory Granule* (Poisner A. M. and Trifaro J. M., eds.), pp. 3-79. Elsevier, Amsterdam.
- Winkler H. and Fischer-Colbrie R. (1992) The chromogranin A and B: the first 25 years and future perspectives. *Neuroscience* **49**, 497-528.
- Wu H. J., Mahata S. K., Mahata M., Webster N. J. G., Parmer R. J., and Oconnor D. T. (1995) A functional cyclic AMP response element plays a crucial role in neuroendocrine cell type-specific expression of the secretory granule protein chromogranin A. *Journal of Clinical Investigation* **96**, 568-578.
- Xiao R. P., Ji X. W., and Lakatta E. G. (1995) Functional coupling of the beta₂-adrenoceptor to a pertussis toxin-sensitive G protein in cardiac myocytes. *Molecular Pharmacology* **47**, 322-329.

- Xu J. and Tse F. W. (1999) Brefeldin A increases the quantal size and alters the kinetics of catecholamine release from rat adrenal chromaffin cells. *Journal of Biological Chemistry* **274**, 19095-19102.
- Yoo S. H. and Albanesi J. P. (1990) Ca^{2+} induced conformational change and aggregation of chromogranin A. *Journal of Biological Chemistry* **265**, 14414-14421.
- Yoo S. H. and Lewis M. S. (1992) Effects of pH and Ca^{2+} on monomer-dimer and monomer-tetramer equilibria of chromogranin A. *Journal of Biological Chemistry* **267**, 11236-11241.
- Zaika O. L., Pochynyuk O. M., Kostyuk P. G., Yavorskaya E. N., and Lukyanetz E. A. (2004) Acetylcholine-induced calcium signalling in adrenaline and noradrenaline-containing adrenal chromaffin cells. *Archives of Biochemistry and Biophysics* **424**, 23-32.
- Zhou Z., Mislis S., and Chow R. H. (1996) Rapid fluctuations in transmitter release from single vesicles in bovine adrenal chromaffin cells. *Biophysical Journal* **70**, 1543-1552.

CHAPTER 2

Materials and Methods

2.1 Chemicals

Dibutyryl cyclic-AMP (dBcAMP), dexamethasone, 3,4-dihydroxy-L-phenylalanine (L-DOPA), collagenase type I, hyaluronidase type I-S, deoxyribonuclease type I, trypsin type I, and bovine serum albumin were purchased from Sigma-Aldrich Ltd. (Oakville, ON, Canada). Forskolin and N^G-monomethyl-L-arginine (L-NMMA) were obtained from Calbiochem (San Diego, CA, U.S.A.). Dulbecco's modified Eagle's medium (DMEM), minimal essential medium (MEM), insulin-transferrin-selenium-A, penicillin G, and streptomycin were obtained from Gibco (Grand Island, NY, U.S.A.).

2.2 Cell preparation and short-term culture

Adult male Sprague-Dawley rats (200 - 250 g) were euthanized with halothane in accordance with the standards of the Canadian Council on Animal Care. Single rat chromaffin cells were prepared according to the procedure described previously (Xu and Tse 1999; Tang *et al.* 2005). Briefly, the adrenal medullae were removed and cut into fragments under a dissecting microscope. The tissue was then dissociated enzymatically at 37°C in a modified Hanks' solution containing collagenase type I (3.0 mg/ml), hyaluronidase type I-S (2.4 mg/ml), and deoxyribonuclease type I (0.2 mg/ml) for 30 min, followed by trypsin type I (0.5 mg/ml) for 10 min. Single chromaffin cells were obtained by trituration with a fire-polished glass pipette. After the removal of enzymes, chromaffin cells

were suspended in DMEM that contained 0.1% (v/v) bovine serum albumin. Cells were plated on uncoated plastic culture dishes (Corning) and allowed to settle before flooding with culture medium. The cells were maintained in a defined medium [MEM supplemented with 1% (v/v) insulin-transferrin-selenium-A] supplemented with 50 U/ml penicillin G and 50 μ g/ml streptomycin.

2.3 Solutions

The standard bath solutions contained (in mM): 150 NaCl, 2.5 KCl, 2 CaCl₂, 1 MgCl₂, 8 glucose, and 10 Na-Hepes (pH 7.4). To stimulate chromaffin cells, [K⁺] in the standard solution was raised to 50 mM (equal molar replacement of NaCl by KCl). The electrochemical measurement was performed at room temperature (21 - 24°C) on cells maintained in culture for 1 or 3 days.

2.4 Electrochemical detection of catecholamine release

Carbon fiber (tip diameter of 7 μ m) amperometry (Wightman *et al.* 1991; Chow and von Ruden 1995; Zhou and Misler 1995) was employed on single rat chromaffin cells to monitor real-time quantal catecholamine release during exocytosis as described previously (Xu and Tse 1999; Tang *et al.* 2005; Xu *et al.* 2005). The fabrication of carbon fiber electrodes was as described by Zhou and Misler (1995). Briefly, the carbon fiber was first insulated with polyethylene, so that the detection of catecholamine was restricted to the tip of the electrode

(Figure 2-1). To ensure intact insulation of the carbon fiber before the tip-cutting process, the polyethylene at the tip was heated to form a thinly insulated region of ~100 μm in length. Because the electrode noise depends significantly on the electrode capacitance, which is proportional to the length of the thinly insulated tip, the tip was cut to a final length of ~20 μm . During the recording, the tip of the carbon fiber electrode was positioned such that it touched the cell surface. A +680 mV potential (D.C.) was applied to the carbon fiber electrode, using a modified Axopatch-1B amplifier (Axon Instruments Inc., Foster City, CA, U.S.A.). The sensitivity and linearity of the carbon fiber electrodes were examined by focal application of known concentrations of dopamine (DA) (0.05, 0.1, or 0.2 mM) (Figure 2-2). According to this procedure, the sensitivity of the electrodes employed in this study varied by < 22%, and were essentially linear for the range of signal recorded. Chromaffin cells were stimulated by bath application of a high K^+ concentration ($[\text{K}^+]$) (50 mM) extracellular solution which typically elevated intracellular Ca^{2+} concentrations ($[\text{Ca}^{2+}]_i$) to 0.5 - 1 μM for several minutes and triggered Ca^{2+} -dependent quantal release of catecholamines (Figure 2-3) (Xu and Tse 1999). In all experiments, data were collected for 5 min while extracellular $[\text{K}^+]$ was raised. To minimize further the slight variation in the sensitivity of individual carbon fiber electrodes, each electrode was used only twice: for one control cell, and for one cell that received the experimental manipulation (in random order).

Amperometric currents were sampled at 10 kHz (filtered at 1 kHz) with the Fetchex function of pCLAMP version 6.03 (Axon Instruments) and then analyzed

with the Mini Analysis Program version 5.24 (Synaptosoft Inc., Decatur, GA, U.S.A.). Quantal size was calculated from the time integral of individual amperometric events (Figure 2-4). All three catecholamines in chromaffin cells, i.e. DA, norepinephrine (NE), and epinephrine (E) oxidize to yield two electrons per molecule (Chow and von Ruden 1995). Therefore, the time integral of each amperometric event (i.e. the quantal charge) provides a reliable estimate of the total amount of catecholamines released from the exocytosis of one granule (i.e. quantal size, Q). In order to have an accurate estimate of quantal size, we restricted our analysis to individual non-overlapping amperometric signals that arose from the exocytosis of one granule occurring at the tip of the carbon fiber electrode (Mosharov and Sulzer 2005). The following criteria were employed to select the amperometric events for analysis: (a) the amplitude of the amperometric event must be $\geq 3 \times$ rms noise; (b) the time integral of the amperometric event must be > 0.01 pC; (c) the 50 - 90% rise-time of the amperometric event must be < 5 ms; (d) the decay time constant (τ) of the amperometric event must be < 40 ms; and (e) the time interval between the peaks of two adjacent amperometric events must be $> 3 \times$ the decay τ of the first amperometric event. Criteria (a) and (b) were employed to distinguish the real amperometric events from electrical noise (Figure 2-5A). Criteria (c) and (d) were employed to eliminate the events that had arisen at a distance from the detection site (Figures 2-5B and C). Criterion (e) was used to eliminate overlapping amperometric events (Figure 2-5D).

2.5 Data analysis

Functions in Origin version 6.0 (OriginLab Corp., Northampton, MA, U.S.A.) or the Mini Analysis Program were employed for the following statistical and curve-fitting procedures. (1) A Student's *t*-test was used when comparing mean cellular cube-root of *Q* ($Q^{1/3}$) between two populations of cells. (2) The distributions of individual sets of data were fitted to one (or more) Gaussian distribution(s): this procedure gave chi-square (χ^2) values for comparing goodness-of-fit. To confirm whether the distribution of each set of data deviated from a Gaussian distribution, we employed a D'Agostino test of normality from GB-STAT version 8.0 (Dynamic Microsystems Inc., Silver Springs, MD, U.S.A.). (3) When comparing distributions and simulations that involve non-Gaussian distributions or the summation of multiple Gaussian distributions, a Kolmogorov-Smirnov test (K-S test) was employed (Van der Kloot 1991; Sulzer and Pothos 2000). The K-S test is based on the absolute differences between two relative cumulative frequency distributions (Sokal and Rohlf 1969). If the maximum vertical difference (d_{\max}) is greater than the critical values, then the d_{\max} is statistically significant. All error bars shown were standard error of the mean (S.E.M.). In all figures, * denotes $p < 0.05$, ** denotes $p < 0.01$, and *** denotes $p < 0.001$.

2.6 Measurement of cellular catecholamine content

For each experiment, chromaffin cells isolated from 2 - 3 rats were grown in 96-well plates. After 1 or 3 days in culture, cells were rinsed twice with phosphate-buffered saline (pH 7.4) and then harvested by scraping into an ice-cold 50 mM sodium acetate buffer (pH 6.2). The cell membrane was disrupted by sonication and a solution containing perchloric acid (2.5 M), ascorbic acid (0.5 mM), and EDTA (3.5 mM) was then added to precipitate the protein and to prevent oxidation of the catecholamines. Following centrifugation, the cell debris was removed and samples of the supernatant were stored at -80°C until determination of catecholamine content by high-performance liquid chromatography (HPLC) with electrochemical detection.

Samples (maintained at 4°C) were injected onto a chromatographic column similar to that described by Parent *et al.* (2001). The HPLC system (Waters Ltd., Mississauga, ON, Canada) was equipped with a Waters Symmetry Guard C18 precolumn and a Waters Symmetry Shield RP8 column (2.1 × 150 mm, 5 μM) maintained at 30°C. The mobile phase, which consisted of (in mM): 60 NaH₂PO₄, 0.9 Na-octyl sulfate, 0.5 EDTA, and 8% (v/v) acetonitrile (pH 2.9 with *o*-phosphoric acid), was pumped with a flow rate of 0.8 ml per min with a Waters Alliance 2690 XE system. The detector (Waters 2465 electrochemical detector) was set at a potential of +600 mV. Standards of known concentration of DA, NE, and E were included with each assay run. The concentrations of DA, NE, and E in each sample were calculated by comparing the peaks and retention

time to those of the standards. The catecholamine content in each sample was normalized to the protein amount, which was quantified with the BCA Protein Assay Reagent Kit (Pierce Biotechnology Inc., Rochford, IL, U.S.A.).

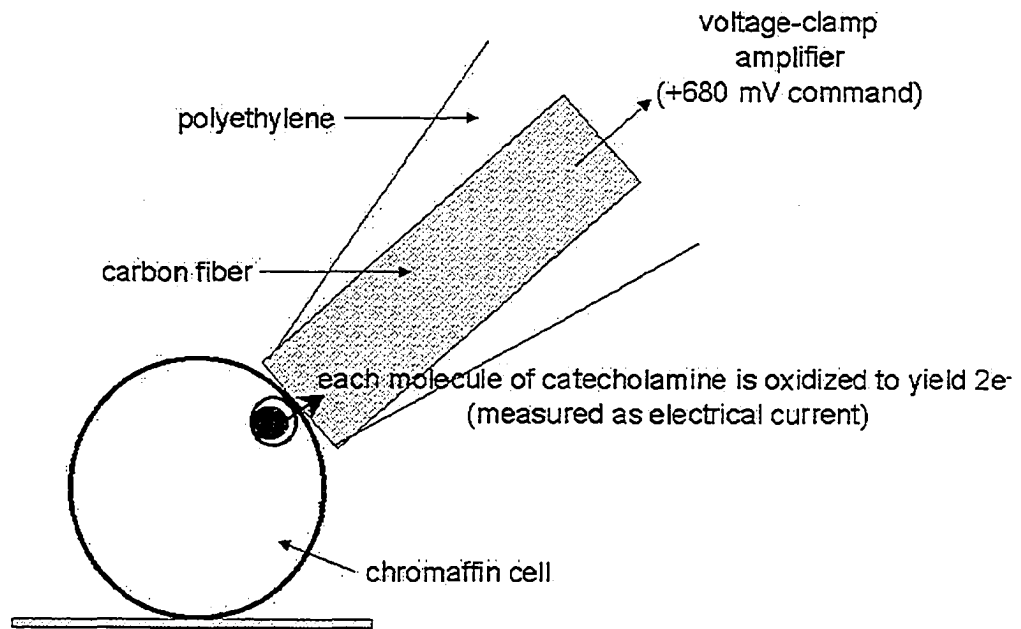


Figure 2-1 Carbon fiber amperometry. Schematic representation of a carbon fiber electrode positioned at an isolated single rat chromaffin.

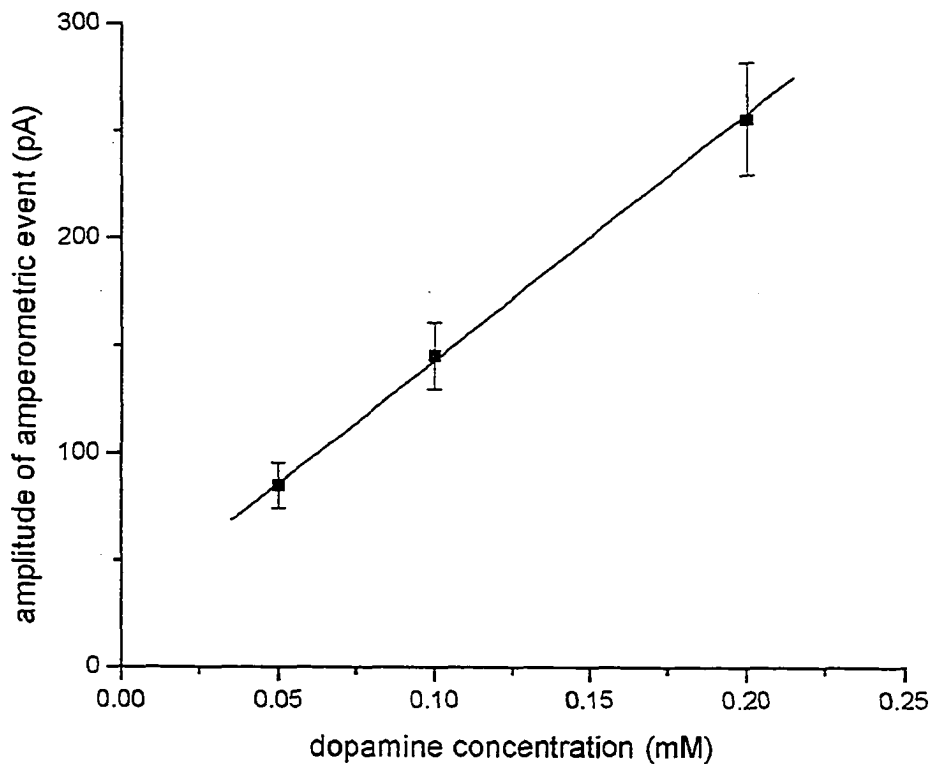


Figure 2-2 Determination of carbon fiber electrode sensitivity. The sensitivity of carbon fiber electrodes was linear over a wide range of DA concentrations. A total of ten electrodes were examined in this study.

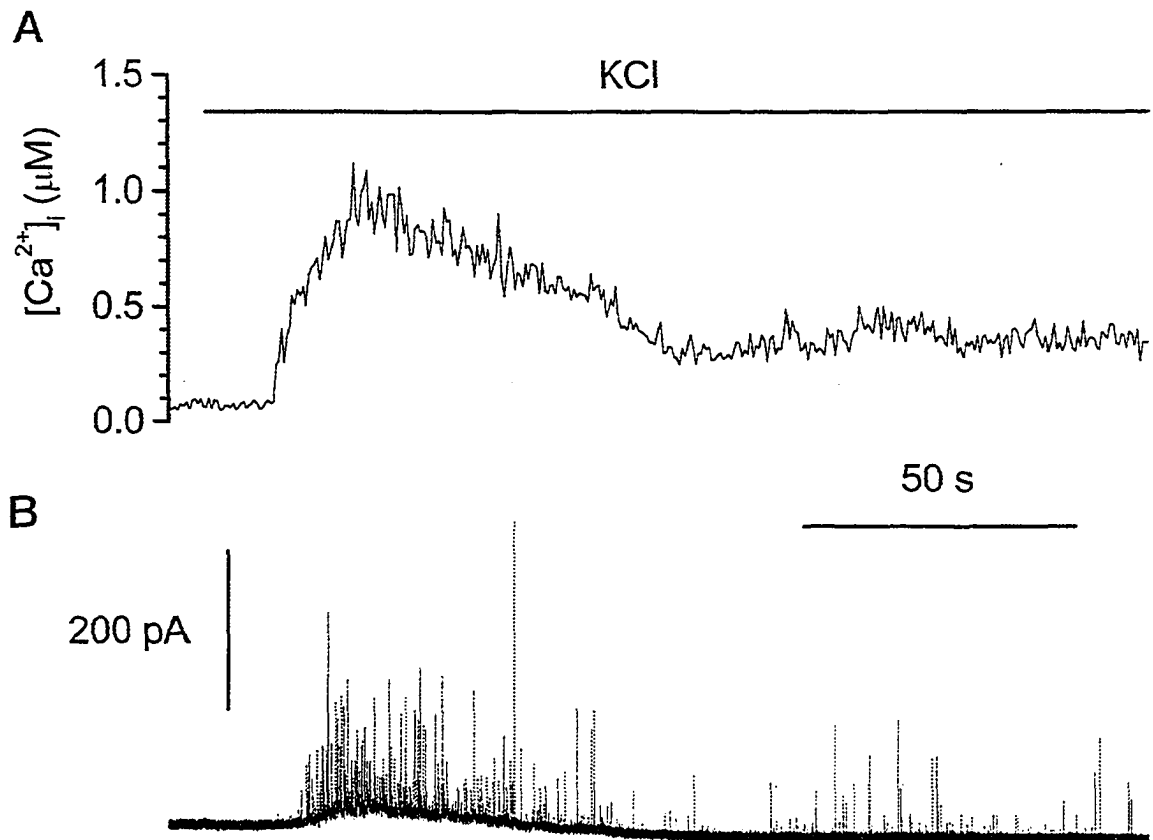


Figure 2-3 $[Ca^{2+}]_i$ transient and amperometric events triggered by bath application of a high $[K^+]$ solution (50 mM). (A) Depolarization by KCl elevated the $[Ca^{2+}]_i$. (B) $[Ca^{2+}]_i$ rise was accompanied by amperometric events. In the continued presence of KCl solution, $[Ca^{2+}]_i$ remained $\sim 0.5 \mu M$, and amperometric events persisted for at least 5 min. The cell was loaded with indo-1-AM as a Ca^{2+} indicator (modified from Xu and Tse, 1999).

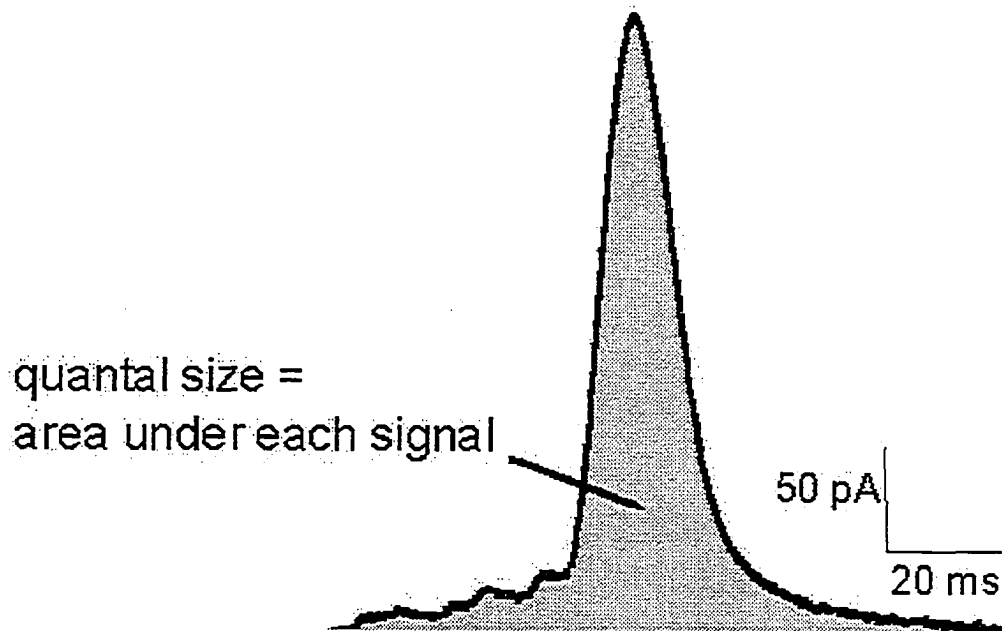


Figure 2-4 An example of amperometric event. Quantal size is the time integral of amperometric current (i.e. area under each amperometric event).

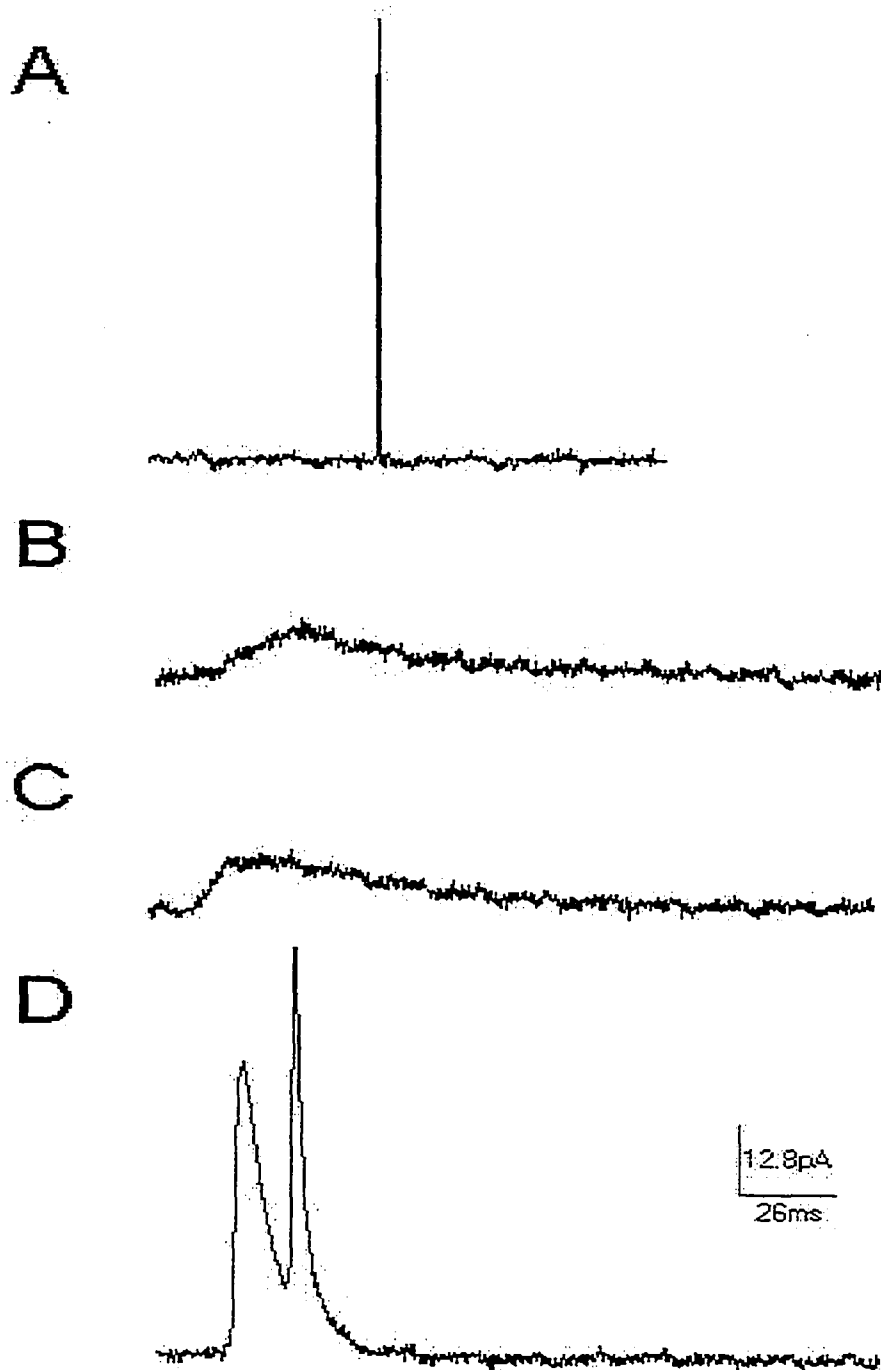


Figure 2-5 Examples of events that were rejected by the selection criteria. (A) Electrical noise with time integral of < 0.01 pC. (B) Amperometric event with slow rising phase (the 50 - 90% rise-time is ~ 13 ms). (C) Amperometric event with slow falling phase (the decay τ is ~ 52 ms). (D) Two overlapping amperometric events.

References

- Chow R. H. and von Ruden L. (1995) Electrochemical detection of secretion from single cells, in *Single-Channel Recording* (Sakmann B. and Neher E., eds.), pp. 245-275. Plenum Press, New York.
- Mosharov E. V. and Sulzer D. (2005) Analysis of exocytotic events recorded by amperometry. *Nature Methods* **2**, 651-658.
- Parent M., Bush D., Rauw G., Master S., Vaccarino F., and Baker G. (2001) Analysis of amino acids and catecholamines, 5-hydroxytryptamine and their metabolites in brain areas in the rat using in vivo microdialysis. *Methods* **23**, 11-20.
- Sokal R. R. and Rohlf F. J. (1969) *Biometry: The principals and practice of statistics in biological research*, W.H. Freeman and Company, San Francisco, CA.
- Sulzer D. and Pothos E. N. (2000) Regulation of quantal size by presynaptic mechanisms. *Reviews in the Neurosciences* **11**, 159-212.
- Tang K. S., Tse A., and Tse F. W. (2005) Differential regulation of multiple populations of granules in rat adrenal chromaffin cells by culture duration and cyclic AMP. *Journal of Neurochemistry* **92**, 1126-1139.
- Van der Kloot W. (1991) The regulation of quantal size. *Progress in Neurobiology* **36**, 93-130.

- Wightman R. M., Jankowski J. A., Kennedy R. T., Kawagoe K. T., Schroeder T. J., Leszczyszyn D. J., Near J. A., Diliberto E. J., and Viveros O. H. (1991) Temporally resolved catecholamine spikes correspond to single vesicle release from individual chromaffin cells. *Proceedings of the National Academy of Sciences of the United States of America* **88**, 10754-10758.
- Xu J., Tang K. S., Lu V. B., Weerasinghe C. P., Tse A., and Tse F. W. (2005) Maintenance of quantal size and immediately releasable granules in rat chromaffin cells by glucocorticoid. *American Journal of Physiology - Cell Physiology* doi:10.1152/ajpcell.00514.2004.
- Xu J. and Tse F. W. (1999) Brefeldin A increases the quantal size and alters the kinetics of catecholamine release from rat adrenal chromaffin cells. *Journal of Biological Chemistry* **274**, 19095-19102.
- Zhou Z. and Misler S. (1995) Action potential-induced quantal secretion of catecholamines from rat adrenal chromaffin cells. *Journal of Biological Chemistry* **270**, 3498-3505.

CHAPTER 3

Differential Regulation of Multiple Populations of Granules by Culture Duration, Cyclic AMP, and Glucocorticoids

The work in this chapter was published in:

Tang K. S., Tse A., and Tse F. W. (2005) Differential regulation of multiple populations of granules in rat adrenal chromaffin cells by culture duration and cyclic AMP. *Journal of Neurochemistry* **92**, 1126-1139.

*Xu J., ***Tang K. S.**, Lu V. B., Weerasinghe C. P., Tse A., and Tse F. W. (2005) Maintenance of quantal size and immediately releasable granules in rat chromaffin cells by glucocorticoid. *American Journal of Physiology - Cell Physiology* doi:10.1152/ajpcell.00514.2004.

* equal contributions to the work

3.1 Introduction

The secretion of epinephrine (E) and norepinephrine (NE) from adrenal chromaffin cells is the most important endocrine output of the autonomic nervous system. Traditionally, the regulation of this output has been considered at two levels. The first level focuses on the triggering of Ca^{2+} -dependent exocytosis and typically involves activation of receptor-coupled second messenger cascades which in turn modulate ion channels, intracellular Ca^{2+} concentrations ($[\text{Ca}^{2+}]_i$) and exocytosis of catecholamine-containing granules. The second level focuses on the amount of catecholamines released from individual granules (quantal size, Q). Studies on the latter typically involve the use of carbon fiber amperometry (Wightman *et al.* 1991; Chow and von Ruden 1995), and quantal size is estimated from the time integral of individual amperometric events. The quantal size of catecholamine-containing granules can be regulated by multiple factors, including catecholamine synthesis, transport, and storage (reviewed by Burgoyne and Barclay 2002). In addition, factors such as compound exocytosis (Machado *et al.* 2001) or kinetics of fusion pore opening and closure (Elhamdani *et al.* 2001; Fisher *et al.* 2001) have also been suggested to play significant roles. In most studies, chromaffin cells were assumed to have a single population of granules, and the change in quantal size arose solely from the modulation of this population of granules. However, morphological studies in rat and bovine chromaffin cells have suggested the presence of sub-populations of chromaffin cells, which stored predominantly E or NE in morphologically distinct dense core

granules (Coupland 1965; Nordmann 1984; Coupland and Tomlinson 1989; Glavinovic *et al.* 1998; Koval *et al.* 2000; 2001). Moreover, even among populations of bovine chromaffin cells that had been enriched for E- or NE-containing cells, sub-populations of cells that predominantly released E, NE, or a mixture of E and NE had been found (Pihel *et al.* 1994). These findings raise the possibility that chromaffin cells may contain distinct populations of granules. Therefore, any modulation of quantal size, particularly those involving catecholamine synthesis, uptake, or storage may not affect the different populations of granules uniformly.

In the present study, we found that rat chromaffin cells contained multiple populations of granules that released small, medium, or large modal amounts of catecholamines. Here, we operationally refer to these populations as small Q, medium Q, and large Q granules. In the majority of cells, multiple populations of granules were released. During short-term culture (1 - 3 days), a time-dependent rundown in the mean cellular quantal size involved a decrease in the proportional release from large Q granules and a reduction in the modal Q of small Q granules. On the other hand, elevation of cyclic AMP (cAMP) level in chromaffin cells increased the mean cellular quantal size. This increase was not associated with changes in the proportional release of multiple populations of granules, and was inconsistent with a random compound exocytosis among fractions of all three populations of granules. Instead, cAMP uniformly increased the modal Q of all populations of granules. In contrast, glucocorticoid prevented the rundown in the mean cellular quantal size as well as the shift in the proportional release of

multiple populations of granules. Thus, our findings suggest that the proportion of release, as well as the modal amount of catecholamines released, from multiple populations of granules in rat chromaffin cells can be differentially regulated.

3.2 Results

3.2.1 Time-dependent rundown of mean cellular quantal size and the effect of dBcAMP

In order to examine whether rat chromaffin cells have distinct populations of granules with different quantal sizes, we collected and analyzed a large number of amperometric events from chromaffin cells maintained in short-term culture (1 or 3 days) in a defined serum-free culture medium. This data was then compared to those recorded from chromaffin cells that were cultured with the membrane-permeable cAMP analog, dibutyryl cyclic-AMP (dBcAMP; 1 mM). cAMP has been reported to increase or maintain the quantal size of catecholamine release from bovine chromaffin cells (Machado *et al.* 2001; Koga and Takahashi 2004) and the effect was selective for granules with large Q (Koga and Takahashi 2004). Therefore, the change in quantal size by cAMP in rat chromaffin cells might allow us to ask whether the granule populations are differentially regulated.

We first examined whether there were any time-dependent changes in the Q values of rat chromaffin cells in short-term culture and whether the Q values were affected by cAMP. This involved comparisons among four different groups

of cells [control or dBcAMP (labeled as cAMP in all figures): 1 day or 3 days in culture] and we plotted the Q distributions from the four groups of cells in Figure 3-1. Note that each Q distribution (10 777 - 49 975 events sampled from 60 - 277 cells) was clearly too skewed to be described as a Gaussian distribution (c.f. Wightman *et al.* 1991). Using the Kolmogorov-Smirnov test (K-S test), we found that each Q distribution was significantly different from the others ($p \ll 0.0001$). We also compared the mean of the cellular values of the cube-root of quantal size ($Q^{1/3}$) which turned out to have a Gaussian distribution (see Figure 3-7 and insets of Figure 3-13A). The value of $Q^{1/3}$ is expected to be proportional to the radius of the granules if the concentration of catecholamines is identical in all granules. Note that our comparison of mean cellular $Q^{1/3}$ (Figure 3-2) did not consider individual amperometric events as independent samples; instead we averaged the $Q^{1/3}$ from different cells in the same treatment group before comparing with other groups. This grouping of data also minimized any sampling bias that might arise from unequal representation of different cells within the sample (Colliver *et al.* 2000a).

Figure 3-2 shows that in control cells when the duration of cell culture was increased from 1 to 3 days, the mean cellular value of $Q^{1/3}$ decreased by 6.5% (from $0.619 \pm 0.006 \text{ pC}^{1/3}$; $n = 277$ cells to $0.585 \pm 0.005 \text{ pC}^{1/3}$; $n = 232$ cells, $p = 9.6 \times 10^{-7}$ for Student's *t*-test), reflecting a 15% rundown in the mean cellular value of Q. When rat chromaffin cells were cultured with dBcAMP for 1 day, there was no significant change in the mean cellular value of $Q^{1/3}$ ($0.625 \pm 0.009 \text{ pC}^{1/3}$; $n = 88$ cells, $p = 0.53$ for Student's *t*-test) in comparison with control cells cultured

for the same duration. However, for cells cultured with dBcAMP for 3 days, the mean cellular value of $Q^{1/3}$ was 0.647 ± 0.013 ($n = 60$), which was ~11% larger ($p = 4.3 \times 10^{-7}$ for Student's t -test) than the control cells cultured for the same duration. In fact, after 3 days of culture with dBcAMP, the mean cellular value of $Q^{1/3}$ was 4.5% larger than that in control cells cultured for 1 day ($p = 2.4 \times 10^{-2}$ for Student's t -test). When the mean cellular values of Q were used instead of $Q^{1/3}$ in the above comparison, culturing in dBcAMP for 3 days increased the mean cellular value of Q by ~14% and ~35%, relative to control cells cultured for 1 day and 3 days, respectively. Thus, in the continuous presence of dBcAMP, the mean quantal size of the rat chromaffin cells increased to an extent that exceeded the time-dependent rundown of quantal size.

3.2.2 The presence of multiple populations of granules with different modal quantal size

The time-dependent rundown in mean cellular quantal size and the enhancement of the mean cellular quantal size by cAMP described above could be due to the modulation of a single uniform population of granules. Alternatively, there might be distinct populations of granules, each with a distinct modal quantal size, and a change in the modal Q values or a shift in the proportional release from the different populations of granules would alter the mean cellular quantal size. Traditionally, when the distribution of $Q^{1/3}$ of individual amperometric events could be adequately described by a single Gaussian (Finnegan *et al.* 1996; Glavinovic *et al.* 1998), the presence of a uniform population of granules was

implicated. Therefore, we employed a similar approach to examine whether rat chromaffin cells possessed distinct populations of granules, each with a distinct quantal size. There were two methods for pooling the data to examine the distribution of $Q^{1/3}$. For the first method, each amperometric event was considered independently and amperometric events from different cells of the same treatment group were pooled for plotting the distribution. An example of this is shown in Figure 3-3A, where the distribution of $Q^{1/3}$ of 49 975 amperometric events (collected from 277 control cells cultured for 1 day) were plotted. For the second method, the distribution of $Q^{1/3}$ for all amperometric events collected from each cell was first generated. This distribution was then averaged for all the cells in the same treatment group. In Figure 3-3B, we plotted the distribution of $Q^{1/3}$ averaged from 277 control cells cultured for 1 day. Note that the distributions of $Q^{1/3}$ generated by the two methods were very similar ($p > 0.05$ in the K-S test). This suggests that with our large number of cells sampled, the relatively small variation in the number of amperometric events analyzed from individual cells caused no significant bias in our sampling on the distribution of quantal size. Therefore, in the following sections (except Figure 3-8), amperometric events from all the cells in the same treatment group are pooled together for comparison (as in Figure 3-3A).

In Figure 3-4, we plotted the distribution of $Q^{1/3}$ for all amperometric events recorded from four groups of cells (control or dBcAMP: 1 or 3 days in culture), along with the best-fitted single Gaussian for each group. Because the proportion of events with $Q^{1/3} > 1.5 \text{ pC}^{1/3}$ (i.e. $Q > 3.4 \text{ pC}$ in Figure 3-1) was small (0.4 -

1.1%), these events were not shown in Figure 3-4. However, they were included in all subsequent analyses. A comparison of the fractional contribution of events with large $Q^{1/3}$ values ($> 1.0 \text{ pC}^{1/3}$) shows that the contribution of these large events was increased by cAMP. In cells cultured under control conditions for 1 day (Figure 3-4A), the fractional contribution of such events was 0.10 and treatment with dBcAMP for 1 day increased the fractional contribution by ~10% (to 0.11; Figure 3-4C). The effect of dBcAMP treatment was more dramatic in cells cultured for 3 days. In cells cultured for 3 days under control conditions, the fractional contribution of the events with $Q^{1/3} > 1.0 \text{ pC}^{1/3}$ was reduced to 0.07 (Figure 3-4B). Treatment with dBcAMP for 3 days increased the fractional contribution by ~57% (to 0.11; Figure 3-4D). Our observation that cAMP increased the fractional contribution of events with large $Q^{1/3}$ was in general agreement with the previous finding by Koga and Takahashi (2004) which showed that inhibition of protein kinase A preferentially reduced the exocytosis of events with large quantal size. Note that while the distributions shown in Figure 3-4 were roughly bell-shaped (c.f. Finnegan *et al.* 1996; Glavinovic *et al.* 1998), they all deviated significantly from a single Gaussian ($p \ll 0.01$ for the D'Agostino test of normality and $p \ll 0.0001$ for the K-S test). The following deviations were found for each plot in Figure 3-4. First, there were too many events with large values of $Q^{1/3}$ ($> 0.8 \text{ pC}^{1/3}$). Second, the peak of each best-fitted Gaussian distribution was located to the right of the mode of the corresponding data set. When the location of the peak of each best-fitted Gaussian distribution in Figure 3-4 was compared with the corresponding mean

cellular value of $Q^{1/3}$ (Figure 3-2), the mean cellular values of $Q^{1/3}$ were consistently larger by ~15 - 18%. Lastly, there were far too few events with small values of $Q^{1/3}$ ($< 0.25 \text{ pC}^{1/3}$). Among these three deviations, only the last one could be partially contributed by our criteria for selecting amperometric events, which always rejected events with amplitude $< 3 \times \text{rms noise}$ or with $Q < 0.01 \text{ pC}$ ($Q^{1/3} < 0.2 \text{ pC}^{1/3}$). Figure 3-4 shows that, in addition to the observation that the distribution of $Q^{1/3}$ clearly deviated from a single Gaussian distribution, the right skew in the distribution of $Q^{1/3}$ was obviously not decreasing smoothly (a distinct hump at $Q^{1/3} \approx 0.75 \text{ pC}^{1/3}$). This suggests that multiple populations of granules (each with distinct modal Q) might be present. Indeed, previous studies (e.g. Finnegan *et al.* 1996; Machado *et al.* 2001) have suggested that, under some experimental conditions, the distribution of $Q^{1/3}$ could be better fitted by models that allowed the existence of multiple populations in quantal size. Therefore, we specifically examined whether our data could be better fitted with more than one Gaussian distribution.

Figure 3-5 shows that when two Gaussian distributions were allowed, the best-fitted simulations deviated much less from the data [which was reflected in 7- to 17-fold decreases in chi-square (χ^2) values]. However, each best-fitted simulation still differed significantly from each data set ($p \ll 0.0001$ for the K-S test). In comparison to Figure 3-4, even at values of $Q^{1/3}$ that were near our lowest limit of selection for amperometric events ($0.2 \text{ pC}^{1/3}$), the best-fitted simulations in Figure 3-5 show much less deviation from each set of data. In Figure 3-5, for all experimental conditions, the peaks of the second Gaussian

distribution were located at 1.6- to 1.7-fold of $Q^{1/3}$ values of the first Gaussian distribution, and the proportion of area under each second Gaussian distribution was always larger than that under the first Gaussian distribution. If the population of the second Gaussian distribution arose from compound exocytosis (of all granule contents) of the population from the first Gaussian distribution, then the simultaneous exocytosis, or perfusion of 4 - 5 granules, from the first Gaussian distribution had to occur in more than 50% of the amperometric events. Despite the many-fold decreases in χ^2 for all four experimental conditions, the best-fitted simulations with two Gaussian distributions still failed to account for the events with large values of $Q^{1/3}$ ($> 1.2 \text{ pC}^{1/3}$), particularly prominent in Figures 3-5B and D.

The last pattern of deviation was essentially eliminated when three Gaussian distributions were allowed (Figure 3-6). In comparison to Figure 3-5 (where only two Gaussian distributions were allowed), the best-fitted simulations with three Gaussian distributions in Figure 3-6 had 2- to 6-fold decreases in the values of χ^2 , and the K-S test improved to $p \simeq 0.01$ for the control data sets. However, p remained < 0.001 for the dBcAMP data sets. Note that although the summation of the three Gaussian distributions essentially overlapped each data set over the range of $0.25 < Q^{1/3} < 1.2$, the K-S test still showed significant differences according to the conventional criterion of $p < 0.05$. When we attempted to fit each set of data with more than three Gaussian distributions, our curve-fitting program could not find any consistent improvement in the goodness-of-fit. Since our data was operationally "best-fitted" by the simulation in Figure 3-

6, we interpret that rat chromaffin cells release catecholamines from at least three populations of granules, each with a distinct modal value of Q (small, medium, or large). Note that in Figure 3-6, the peaks of the three best-fitted Gaussian distributions for the four groups of cells were located at $0.39 - 0.43 \text{ pC}^{1/3}$, $0.57 - 0.60 \text{ pC}^{1/3}$, and $0.82 - 0.88 \text{ pC}^{1/3}$, respectively. Thus, the peaks of the second and third Gaussian distributions in Figure 3-6 were located at a $Q^{1/3}$ value of ~ 1.4 - and ~ 2.1 -fold, respectively of the first Gaussian distribution. This suggests that the modal Q values of the second and third Gaussian distributions were ~ 2.7 - and ~ 9.3 -fold that of the first Gaussian distribution. If the third Gaussian distribution arose strictly from the compound exocytosis of granules in the first Gaussian distribution, then more than nine granules from the first Gaussian would have had to fuse into a single large granule. Considering that each fitted Gaussian distribution contributed $\sim 30\%$ of the area under the entire distribution, the right half of the third Gaussian distribution represented $\sim 15\%$ of the total number of amperometric events. Therefore, the fusion of more than nine small Q granules had to occur in $\sim 15\%$ of the amperometric events to account for the right half of the third Gaussian distribution. Since compound exocytosis of this magnitude was only observed in electron micrographs of rat pituitary lactotrophs (Cochilla *et al.* 2000) but not in chromaffin cells, we consider it very unlikely that the second and third Gaussian distributions arose from the compound exocytosis.

There are at least two possible explanations for the existence of multiple populations of granules in rat chromaffin cells. First, every cell can release

multiple populations of granules. Second, there may be multiple subtypes of rat chromaffin cells such that each subtype releases catecholamines with a distinct modal quantal size. Interestingly, the relative positions of the modal $Q^{1/3}$ of the three fitted Gaussian distributions in Figure 3-6 roughly correspond to the relative modal granular diameters of four types of bovine chromaffin cells described by Koval *et al.* (2000). In Figure 4 of Koval *et al.* (2000), two types of cells had similar modal diameter $\simeq 150$ nm, another type $\simeq 200$ nm, and yet another $\simeq 300$ nm. As shown in Figure 3-7, the mean cellular quantal size of individual rat chromaffin cells ($n = 277$ control day 1 cells in this example) indeed had a wide range of values. Therefore, we selected three subsets of chromaffin cells with mean cellular $Q^{1/3}$ values that matched closely the modal $Q^{1/3}$ values of each of the Gaussian distribution in Figure 3-6. The first subset of cells had small mean cellular values of $Q^{1/3}$ (range: 0.37 - 0.42 $\text{pC}^{1/3}$), and the second and third subset of cells had mean cellular $Q^{1/3}$ values that were either intermediate (range: 0.61 - 0.62 $\text{pC}^{1/3}$) or large (range: 0.79 - 0.88 $\text{pC}^{1/3}$). We then examined whether the distribution of $Q^{1/3}$ from these subsets of cells corresponded to the presence of a single or multiple population(s) of granules. The distribution of $Q^{1/3}$ from each of the three subsets (averaged from five day 1 control cells using the method shown in Figure 3-3B) was plotted in Figures 3-8A, B, and C, respectively. For comparison, the corresponding Gaussian distributions from Figure 3-6A (scaled up to have an area of 100%) were superimposed on Figures 3-8A, B, and C respectively. As shown in Figure 3-8A, the distribution for cells with small mean cellular $Q^{1/3}$ could be almost covered by the Gaussian distribution with small

modal Q, but the small fraction of data with $Q^{1/3} > 0.6 \text{ pC}^{1/3}$ was probably contributed by the Gaussian distribution with medium modal Q. In contrast, the distributions for cells with intermediate (Figure 3-8B) or large values of mean cellular $Q^{1/3}$ (Figure 3-8C) were multi-modal and straddled the ranges of all three Gaussian distributions from Figure 3-6A. Note that the location of the peaks of the data in Figures 3-8A, B, and C did not correspond precisely to the peaks of the three Gaussian distributions. This observation suggests that the modal Q value of each population of granules may be slightly different in individual cells. Most interestingly, the three distributions in Figure 3-8 also resembled the distribution of granule diameter in the distinct population of cells described by Koval *et al.* (2000). Thus, each best-fitted Gaussian distribution in Figure 3-6 may reflect the variation in Q among a population of granule in each cell, as well as the variation in modal Q of that population of granules among different cells (or subtypes of cells). Nevertheless, the results in Figures 3-8B and C suggest that in the majority of rat chromaffin cells where the mean cellular quantal size was intermediate or large, multiple populations of granules were released. However, in a small fraction of cells that had very small mean cellular quantal size, the release of granules with the small modal Q dominated.

3.2.3 Differential regulation of the multiple populations of granules by culture duration and cAMP

The results from Figure 3-2 showed that the mean cellular quantal size of rat chromaffin cells could be modulated by culture duration as well as by cAMP.

Therefore, we examined whether these changes in mean cellular quantal size uniformly affected all populations of granules. We first examined whether the rundown in mean cellular quantal size during short-term culture affected the modal Q value or the relative proportion of multiple populations of granules. Based on the location of the peaks for the three best-fitted Gaussian distributions in Figure 3-6A, we estimated that in control cells cultured for 1 day, the modal Q values of the small, medium, and large granules were 0.06, 0.17, and 0.56 pC, respectively. A similar analysis was applied to Figure 3-6B to obtain the modal Q values of all populations of granules from control cells cultured for 3 days. These values were compared to those from control cells cultured for 1 day and plotted in Figure 3-9A. Note that despite a 14% reduction in the mean cellular quantal size in control cells cultured for 3 days, there was only a small reduction (< 0.01 pC) in the modal Q value of each of the populations of granules in these cells when compared to those cultured for 1 day (Figure 3-9A). In Figure 3-9B, we expressed the same data as percentage changes in modal Q values relative to the corresponding granule populations for control day 1 cells. Note that there was ~19% and ~6% reduction in the quantal size of the small granules and medium Q granules, but the large Q granules were hardly affected ($< 1\%$ reduction). We then examined whether the rundown in mean cellular quantal size during short-term culture was associated with any shift in the proportional release of multiple populations of granules. Based on the fraction of area under each of the Gaussian distribution (relative to the summation of the three Gaussian distributions) in Figure 3-6A, we estimated that in control cells cultured for 1 day,

the proportional release from small, medium, and large Q granules was 33%, 28%, and 39%, respectively. When a similar analysis was applied to control cells cultured for 3 days, there was little change (~1%) in the fractional contribution from the small Q granules (Figure 3-9C). Instead, the phenomenon of time-dependent rundown in quantal size was mainly associated with an increase in the relative contribution from the medium Q granules (~12%) and a parallel reduction in the contribution from the large Q granules (~11%; Figure 3-9C). Thus, the above analyses suggest that the time-dependent rundown of mean cellular quantal size was mainly associated with a shift in the proportional release between the medium Q and the large Q granules, as well as a larger fractional reduction in the modal quantal size of the small Q granules.

When a similar analysis was applied to the cells cultured with dBcAMP, a different picture emerged. Since the change in mean cellular Q value for cells cultured for 1 day with dBcAMP was statistically insignificant from their time-matched controls (Figure 3-2), we focused only on cells cultured with dBcAMP for 3 days. The significant (~35%) increase in mean cellular Q for cells cultured with dBcAMP for 3 days (Figure 3-2) was mainly associated with a rather uniform increase (~30%) in the modal quantal size for each of the populations of granules in comparison to the time-matched control (3 days). (Figure 3-9B). As shown in Figure 3-9C, there was little (< 4%) change in the proportional release of multiple populations of granules in these cells when compared to the time-matched control (3 days).

The analyses above suggest that cAMP caused uniform increases in the modal Q of all populations, but the time-dependent rundown during cell culture mainly affected the proportional release. However, note that the analyses above relied on the accurate fitting of the three Gaussian distributions, and we cannot rule out the possibility that our criteria for selecting amperometric events introduced some uncertainty in the fitting of the Gaussian distributions. In our study, all amperometric events with amplitude $< 3 \times \text{rms noise}$, or $Q < 0.01 \text{ pC}$ were excluded. If a significant number of granules with very small Q were indeed released from rat chromaffin cells, the under-sampling of these granules would create errors in the modal value as well as the area of the best-fitted Gaussian distribution with small modal Q. Such errors might also cause a systematic bias in the fitting of the other two granule populations with medium or large modal values of Q. In view of these potential problems, we employed the following analysis, which is not dependent on the best-fitted Gaussian distributions to further analyze our data. This analysis is based on the assumption that when there is no change in the proportional release from the different granule populations, the cumulative frequency histograms of $Q^{1/3}$ distributions of all the amperometric events collected from the two groups of cells (with the same value in mean Q) should be similar (according to the K-S test). We first pooled the amperometric events collected from all the cells in the same treatment group. The fraction of amperometric events with different values of $Q^{1/3}$ (bin size of $0.05 \text{ pC}^{1/3}$) was then plotted as a cumulative frequency histogram. Since the majority of the amperometric events had $Q^{1/3}$ values $< 1.2 \text{ pC}^{1/3}$ (Figure 3-3), the

cumulative fraction of events approached the value of ~ 1 at $Q^{1/3} = 1.2$. For clarity, all cumulative frequency histograms were shown as lines instead of bar graphs. In Figure 3-10A, we plotted the $Q^{1/3}$ distributions of control cells day 1 and day 3 (same data in Figures 3-6A and B) as cumulative frequency histograms. The K-S test shows that the two sets of data were significantly different ($p \ll 0.0001$). Since the rundown in the mean value of Q between cells cultured for 1 and 3 days was 15% (when individual amperometric events instead of cellular means were considered), we examined whether a uniform decrease of 15% in the Q value of every amperometric events recorded from day 1 control cells would generate a cumulative frequency histogram similar to that from control cells cultured for 3 days (Figure 3-10B). Note that although the two histograms in Figure 3-10B had less deviations than those shown in Figure 3-10A, the K-S test shows that a uniform decrease of 15% in the Q value of every granule released from day 1 control cells still differed very significantly from the data obtained from day 3 control cells ($p \ll 0.0001$). Thus, the phenomenon of rundown could not arise from a uniform decrease in the modal value of Q by the same percentage in every population of granules. Note that this observation is consistent with our earlier analysis that was based on the three best-fitted Gaussian distributions (Figure 3-9).

When the cumulative frequency histogram of $Q^{1/3}$ from cells treated with dBcAMP for 3 days was compared with their time-matched controls (Figure 3-11A), the two sets of data were significantly different ($p \ll 0.0001$ for the K-S test). Since dBcAMP increased the mean value of Q (calculated from every

amperometric event) by 35%, we examined whether a uniform increase of 35% in the Q value of every amperometric event recorded from day 3 control cells would generate a cumulative frequency histogram similar to that from cells cultured with dBcAMP for 3 days. As shown in Figure 3-11B, the two histograms were not significantly different ($p > 0.05$ for the K-S test). This observation further supports our earlier analyses of the three best-fitted Gaussian distributions (Figure 3-9) that a uniform increase in the modal value of all populations of granules by roughly the same percentage can account for the effect of cAMP.

Since a previous study has suggested that the effect of cAMP was also consistent with compound exocytosis involving random perfusion among a fraction of granules (Machado *et al.* 2001), we examined whether this mechanism could also account for the effect of cAMP observed here (Figure 3-11A). We simulated the random fusion of any two granules drawn from the Q distribution of control cells cultured for 3 days (Figure 3-1B). In order to increase the mean quantal size by 35%, we had to allow the compound exocytosis (involving perfusing two granules) to occur in 40% of the amperometric events. Figure 3-11C shows that the cumulative frequency histogram generated from the simulation of 40% random compound exocytosis among day 3 control cells was significantly different from the data from cells treated with dBcAMP for 3 days ($p \ll 0.0001$ for the K-S test).

The analyses in both Figures 3-9 and 3-11A - B suggest that dBcAMP uniformly increased the value of Q by a certain percentage in all populations of granules (which is very similar to increasing the modal Q of the three best-fitted

Gaussian distributions by the same percentage). Since a short exposure to 3,4-dihydroxy-L-phenylalanine (L-DOPA) has been reported to increase the mean quantal size of granules (Pothos *et al.* 2002) and this action is expected to increase the value of Q in every granule, we examined whether treatment with L-DOPA could mimic the effect of cAMP. In Figure 3-11D, we plotted the cumulative frequency histogram of $Q^{1/3}$ from a much smaller sample of day 1 cells ($n = 19$) exposed to L-DOPA (50 μ M for 1 hour) and their time-matched controls ($n = 19$). Although the sample size in Figure 3-11D (3119 events for control and 2651 events for L-DOPA cells) was too small for a reliable analysis of multiple distributions, the treatment with L-DOPA indeed caused a shift in the cumulative frequency histogram that was similar to the effect of dBcAMP in Figure 3-11A. In this experiment, L-DOPA increased the mean quantal size by 19%. As shown in Figure 3-11E, a uniform increase of 19% in the Q value of every amperometric event recorded from control cells would generate a cumulative frequency histogram similar to that from cells treated with L-DOPA ($p > 0.05$ for the K-S test).

3.2.4 The changes in quantal size were not always correlated to changes in cellular catecholamine content

One possible explanation for the time-dependent rundown in mean cellular quantal size of chromaffin cells in culture is a general reduction in catecholamine biosynthesis. For example, a recent study employing intracellular patch electrochemistry has reported that the concentration of catecholamines in the

cytosol (i.e. the most metabolically active pool) of individual cultured chromaffin cells decayed with a time constant of ~4 days (Mosharov *et al.* 2003). Since chromaffin cells have been reported to release predominantly E and NE (Pihel *et al.* 1994), we employed high-performance liquid chromatography (HPLC) to examine whether any of the changes in the multiple populations of granules were correlated with the total amount or the relative proportion of the dominant catecholamines in these cells. Figure 3-12A shows that the effect of time-dependent rundown and cAMP on the total cellular catecholamine content (normalized to the value for day 1 control cells). The three main catecholamines that could be detected by our HPLC procedure included the two dominant catecholamines (E and NE) in chromaffin cells as well as their precursor, dopamine (DA). Not surprisingly, the rundown in quantal size in control cells between the first and third day in culture, as well as the small increase in quantal size with 1 day exposure to dBcAMP, were correlated with parallel decrease (25%) and increase (13%) in total cellular catecholamines, respectively. Unexpectedly, the 35% increase in mean cellular quantal size in cells cultured for 3 days with dBcAMP (relative to their time-matched controls) was associated with a 48% decrease in total cellular catecholamines. When we analyzed the relative contributions of the three cellular catecholamines (Figure 3-12B), there was another unexpected finding. The relative proportions of E : NE : DA (63 - 69% : 28 - 32% : 3 - 6%) were similar among the control cells (1 day and 3 days in culture) and the cells cultured for 1 day in dBcAMP. For cells cultured with dBcAMP for 3 days, the relative contribution of E dropped to 57% while the

relative contribution of DA increased to 16%. Although none of the above changes were statistically significant ($p > 0.05$ for Student's *t*-test; probably due to the large variations in the amount of catecholamine content among different batches of cultured cells), the overall patterns suggest that changes in the cellular value of Q do not always result in parallel changes in the total cellular catecholamines. Nevertheless, this finding suggested that the rundown in quantal size might be related to a general reduction in catecholamine biosynthesis.

3.2.5 Dexamethasone prevented the rundown in mean cellular quantal size after 3 days of culture

An important factor that regulates catecholamine biosynthesis is glucocorticoids. Glucocorticoids were reported to affect key enzymes involved in catecholamine biosynthesis (Hodel 2001). In rat PC18 cells (Tank *et al.* 1986) and chromaffin cells in long-term (30 days) culture (Tischler *et al.* 1982), glucocorticoids enhanced the activity of tyrosine hydroxylase, the rate-limiting enzyme in the synthesis of L-DOPA which is the precursor of all catecholamines. In bovine chromaffin cells cultured for 6 - 21 days, glucocorticoids increased the activity of the enzyme phenylethanolamine N-methyltransferase (PNMT) which converts NE to E (Kelner and Pollard 1985; Betito *et al.* 1992). For cells in short- or long-term culture, both tyrosine hydroxylase and PNMT were reported to be down-regulated (Doupe *et al.* 1985; Kelner and Pollard 1985). *In vivo*, the local blood circulation within the adrenal gland exposes chromaffin cells in the medulla to high concentrations of glucocorticoids that are secreted by cortical cells of the

adrenal cortex (Raum 1997; Hodel 2001). Therefore, one possible explanation for the rundown in mean cellular quantal size during our short-term culture of chromaffin cells is the loss of the paracrine action of glucocorticoids which in turn leads to reduction in catecholamine biosynthesis. In the following study, we examined whether glucocorticoids could prevent the rundown of mean cellular quantal size in rat chromaffin cells kept in short-term culture for 3 days.

Figure 3-13A shows the distributions of $Q^{1/3}$ generated by pooling individual amperometric events collected from different cells cultured for 1 or 3 days in the defined serum-free culture medium. Note that in comparison to the control cells cultured for 1 day (Figure 3-13Ai), the distribution of $Q^{1/3}$ of the amperometric events from control cells cultured for 3 days (Figure 3-13Aii) was shifted to the left, reflecting a rundown in quantal size during the two extra days of culture. However, a quantitative comparison between the treatment groups was complicated by the presence of multiple populations of granules in rat chromaffin cells (Tang *et al.* 2005). In our previous analysis of a large number (~10 000 - 50 000) of amperometric events (Section 3.2.2), we found that the distribution of $Q^{1/3}$ could be reasonably described by the summation of at least three Gaussian distributions (Figure 3-6), suggesting that the presence of at least three populations of granules, each with a different modal Q . In Section 3.2.3, we have also shown that the rundown in quantal size was mainly associated with a shift in the proportional release from the different populations of granules (Figures 3-9C and 3-10). Due to the much smaller number of amperometric events (~1500 - 4500) in this experiment (Figure 3-13A), it was not possible to fit

the distribution of $Q^{1/3}$ with multiple Gaussian distributions reliably to examine the contribution of the different populations of granules. Although each distribution of $Q^{1/3}$ of individual amperometric events in Figure 3-13A appeared to have a smooth bell-shape, the K-S test indicated that they all deviated significantly from a single Gaussian distribution ($p < 0.05$ in the K-S test). We have shown in Section 3.2.2 that the distribution of the $Q^{1/3}$ of individual cells (generated by averaging the $Q^{1/3}$ values of all amperometric events collected from the same cell) in the same treatment group (60 - 277 cells) could be well described by a single Gaussian distribution (Figure 3-7). In the current experiment, although the number of cells (18 - 22) is much smaller, the distribution of the mean $Q^{1/3}$ from individual cells in each treatment group (insets of Figure 3-13A) did not deviate significantly from a single Gaussian distribution ($p > 0.05$ in the K-S test). As shown in Figure 3-13B, the mean value of $Q^{1/3}$ in cells cultured for 1 day was $0.632 \pm 0.013 \text{ pC}^{1/3}$ ($n = 18$ cells). The mean $Q^{1/3}$ for cells cultured for 3 days was $0.533 \pm 0.025 \text{ pC}^{1/3}$ ($n = 20$ cells). Thus, in comparison to cells cultured for 1 day, the mean $Q^{1/3}$ of cells cultured for 3 days in defined medium was reduced by ~16% ($p = 1.4 \times 10^{-3}$ for Student's *t*-test), reflecting a decrease by ~40% of the mean cellular quantal size (Figure 3-13B).

To examine whether this rapid rundown in quantal size in isolated chromaffin cells was related to the loss of the paracrine actions of glucocorticoids during culture, we measured the quantal size of chromaffin cells cultured in defined medium supplemented with dexamethasone ($1 \mu\text{M}$), a glucocorticoid agonist. We found that the $Q^{1/3}$ distribution for cells cultured for 1 day in defined

medium supplemented with dexamethasone (Figure 3-13Aiii) was similar to that of the control cells cultured for 1 day (Figure 3-13Ai). However, the $Q^{1/3}$ distribution for cells cultured for 3 days with dexamethasone (Figure 3-13Aiv) was shifted to the right when compared with the time-matched controls (Figure 3-13Aii). The mean cellular $Q^{1/3}$ values with dexamethasone treatment for 1 and 3 days were $0.598 \pm 0.014 \text{ pC}^{1/3}$ ($n = 20$ cells) and $0.608 \pm 0.015 \text{ pC}^{1/3}$ ($n = 21$ cells), respectively. We found that these values were similar to that of the control cells cultured for 1 day ($p = 0.2$ for Student's t -test), but significantly larger than that of control cells cultured for 3 days ($p = 0.013$ for Student's t -test) (Figure 3-13B). The overall results in Figure 3-13B indicated that dexamethasone ($1 \text{ } \mu\text{M}$) did not cause any significant increase in the mean cellular quantal size after 1 day of culture, but prevented the rundown of mean cellular quantal size by $\sim 40\%$, which would otherwise occur with two extra days of culture.

Since dexamethasone ($1 \text{ } \mu\text{M}$) prevented the rundown of the cellular mean value of $Q^{1/3}$, we examined whether this effect of dexamethasone could be observed at lower concentration. We found that dexamethasone at $1 \text{ } \mu\text{M}$, but not at 10 nM , was effective in increasing the quantal size of cells cultured with defined medium. The mean $Q^{1/3}$ value for cells treated with 10 nM dexamethasone for 3 days was $0.486 \pm 0.014 \text{ pC}^{1/3}$ ($n = 16$ cells) which was not significantly different from that obtained from the time-matched controls ($0.503 \pm 0.017 \text{ pC}^{1/3}$; $n = 34$ cells; $p = 0.51$ for Student's t -test). For cells cultured with 100 nM dexamethasone in serum-supplemented medium for 3 days, the increase in the mean cellular quantal size was similar to that produced by $1 \text{ } \mu\text{M}$

dexamethasone (Xu *et al.* 2005). The above results suggested that ~100 nM - 1 μ M dexamethasone was required to maintain the quantal size in rat chromaffin cells.

3.2.6 Dexamethasone prevented the shift in proportional release of different populations of granules

We have shown in Section 3.2.3 that the phenomenon of rundown in quantal size after 3 days of culture was mainly associated with a shift in the proportion released from the different granule populations (Figures 3-9C and 3-10). While the result from Figure 3-13B suggested that dexamethasone could prevent the decrease in mean cellular quantal size during culture, it was not clear whether dexamethasone could also prevent the shift in the proportional release from different granule populations. In the current experiment, the sample size was too small for fitting multiple Gaussian distributions to dissect out the contribution from the different granule populations. Nevertheless, we have indicated in Section 3.2.3 that a comparison (with the K-S test) between the cumulative frequency histograms of $Q^{1/3}$ distributions of all the amperometric events collected from the two groups of cells (after the two data sets were scaled to have matching values in mean Q) would reveal whether there is any change in the proportional release. Figure 3-14A shows the cumulative histograms obtained from control cells cultured for 1 or 3 days. In this plot, the Q value of individual amperometric events from control day 1 cells was scaled down by 37%, such that their mean Q matched the mean Q value of control day 3 cells. Thus, if the

rundown in culture is solely a result of a uniform decrease in the Q value of every granule by 37%, the two cumulative frequency histograms should be similar. Note that the two histograms were significantly different ($p = 0.025$ in the K-S test). For control cells cultured for 3 days, there was an increase in the proportional release of granules with medium values of $Q^{1/3}$ ($\sim 0.4 - 0.7 \text{ pC}^{1/3}$; denoted by thick arrow; critical for the K-S test) and a reduction in the proportional release from granules with small $Q^{1/3}$ ($< 0.3 \text{ pC}^{1/3}$; denoted by thin arrow) and large $Q^{1/3}$ ($> 0.7 \text{ pC}^{1/3}$; denoted by thin arrow). This result was similar to that observed previously in Figure 3-10B. To examine whether dexamethasone altered the proportional release of granules, we compared the cumulative frequency histogram of $Q^{1/3}$ of control day 1 cells to that obtained from dexamethasone-treated day 1 cells (Figure 3-14B). Note that even without any scaling for mean Q, the two histograms were not significantly different ($p = 0.33$ in the K-S test). Thus, dexamethasone treatment for 1 day did not have any significant effect on proportional release (Figure 3-14B). A comparison between the cumulative frequency histogram of control 1 day cells (scaled down by 13%) and that obtained from dexamethasone treated 3 days cells shows that there was no significant difference ($p = 0.46$ in the K-S test; Figure 3-14C). Thus, if the relatively small ($\sim 13\%$) uniform decrease in Q of every granule was compensated, dexamethasone indeed prevented the shift in proportional release during the two additional days of culture.

3.2.7 *The prevention of mean quantal size rundown by dexamethasone could not be mimicked by an inhibitor of nitric oxide synthase*

In addition to its action as a glucocorticoid agonist, dexamethasone has also been reported to be an inhibitor of nitric oxide synthase (NOS) (Radomski *et al.* 1990). In primary cultures of bovine chromaffin cells, immunoreactivity of NOS was found in the majority of chromaffin cells (Schwarz *et al.* 1998). The action of nitric oxide (NO) on chromaffin cells is controversial. Inhibitors of NOS have been reported to enhance (Torres *et al.* 1994; Schwarz *et al.* 1998) or reduce (Uchiyama *et al.* 1994) catecholamine release in cultured bovine chromaffin cells, as well as to inhibit the activity of tyrosine hydroxylase in rat adrenal medulla (Kumai *et al.* 1999). A recent study in bovine chromaffin cells has shown that NO slowed down the emptying of catecholamine-containing granules during exocytosis (Machado *et al.* 2000). Interestingly, in the same study, acute incubation with NOS inhibitors or NO scavengers caused a reduction in the quantal size. Therefore, we examined whether 3 days of treatment with a potent inhibitor of NOS, N^G-monomethyl-L-arginine (L-NMMA; 300 μ M), affected the quantal size of rat chromaffin cells in defined medium. We found that the mean $Q^{1/3}$ value for cells treated with L-NMMA for 3 days was 0.646 ± 0.020 pC^{1/3} (n = 20 cells) which was not significantly different from that obtained from the time matched controls (0.654 ± 0.016 pC^{1/3}; n = 20 cells; $p = 0.77$ for Student's *t*-test). Thus, the NOS inhibitor, L-NMMA could not mimic the effect of dexamethasone in preventing the rundown of quantal size.

3.2.8 Dexamethasone also prevented the rundown in cellular catecholamine content during short-term culture

Similar to the rundown in quantal size, the reduction in cellular catecholamine content could be prevented by dexamethasone. In these batches of cell culture, we found that the total cellular catecholamine content in cells cultured for 3 days was reduced by ~20% in comparison to the cells cultured for 1 day (Figure 3-15A). In the presence of dexamethasone (1 μ M), the total cellular catecholamine content after 3 days of culture was ~110% of the control cells cultured for 1 day. In comparison to the control cells cultured for 1 day, dexamethasone treatment for 1 day caused a ~25% increase in the total cellular catecholamine content. Although a similar trend was observed in three separate batches of cell culture, there was no statistically significant difference between any of the experimental conditions. The increase in the cellular catecholamine content by dexamethasone is consistent with the stimulatory action of dexamethasone on tyrosine hydroxylase, the rate-limiting enzyme for catecholamine biosynthesis. Since dexamethasone is also known to stimulate PNMT, which may selectively increase E, we examined whether the change in total catecholamine content was accompanied by a change in the proportions of DA, NE, and E in the chromaffin cells. Figure 3-15B showed that despite the rundown in total cellular catecholamine content, we found that the proportions of DA, NE, and E in rat chromaffin cells cultured for 3 days were similar to those in cells cultured for 1 day. For cells treated with dexamethasone, the proportions of the three catecholamines were also similar to the control cells. Thus,

dexamethasone tended to increase the total cellular catecholamine content without affecting the proportions of DA, NE, and E in rat chromaffin cells.

3.3 Discussion

3.3.1 Presence of multiple populations of granules

By analyzing large samples (~10 000 - 50 000) of amperometric events, we found that the distribution of $Q^{1/3}$ of quantal release from rat chromaffin granules could be reasonably described when at least three Gaussian distributions were allowed (Figure 3-6). This finding implicated the presence of at least three populations of granules, with small, medium, or large modal quantal size. In subpopulations of rat chromaffin cells that had either intermediate or large mean cellular Q values (Figure 3-7), the distributions of $Q^{1/3}$ from these cells were conspicuously multi-modal (Figures 3-8B and C), suggesting that multiple populations of granules (in different proportions) were released from the majority of cells. Our comparisons of the distributions of each of the three granule populations with the three subpopulations of cells (Figure 3-7) suggest that there were considerable cell-to-cell variations in the modal Q of each of the granule populations. This is consistent with the analysis of granular concentrations of catecholamines by Gong *et al.* (2003), which showed that while the catecholamine concentrations were remarkably constant among granules from the same cell, there were considerable cell-to-cell variations.

The notion that individual chromaffin cells might contain multiple types of dense core granules was supported by a previous electron microscopic study of bovine chromaffin cells, which reported the presence of five types of dense core granules based on the granule diameters and morphology (Koval *et al.* 2001). However, based on cellular ultrastructure, Koval *et al.* (2000) suggested that there were also at least four subtypes of bovine chromaffin cells, each with a distinct distribution for the diameter of dense core granules (although the distributions were less conspicuously multi-modal in comparison to Figure 3-8, and the modal value of two subtypes was similar). Because rat chromaffin cells have both E- and NE-containing granules (Coupland 1965; Nordmann 1984; Coupland and Tomlinson 1989), it is difficult for us to make any direct comparison of the distribution of $Q^{1/3}$ in this study with the diameters of the different types of granules reported in the electron microscopic study employing glutaraldehyde fixation. The differential solubility of the E- or NE-glutaraldehyde complex (formed during the fixation procedure for electron microscopy) was reported to cause osmotic swelling of granules (Coupland and Hopwood 1966) and thus might affect some of the morphological characteristics (particularly the size of the dense core granules). Nevertheless, in a study employing cryofixation of bovine chromaffin cells, the distribution of granule diameter was clearly right-skewed (Plattner *et al.* 1997), indicating that there might be at least two distinct populations of granules with two different mean diameters. Most interestingly, the distribution $Q^{1/3}$ for bovine chromaffin cells was also right-skewed (Finnegan *et al.* 1996). The similarity between the skewed distributions in $Q^{1/3}$ and granule

diameter raised the possibility that bovine chromaffin cells (that secrete mainly E) might contain at least two distinct populations of granules with different quantal size and granule diameter. Therefore, among a population of rat chromaffin cells that secrete either predominantly E, NE, or both from each cell, it is indeed possible that there are at least three populations of granules.

Note that the argument above is based on the assumption that quantal size directly reflects the diameter of individual granules. However, the above comparison of quantal size with granule diameters is complicated by an important observation from Elhamdani *et al.* (2001) which suggested that an increase in voltage-gated Ca^{2+} entry could dramatically increase the quantal size via regulation of the fusion pore to allow more complete release of individual granules. This mechanism may not uniformly affect every granule because of different degrees of co-localization of VGCC with subpopulations of granules. Under this condition, it is possible that granules of identical diameter and containing the same amount of catecholamines can give rise to different quantal sizes.

Nevertheless, the presence of multiple populations of granules in rat chromaffin cells is further supported by our finding that the populations of granules could be differentially regulated. Between the first day and the third day of culture, the mean cellular quantal size decreased by 15 - 40% (Figures 3-2A and 3-13B). Interestingly, this rundown in mean cellular quantal size did not reduce the modal quantal size of all populations of granules by the same percentage (Figures 3-9B and 3-10). Instead, the small Q granules had the

largest percentage decrease (~19%). This may reflect the involvement of a mechanism (e.g. a transporter) that becomes more prominent when the surface area to volume ratio is large (e.g. in granules with small radius). Indeed, direct or indirect manipulations of amine transport into granules have been reported to regulate quantal size in rat pheochromocytoma (PC12) cells (Pothos *et al.* 2000; 2002).

The modal $Q^{1/3}$ value of the small Q granules in rat chromaffin cells was ~0.4 pC^{1/3} (Figure 3-6), similar to the $Q^{1/3}$ value reported for the granules in PC12 cells (Finnegan *et al.* 1996; Colliver *et al.* 2000b; Elhamdani *et al.* 2000). PC12 cells have been reported to have very little mRNA for PNMT, the enzyme that converts NE to E (Unsworth *et al.* 1999), and they secrete mainly NE and DA (Kumar *et al.* 1998). On the other hand, the modal $Q^{1/3}$ value of the large granules in rat chromaffin cells was ~0.8 pC^{1/3}, similar to the distribution of bovine chromaffin cells which was enriched for E-containing cells (Figure 2B in Finnegan *et al.* 1996). It is tempting to speculate that the large granules in rat chromaffin cells may be similar to the granules in the E-enriched bovine chromaffin cells and secrete predominantly E, and the small granules are similar to the PC12 granules and secrete mainly NE and DA. Unfortunately, the current study cannot directly address these possibilities.

3.3.2 Time-dependent rundown of mean cellular quantal size and its prevention by glucocorticoids

Our results show that dexamethasone was able to prevent the rundown in mean cellular quantal size (Figure 3-13B) as well as preventing the shift in proportional release of different populations of granules (Figure 3-14C). One major difference between chromaffin cells in culture and *in vivo* is the drastic reduction of glucocorticoids that are secreted by the cortical cells. Due to the local blood circulation within the adrenal gland, chromaffin cells in the medulla are exposed to high concentrations of glucocorticoids released from the adrenal cortex (Raum 1997; Hodel 2001). Here, we found that relatively high concentrations of dexamethasone (~100 nM - 1 μ M) were required to prevent the rundown in mean quantal size. This range of dexamethasone concentration is physiologically relevant as the plasma level of the main glucocorticoid (cortisone) in rats was reported to reach ~1 μ M (Honma *et al.* 1984; Sargent 1985). Thus, our results suggest that the continued presence of a high level of glucocorticoids is essential for the maintenance of the amount of catecholamine stored in the granules of rat chromaffin cells.

The quantal size of chromaffin cells can be influenced by multiple factors, including inhibition of NOS, extracellular Ca^{2+} entry, as well as catecholamine biosynthesis or storage (Hodel 2001). Although dexamethasone has been reported to be an inhibitor of NOS (Radomski *et al.* 1990), we found that the effect of dexamethasone on quantal size in rat chromaffin cells could not be mimicked by the NOS inhibitor, L-NMMA, suggesting that the involvement of

NOS inhibition was unlikely. In PC12 cells, dexamethasone treatment for 5 - 7 days was reported to double the mean quantal size; however, this effect was accompanied by ~3-fold increase in VGCC density (Zerby and Ewing 1996; Elhamdani *et al.* 2000). For chromaffin cells cultured in defined medium, dexamethasone did not affect the VGCC density (Xu *et al.* 2005). This may explain why dexamethasone did not cause any measurable change in quantal size in cells cultured in defined medium for 1 day (Figures 3-13B and 3-14B). However, note that even without any change in VGCC density, dexamethasone was effective in preventing the rundown in quantal size as well as the shift in proportional release in cells cultured with defined medium (Figures 3-13B and 3-14C). Therefore we conclude that dexamethasone maintained the quantal size via a mechanism that was independent of the regulation of VGCC density (and thus of extracellular voltage-gated Ca^{2+} entry). In contrast, we found that the rundown in quantal size appeared to occur in parallel with a reduction in total cellular catecholamine content of the rat chromaffin cells, suggesting that a reduction in catecholamine biosynthesis might contribute to this rundown. Consistent with this notion, dexamethasone, which was reported to affect catecholamine synthesis, also prevented the rundown in cellular catecholamine content. Although dexamethasone was reported to stimulate both tyrosine hydroxylase (Tischler *et al.* 1982) and PNMT (Kelner and Pollard 1985), the dexamethasone-mediated increase in total cellular catecholamine content in chromaffin cells was not accompanied by any significant change in the proportion of DA, NE, and E. Any significant stimulation of PNMT may increase E

selectively. Therefore, our results suggest that dexamethasone maintains the quantal size in chromaffin cells mainly via its stimulatory action on tyrosine hydroxylase, the rate-limiting enzyme in catecholamine synthesis. The importance of tyrosine hydroxylase activity in the maintenance of quantal size was shown in PC12 cells where inhibition of tyrosine hydroxylase reduced the quantal size by ~50% (Pothos *et al.* 1998). In addition, dexamethasone may increase the storage of catecholamine in chromaffin cells via the enhanced expression of chromogranin A (Rozansky *et al.* 1994), which is a main component of the dense core matrix where catecholamines are packaged. Our overall evidence is consistent with the idea that an increase in biosynthesis and storage of catecholamine is the major mechanism underlying the prevention of quantal size rundown in rat chromaffin cells by dexamethasone.

3.3.3 *Regulation of quantal size by cAMP*

The action of 3 days treatment with dBcAMP was mainly associated with a uniform (~35%) increase in the size of every granule released (Figure 3-11B), and this change was reflected as an increase in the modal quantal size of each population of granules (Figure 3-9B). However, unlike dexamethasone, cAMP could not prevent the shift in the proportional release of different populations of granules between the first and third day of cell culture. Interestingly, the total cellular catecholamine content in cells treated with dBcAMP for 3 days was reduced below the level of the rundown for the same duration of culture. Recent studies have suggested that the quantal size in chromaffin cells can be regulated

both at the stage of synthesis and storage of catecholamines, as well as via the kinetics of the fusion pore (Burgoyne and Barclay 2002). The details of the effects of cAMP on the kinetics of the amperometric events will be described in Chapter 4. Here, we shall focus our discussion on other mechanisms, which may be involved in the action of cAMP on quantal size.

The first possible mechanism is an increase in catecholamine synthesis. Elevated levels of cAMP were reported to have stimulatory effect on tyrosine hydroxylase (Hwang *et al.* 1994), the rate-limiting enzyme in catecholamine synthesis (Levitt *et al.* 1965). This mechanism is consistent with our observation that a uniform increase in the value of Q of all populations of granules could account for the effect of cAMP (Figures 3-9B and 3-11B). However, we found that there was a reduction in total cellular catecholamine content in cells treated with dBcAMP for 3 days. An explanation for this discrepancy is that the total cellular catecholamine content simply does not accurately reflect the vesicular catecholamine content.

The second possible mechanism is that cAMP enhances the uptake of catecholamines into every granule, thus increasing the modal quantal size in every population of granules. As mentioned earlier in the context of rundown, when the surface area to volume ratio is taken into consideration, this mechanism should, in theory, increase the catecholamine concentration in small diameter granules by a larger percentage. However, Gong *et al.* (2003) have shown that chromaffin cell granules have additional mechanisms to maintain the concentration of catecholamines within a narrow range. Therefore, it is still

possible that an increase in catecholamine uptake can ultimately manifest as a uniform percentage increase in quantal size in all populations of granules. In chromaffin cells, the uptake of catecholamines is mediated via the vesicular monoamine transporter (VMAT). Overexpression of VMAT in PC12 cells indeed led to a robust increase in the quantal size of the PC12 granules (Pothos *et al.* 2000). However, cAMP was reported to inhibit the activity of VMAT in PC12 cells (Nakanishi *et al.* 1995), and it is not clear whether a similar inhibition of VMAT by cAMP also occurs in rat chromaffin cells. The driving force for VMAT to accumulate catecholamines into granules is provided by the pH gradient generated by a vacuolar proton pump (Reimer *et al.* 1998). Inhibition of the vacuolar proton pump has been shown to reduce quantal size (Pothos *et al.* 2002). Therefore, it is also possible that cAMP may increase quantal size via actions on the pH gradient.

The third possible mechanism is granule-granule fusion or compound exocytosis that is triggered by cAMP [e.g. as reported in lactotrophs by Cochilla *et al.* (2000)]. In chromaffin cells, Machado *et al.* (2001) suggested that the random compound exocytosis (of a certain fraction of granules) could better account for the forskolin-induced changes in the frequency histogram (of $Q^{1/3}$) than a uniform increase in the value of Q of every granule by a fixed percentage. In contrast, our analysis in Figure 3-11 led to an opposite conclusion. However, there is a fundamental difference between our analysis and that of Machado *et al.* (2001). Our simulations in Figure 3-11 were generated from actual data whose distribution of $Q^{1/3}$ was not a Gaussian distribution; the simulations in

Machado *et al.* (2001) assumed a Gaussian distribution for the $Q^{1/3}$ values in the control data (although their data set was also right-skewed). Note that in both simulations, the random perfusion had to occur in ~40% of the amperometric events. Since compound exocytosis was rarely detected in electron micrographs of stimulated bovine chromaffin cells (e.g. Pothos *et al.* 2002), we consider this possibility unlikely unless rat chromaffin cells are fundamentally different.

The fourth possible mechanism is that cAMP may regulate dissolution of the dense core after exocytosis, thus affecting the quantal size. In rat pituitary lactotrophs, a decrease in cellular cAMP level has been shown to cause solubilization of dense cores (Angleton *et al.* 1999). An increase in solubilization of dense cores in chromaffin cells during or after exocytosis could lead to a more complete catecholamine release and thus an increase in quantal size. Since the cellular cAMP level was elevated in our study (by dBcAMP), an increase in solubilization of dense cores was unlikely. However, if elevated cellular cAMP leads to a more condensed dense core, the dense core may store more catecholamines. Under this condition, a complete discharge of the granule will increase the amount of catecholamines released and thus the quantal size. On the other hand, it is also possible that the dissociation of the more condensed dense core may be less complete before fusion pore closure. Studies in Chapter 4 attempt to address this issue.

Overall, among the four possible mechanisms discussed here, we consider the stimulatory action of cAMP on tyrosine hydroxylase as the most probable mechanism for the increase in quantal size in rat chromaffin cells. The

increase in catecholamine synthesis in turn results in more storage in all populations of granules, and thus uniformly increases the quantal size of every granule by roughly the same percentage. Consistent with this, supplying chromaffin cells with L-DOPA, the precursor of all catecholamines also resulted in a uniform percentage increase in the quantal size of every granule (Figure 3-11E).

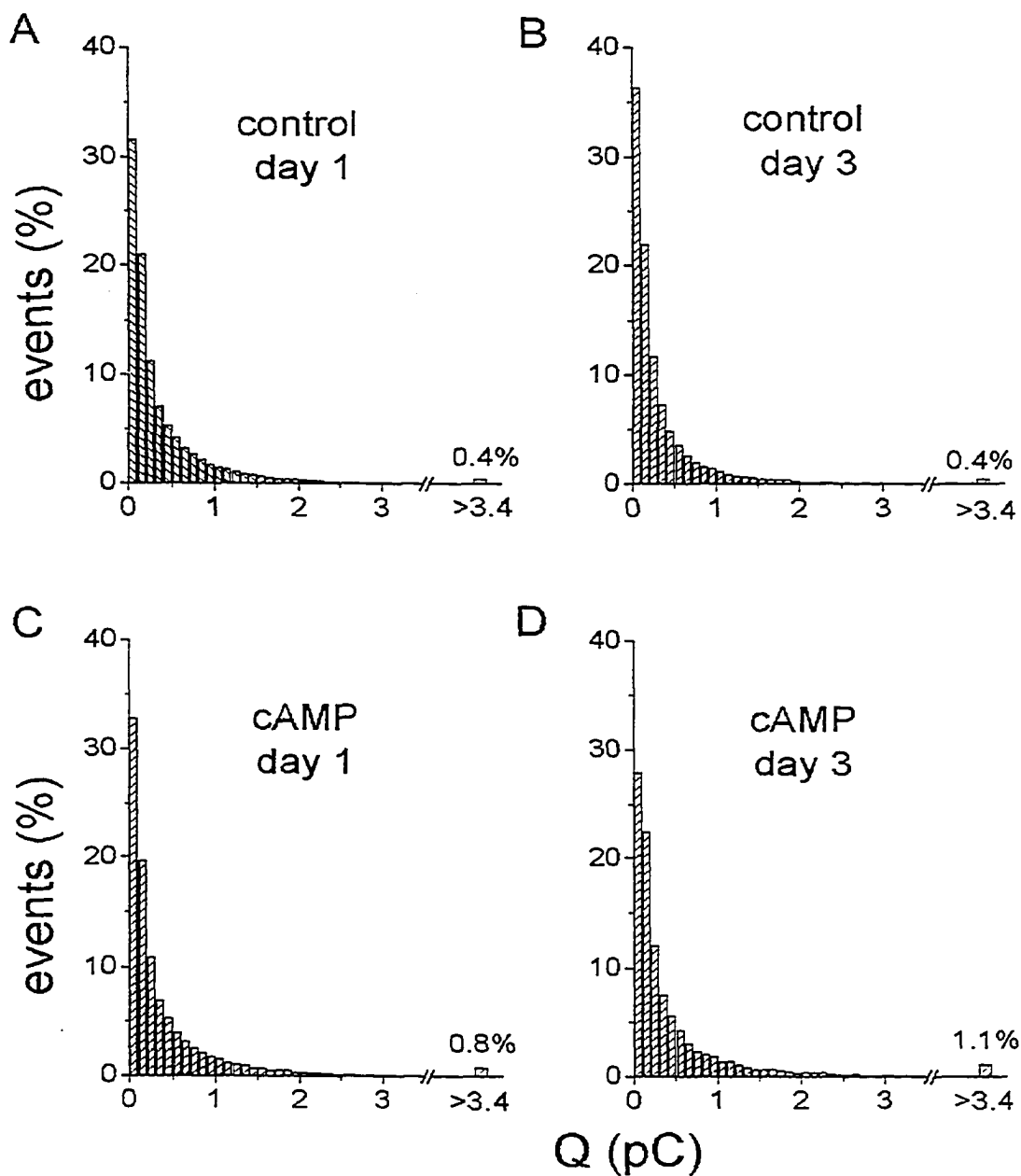


Figure 3-1 The distribution of Q generated by pooling individual amperometric events collected from cells in four treatment groups. (A) Data from cells cultured for 1 day in control condition (49 975 events from 277 cells). (B) Data from cells cultured for 3 days in control conditions (20 170 events from 88 cells). (C) Data from cells cultured for 1 day with 1 mM dBcAMP (39 778 events from 232 cells). (D) Data from cells cultured for 3 days with 1 mM dBcAMP (10 777 events from 60 cells). Note that in each treatment group, events with Q > 3.4 pC were pooled together and shown as a single bar in the histogram. In this and all subsequent figures, groups of cells treated with dBcAMP are labeled as cAMP.

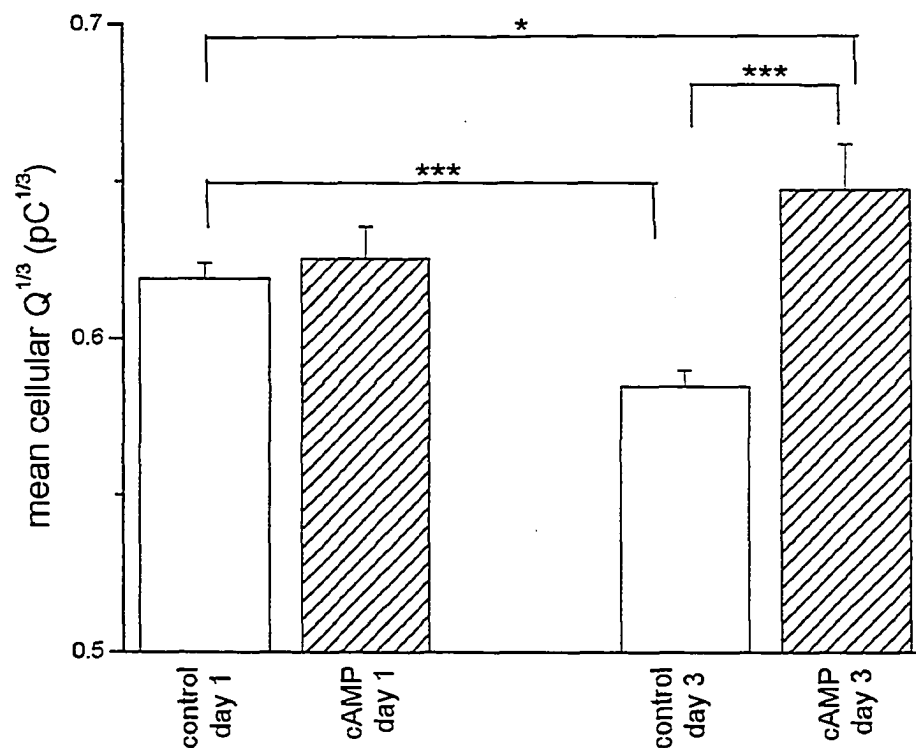


Figure 3-2 Changes in the mean cellular quantal size with duration of culture and cAMP. When the $Q^{1/3}$ value of control cells cultured for 1 day was compared with that from control cells cultured for 3 days, there was a significant ($p = 9.6 \times 10^{-7}$) rundown in $Q^{1/3}$ (marked with ***). For cells treated with dBcAMP (1 mM) for 3 days, there was a significant ($p = 4.3 \times 10^{-7}$) increase in $Q^{1/3}$ when compared to control cells cultured for 3 days (marked with ***). In fact, the $Q^{1/3}$ value of cells treated with dBcAMP for 3 days was significantly ($p = 2.4 \times 10^{-2}$) larger than that in control cells cultured for 1 day (marked with *). For cells treated with dBcAMP for 1 day, the small increase in $Q^{1/3}$ was insignificant ($p = 0.53$) when compared with control cells cultured for 1 day. The $Q^{1/3}$ of individual cell was generated by averaging the $Q^{1/3}$ of all amperometric events collected from the same cell. For each treatment group, a mean cellular $Q^{1/3}$ value was then obtained from the average of 60 - 277 individual cells.

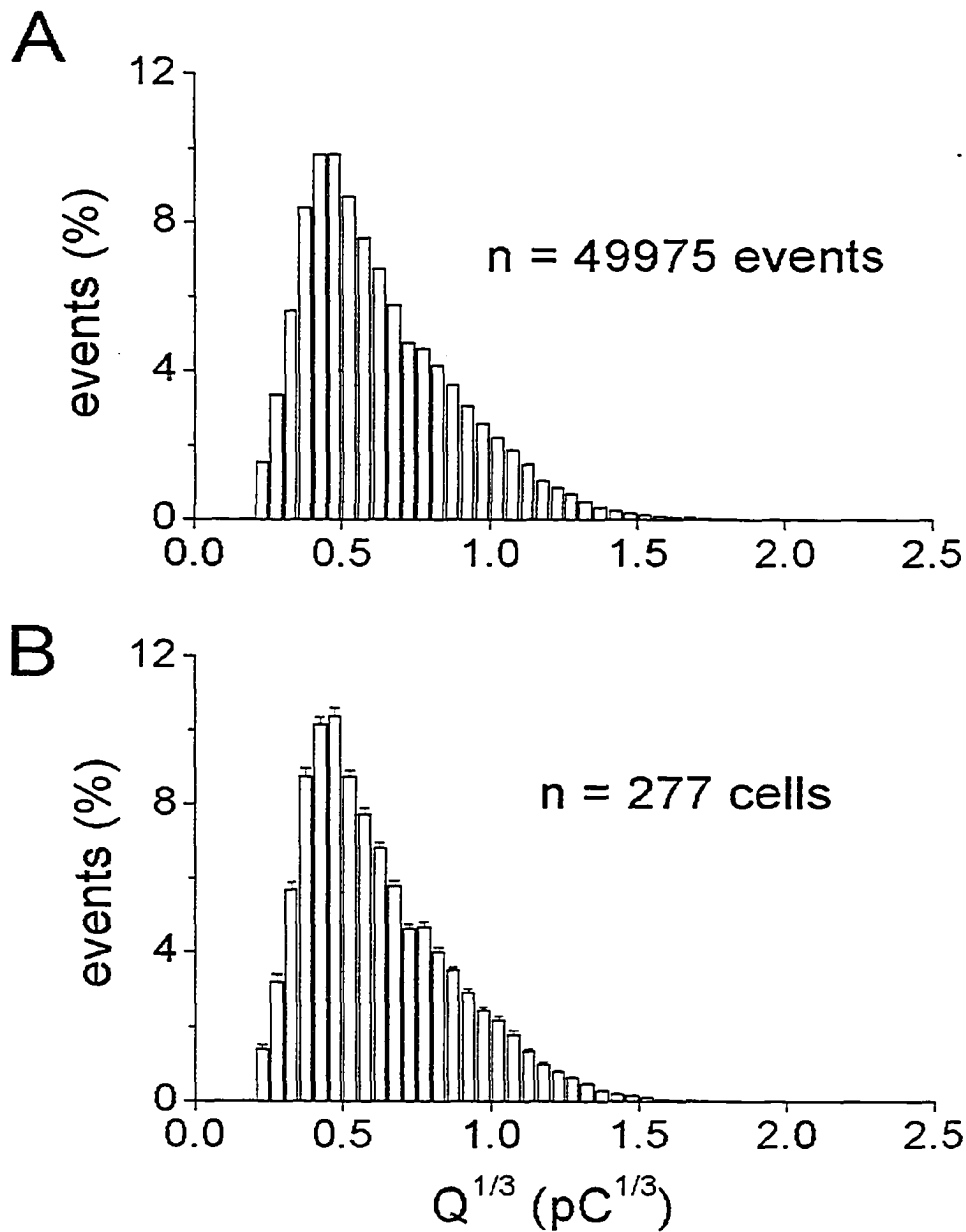


Figure 3-3 Two different ways of generating the distribution of $Q^{1/3}$. The distribution of $Q^{1/3}$ generated by (A) pooling individual amperometric events collected from different cells in the same treatment group was similar to that generated by (B) averaging the distribution of $Q^{1/3}$ from individual cells in the same group. The data plotted in (A) was the distribution of 49 975 amperometric events collected from 277 control cells cultured for 1 day. In (B), the plot was averaged from the distribution generated for each of the 277 cells. The K-S test for comparing (A) and (B) has $p > 0.05$.

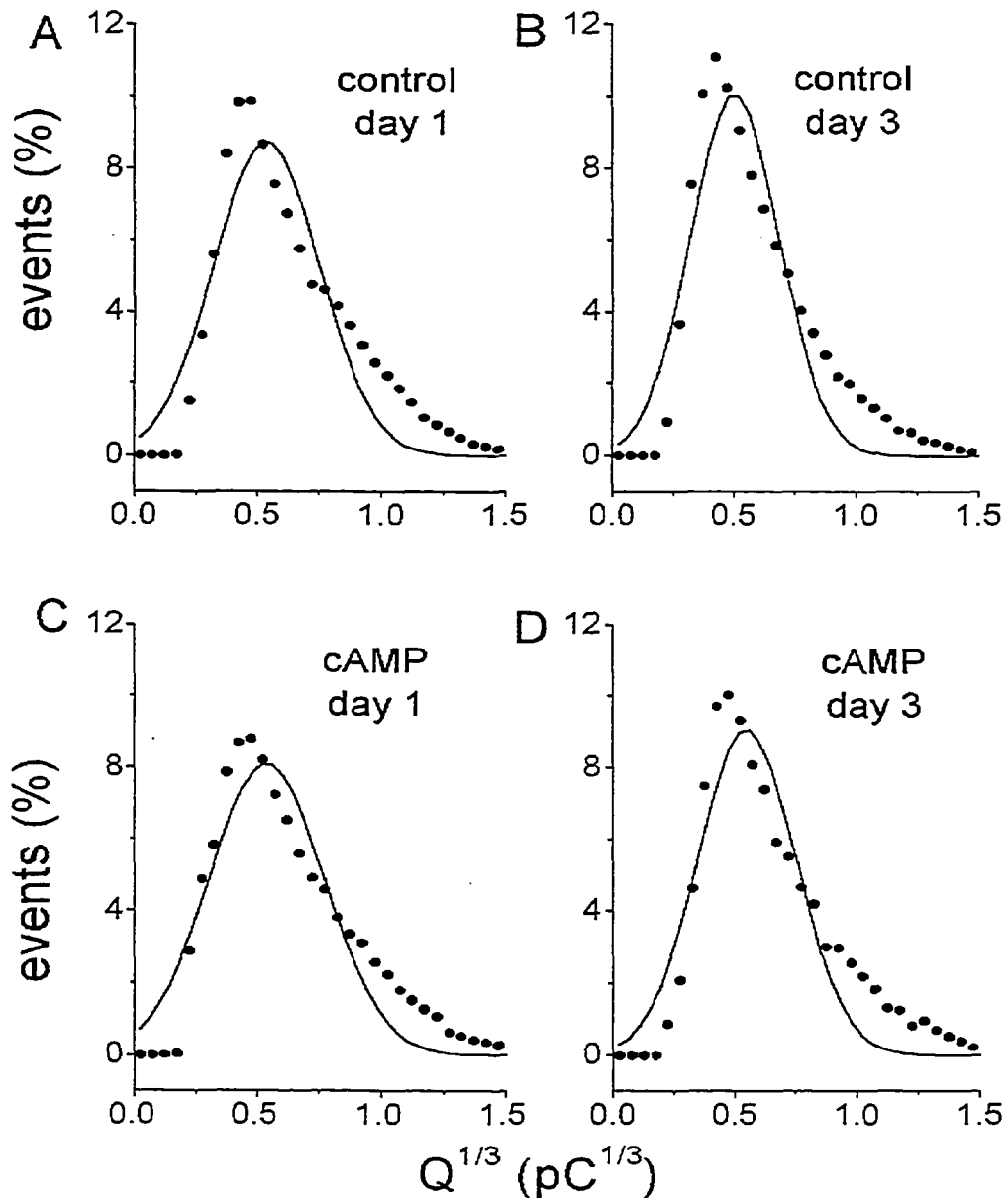


Figure 3-4 Presence of more than one population of granules. The distribution of $Q^{1/3}$ for control cells cultured for 1 day (A) or 3 days (B); cells treated with dBcAMP for 1 day (C) or 3 days (D) could not be adequately described by a Gaussian distribution (solid line). For better visual comparison of the deviation of the data (closed circles) from each best-fitted Gaussian distribution, all data with $Q^{1/3} > 1.5 \text{ pC}^{1/3}$ were not shown. The number of events involved in each histogram ranged from 10 777 (D) to 49 975 (A). When the D'Agostino test of normality or the K-S test was applied to each set of data, the p value was < 0.01 or $\ll 0.0001$, respectively.

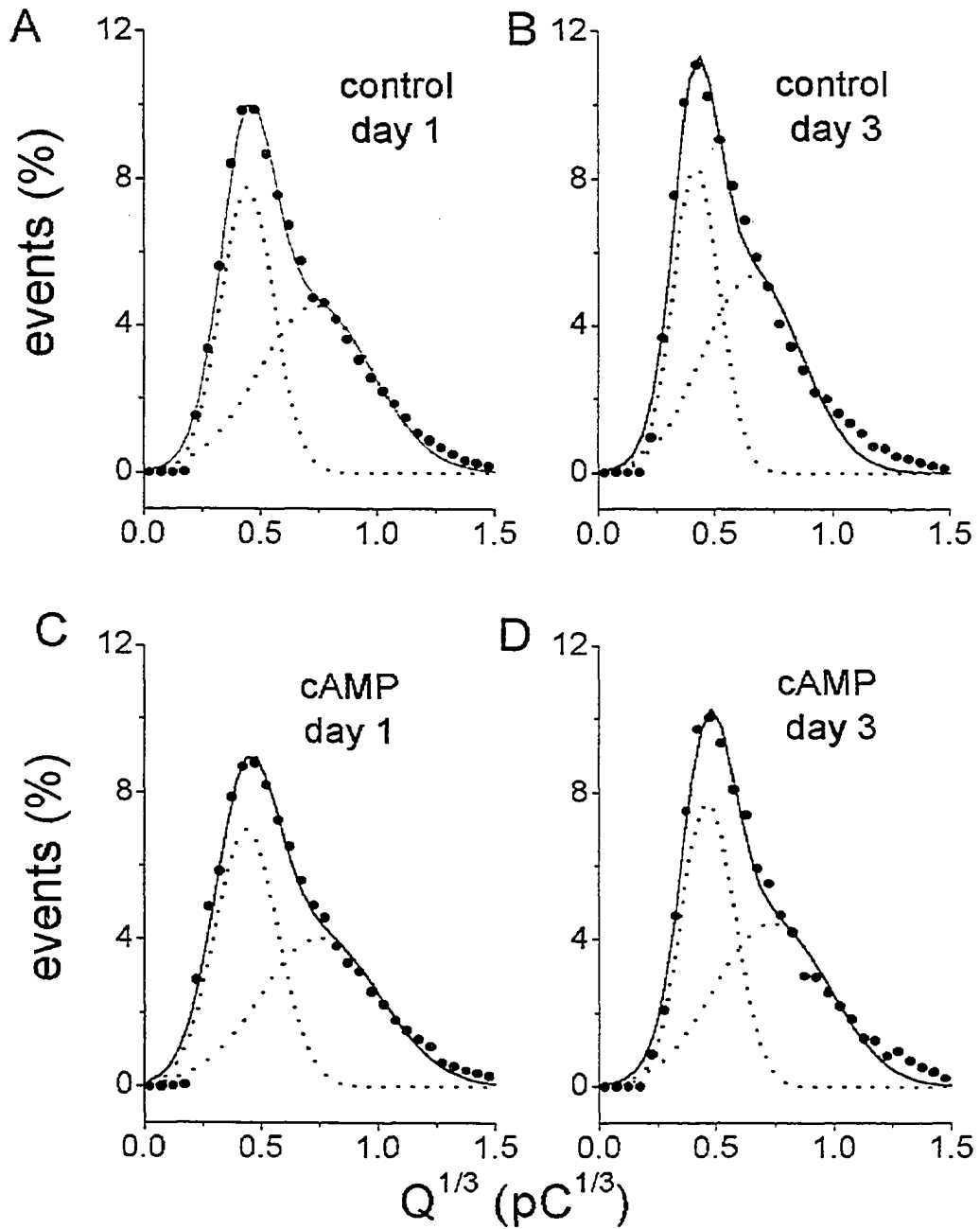


Figure 3-5 Presence of more than two populations of granules. The distribution of $Q^{1/3}$ in each of the four experimental conditions (A-D) could not be adequately described by two Gaussian distributions (dotted lines, $p \ll 0.0001$ in the K-S test). Note that the data clearly deviated from the summation of two Gaussian distributions (solid line) at large values of $Q^{1/3}$ (most noticeable at B and D).

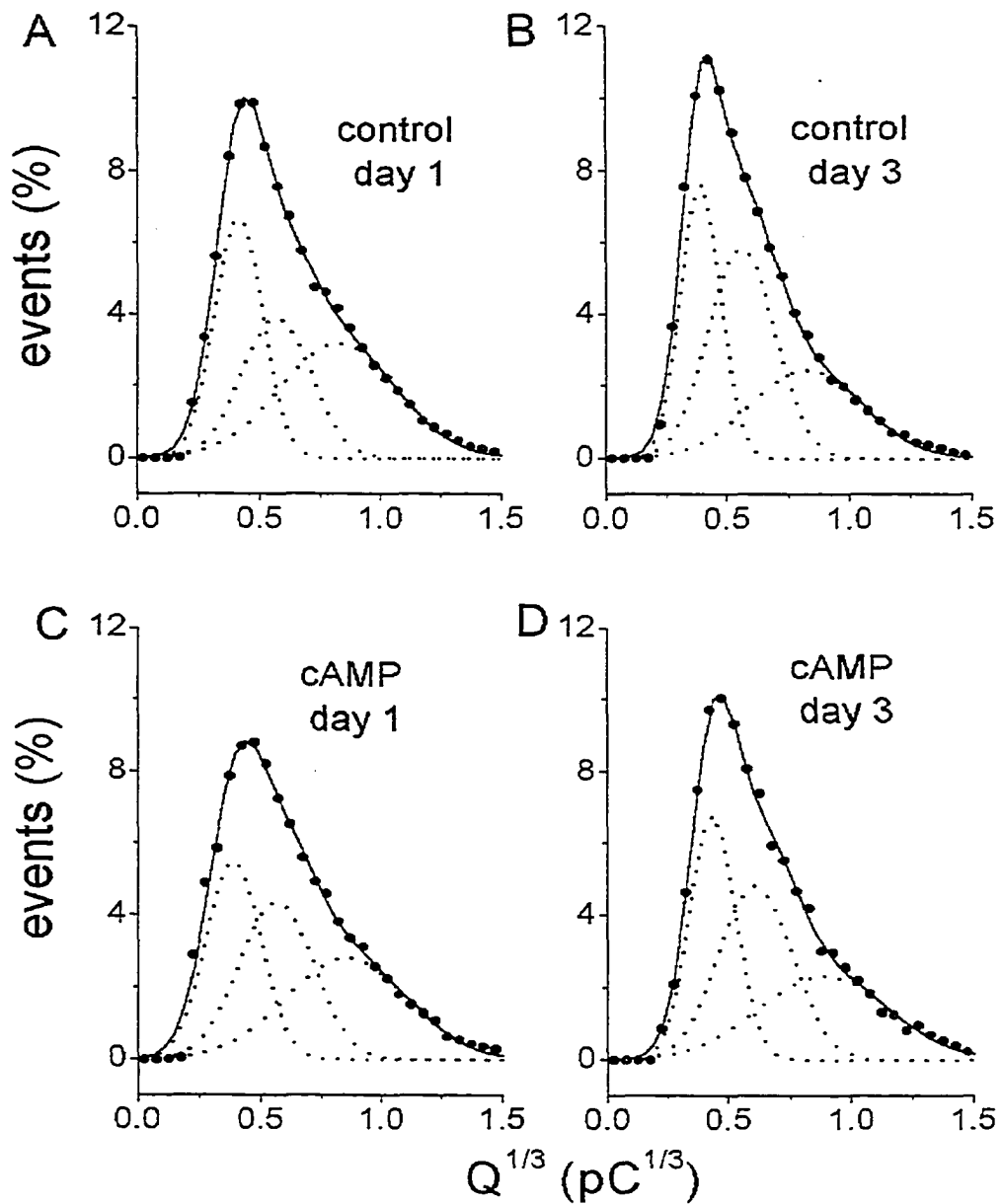


Figure 3-6 Presence of at least three populations of granules. The data (closed circles) from each experimental condition (A-D) were reasonably described by the summation of three Gaussian distributions (solid line, $p \simeq 0.01$ in the K-S test for control data sets; $p < 0.001$ in the K-S test for cAMP data sets). The peaks of the three Gaussian distributions (dotted lines) were located at (in units of $\text{pC}^{1/3}$): 0.413, 0.568, and 0.825 for (A), 0.390, 0.557, and 0.824 for (B), 0.389, 0.565, and 0.857 for (C), 0.433, 0.606, and 0.886 for (D).

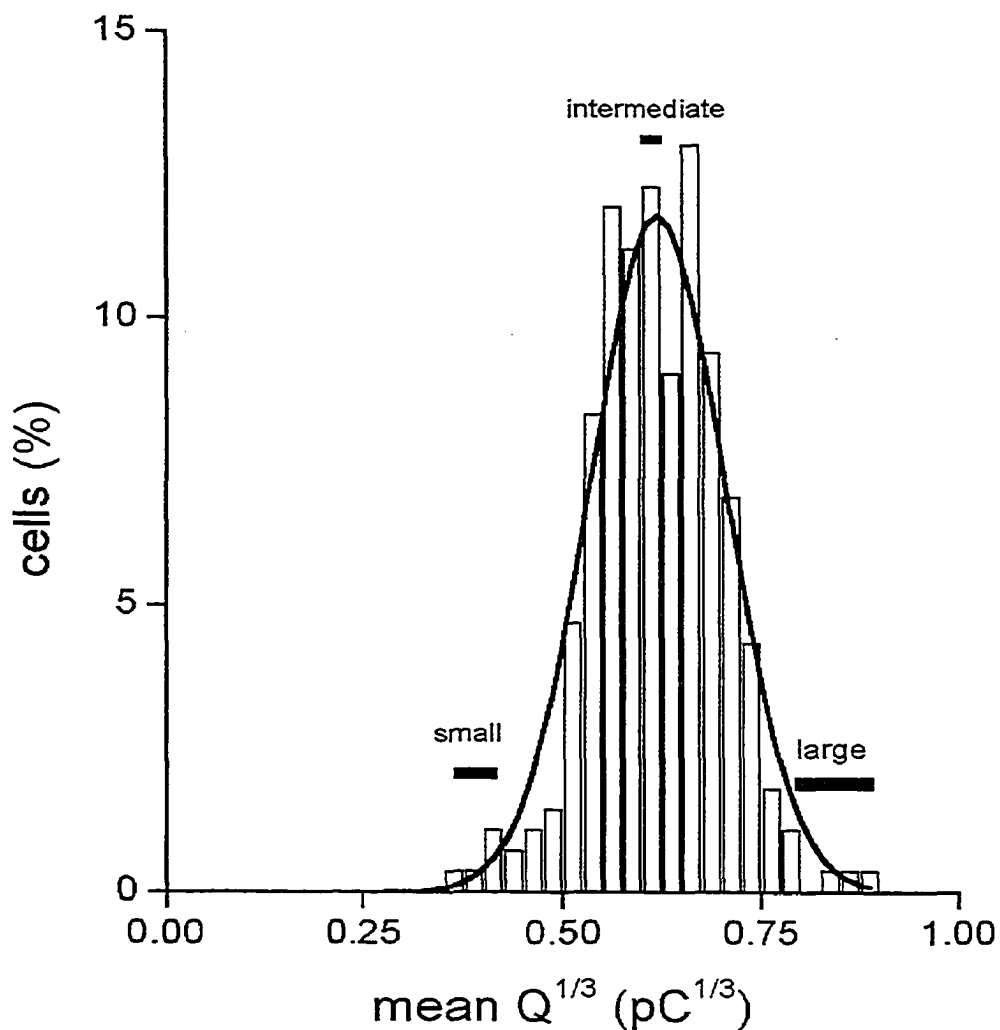


Figure 3-7 Wide range of distribution of the mean of cellular quantal size. Plot of the distribution of mean $Q^{1/3}$ from 277 chromaffin cells cultured under control conditions for 1 day. For each cell, the mean $Q^{1/3}$ was obtained from all amperometric events collected from the same cell. The range of cellular mean $Q^{1/3}$ value for each of the three subsets of cells was shown in Figure 3-8, with $Q^{1/3}$ values that were "small", "intermediate", or "large" denoted by a horizontal bar.

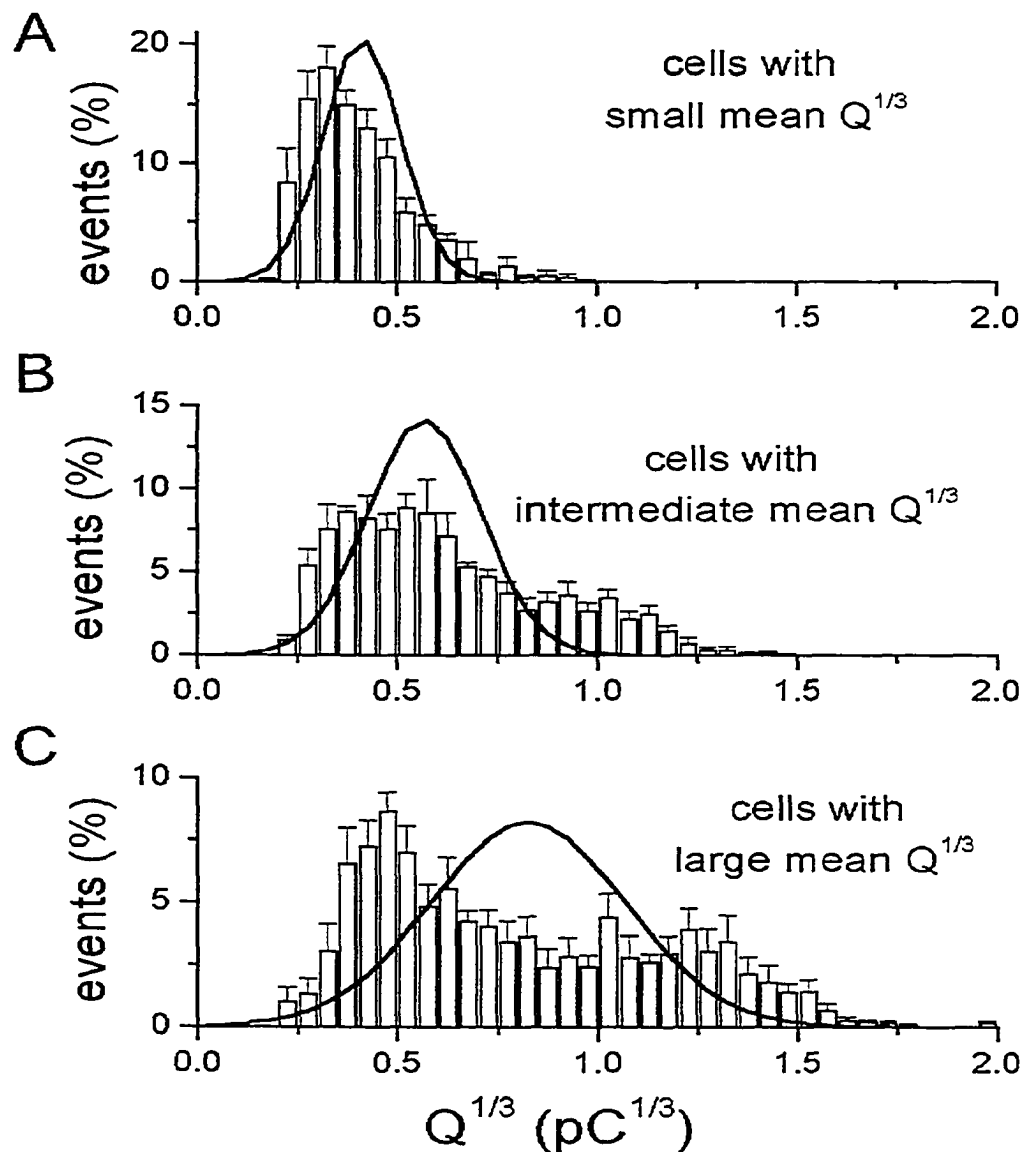


Figure 3-8 Multiple populations of granules were released in the majority of cells. Plots of the distributions of $Q^{1/3}$ from three subsets of control day 1 cells with small mean cellular quantal size (A), intermediate quantal size (B), and large quantal size (C). Each distribution (A - C) was averaged from 5 cells selected from the 3 subsets of cells, whose range in mean cellular $Q^{1/3}$ was shown as one of the three horizontal bars in Figure 3-7. For comparison, the three best-fitted Gaussian distributions from Figure 3-6A with the matched modal value of Q (solid line) were scaled to cover an area of 100% and shown with the corresponding subset. Note that the distribution in (A) could be almost covered by the first Gaussian distribution but the distributions in (B) and (C) were clearly multi-modal.

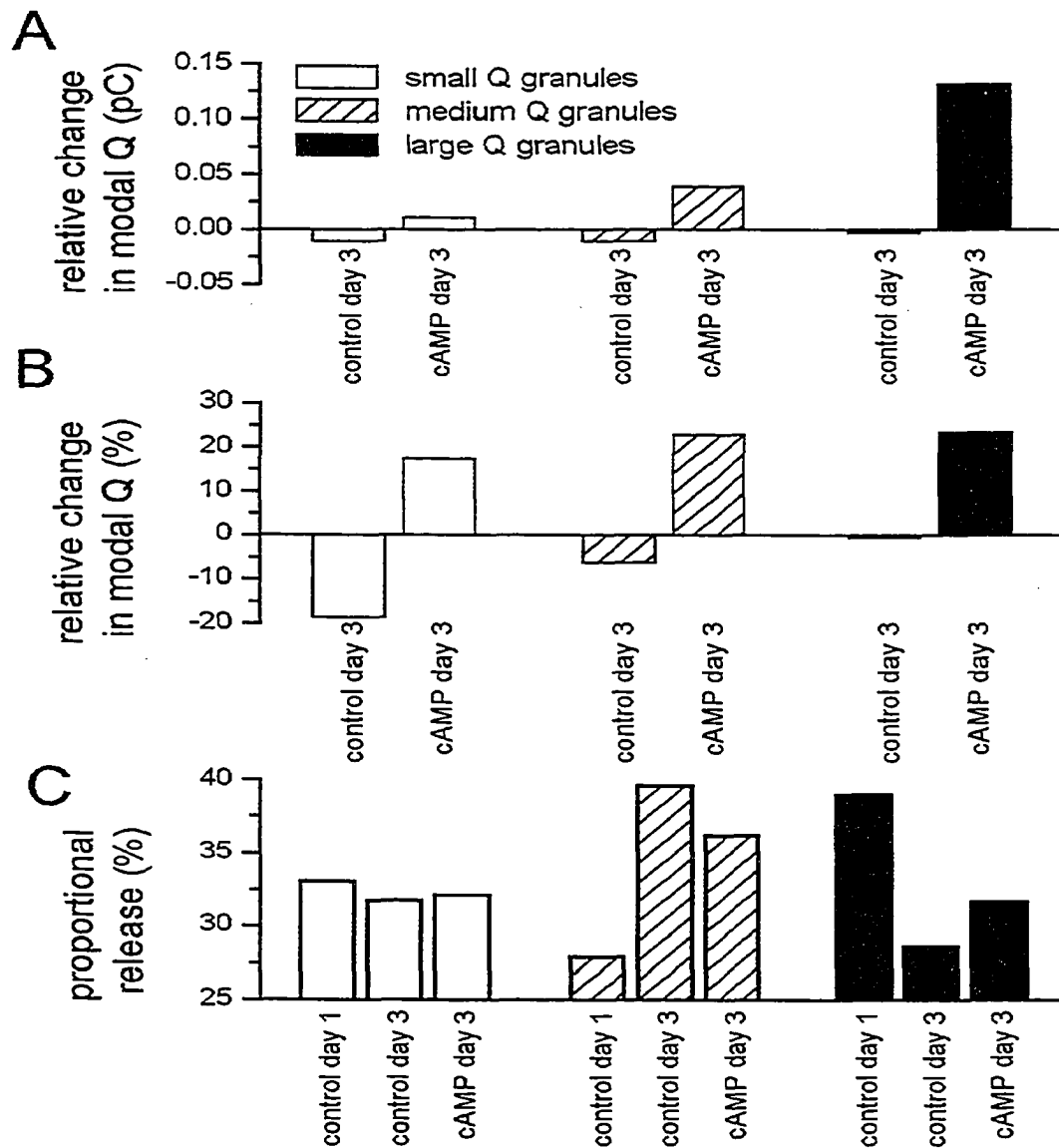


Figure 3-9 Differential regulations of the multiple populations of granules. (A) Plot of the absolute changes in modal quantal size of three granule populations under each condition (relative to control day 1 cells). The modal quantal size of the three granule populations was estimated from the location of the peak of the three best-fitted Gaussian distributions in Figure 3-6. (B) Plot of the percentage changes in modal quantal size of the three granule populations (when compared to control day 1 cells and normalized to the appropriate modal value). (C) Plot of the relative contribution of release from the three granule populations. The proportional release for each granule population was estimated from the fraction of area under each of the best-fitted Gaussian distribution (relative to the summation of the three Gaussian distributions) in Figure 3-6.

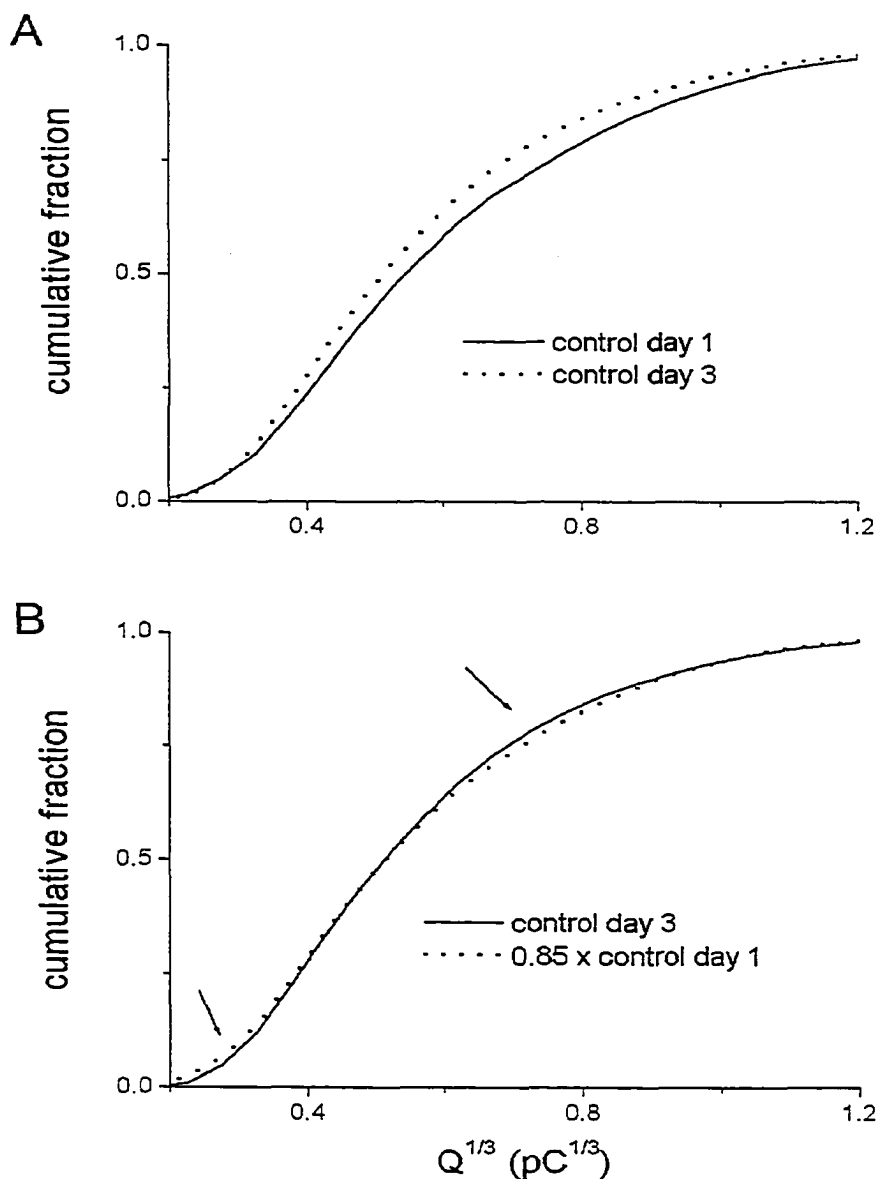


Figure 3-10 The rundown in quantal size during cell culture was not due to a uniform percentage decrease in the quantal size of every granule. (A) Plots of the cumulative distributions of $Q^{1/3}$ for all amperometric events collected from day 1 and day 3 control cells. The two sets of data were very significantly different ($p \ll 0.0001$ in the K-S test). (B) The cumulative histogram generated by uniformly reducing the Q value of all amperometric events from day 1 control cells by 15% was still significantly different from the data of the day 3 control cells ($p < 0.001$ in the K-S test). The arrows denote the two major regions of difference between the simulated distribution and the data from control day 3 cells.

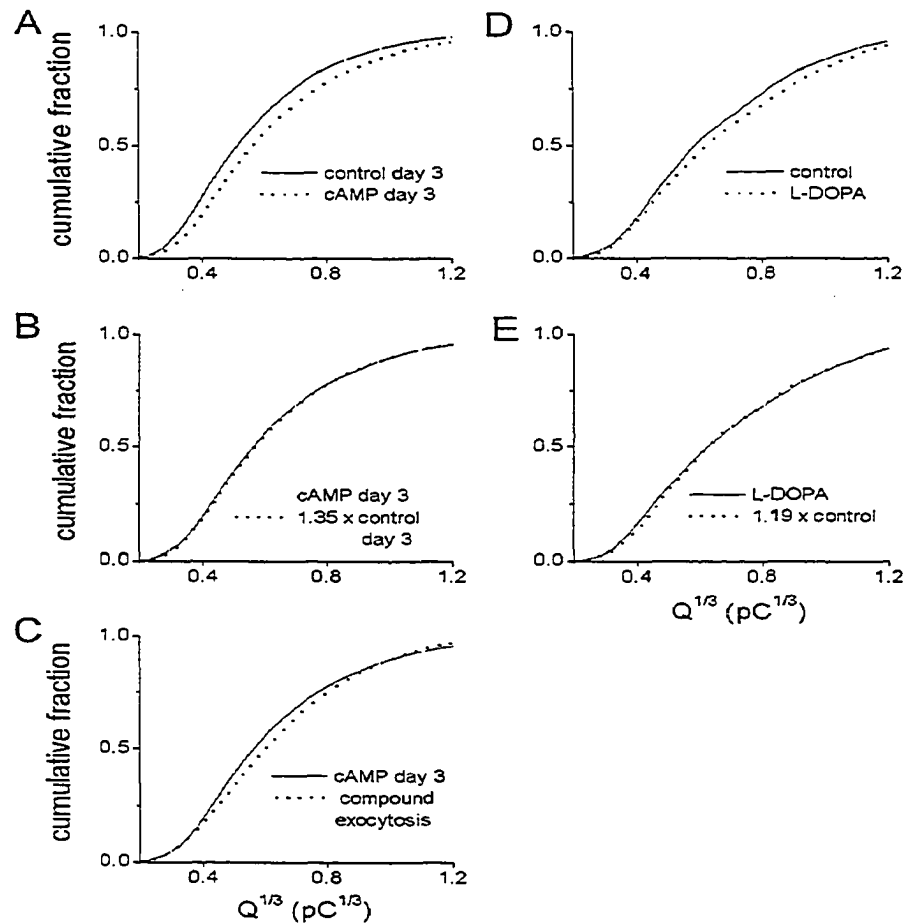


Figure 3-11 The quantal size of every granule was uniformly increased (by ~35%) with 3 days of cAMP treatment. (A) Plots of the cumulative distributions of $Q^{1/3}$ for all amperometric events collected from cells cultured for 3 days under control conditions or in the presence of 1 mM dBcAMP. Note that the two data sets were very significantly different ($p \ll 0.0001$ in the K-S test). (B) The cumulative frequency histogram generated by uniformly increasing the Q value of all amperometric events from day 3 control cells by 35% was not significantly different from the data from cells treated with dBcAMP for 3 days ($p > 0.05$ in the K-S test). (C) The cumulative frequency histogram generated from the simulation of 40% random compound exocytosis among day 3 control cells was significantly different from the data from cells treated with dBcAMP for 3 days ($p < 0.001$ for the K-S test). (D) Plots of the cumulative distributions of $Q^{1/3}$ for all amperometric events collected from cells cultured with L-DOPA (50 μ M) for 1 hour and their time-matched controls. The two data sets were very significantly different ($p \ll 0.0001$ in the K-S test). (E) The cumulative frequency histogram generated by uniformly increasing the Q value of all amperometric events from control cells by 19% was not significantly different from the data from cells treated with L-DOPA ($p > 0.05$ in the K-S test).

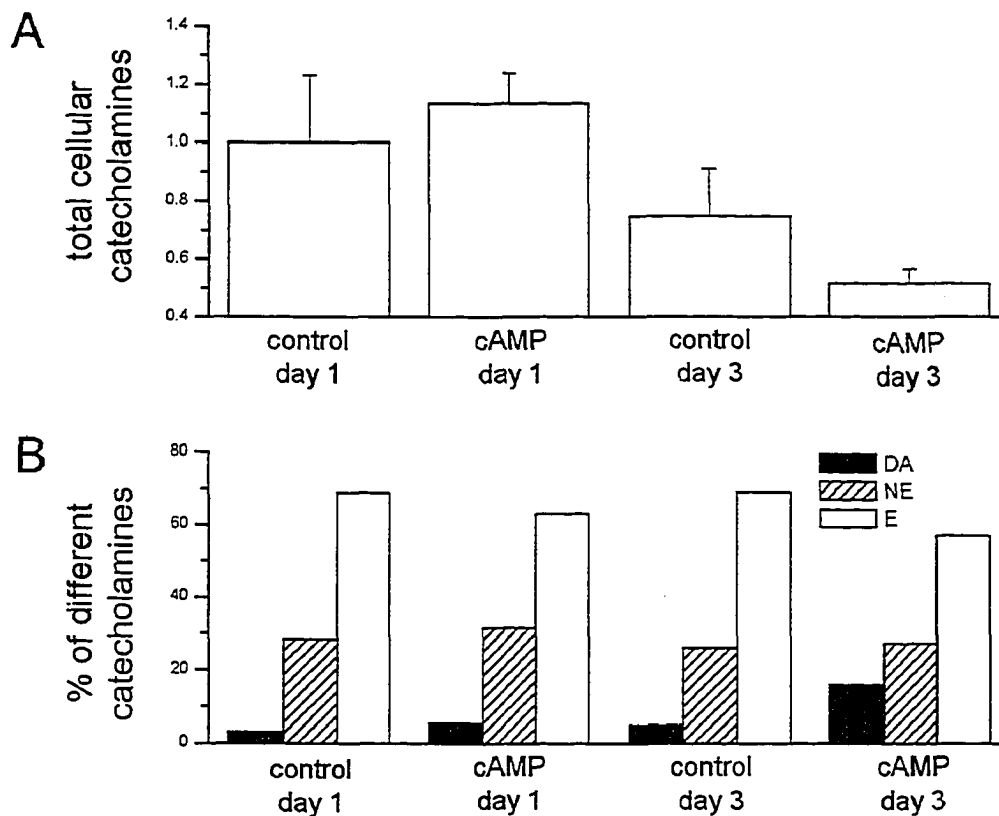


Figure 3-12 Changes in the cellular catecholamine content and the proportion of different catecholamines with culture duration and cAMP. (A) HPLC measurements of the total cellular catecholamine content under different culture conditions. Each value was the average from three cell culture preparations and was normalized to the values from cells cultured for 1 day. For cells treated with dBcAMP for 1 day, there was a small increase in the total cellular catecholamine content. In cells cultured for 3 days (control- or dBcAMP-treated), however, the total cellular catecholamine content was reduced. (B) There was little change in the proportion of the three catecholamines with time of culture or dBcAMP treatment for 1 day. For cells treated with dBcAMP for 3 days, there was an increase in the proportion of DA that was accompanied by a decrease in the proportion of E.

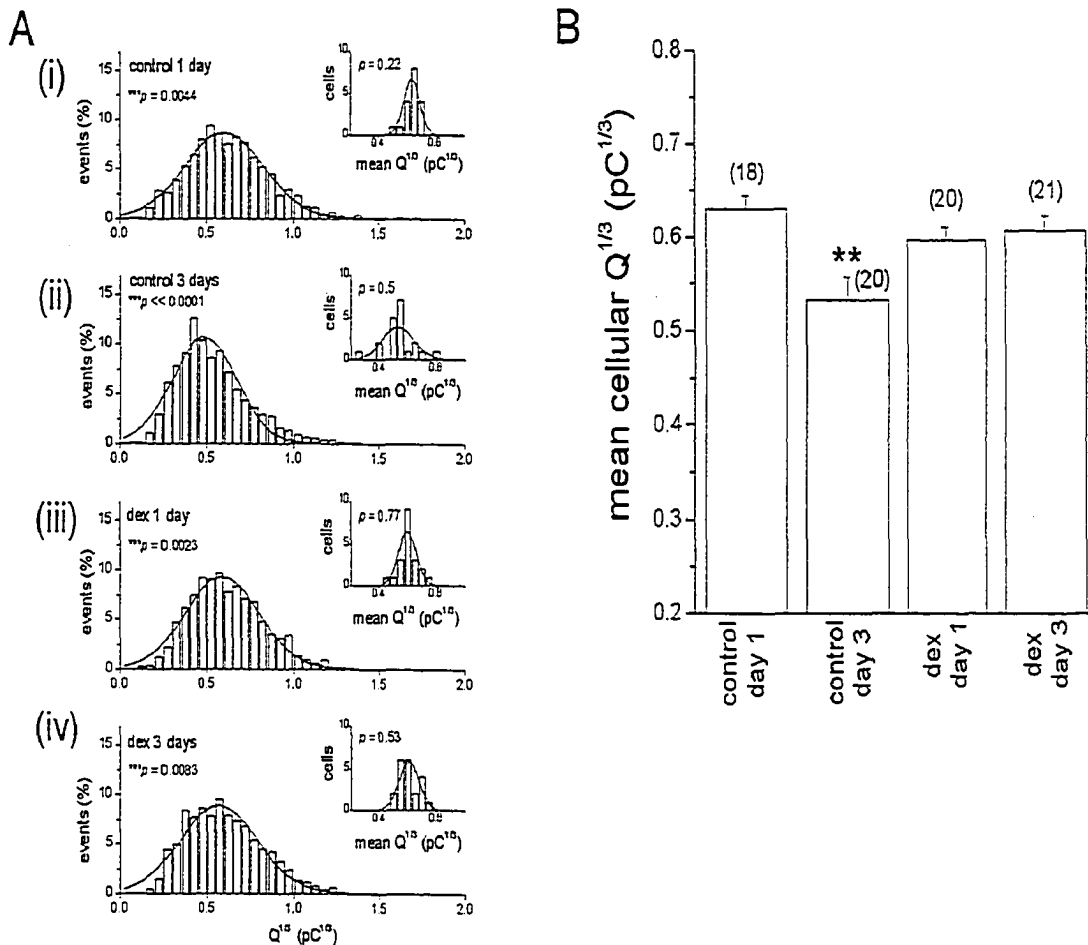


Figure 3-13 The distribution of $Q^{1/3}$ of individual amperometric events deviated significantly from a single Gaussian distribution but not for the distribution of cellular mean $Q^{1/3}$. (A) Distributions of events collected from cells cultured for: (Ai) 1 day (1522 events from 18 cells); (Aii) 3 days (1979 events from 20 cells); (Aiii) 1 day with 1 μM dexamethasone (1841 events from 20 cells); (Aiv) 3 days with 1 μM dexamethasone. Note that each distribution deviated significantly from a single Gaussian distribution (solid line; $p < 0.05$ in the K-S test; marked with asterisk). The inset of each plot shows the distribution of the $Q^{1/3}$ of individual cells in the same treatment group (obtained by averaging the amperometric events collected from individual cells). Note that the distribution of the cellular mean $Q^{1/3}$ values did not deviate from a single Gaussian distribution (solid line; $p > 0.05$ in the K-S test). (B) Mean $Q^{1/3}$ of cells cultured in the absence (control) or presence of dexamethasone (1 μM). The mean $Q^{1/3}$ value that was statistically significant different from control cells cultured for 1 day was marked with **. Note that dexamethasone treatment for 1 day caused no significant effect, but for 3 days, dexamethasone prevented the time-dependent rundown of quantal size. The number of cells for each treatment is shown in brackets.

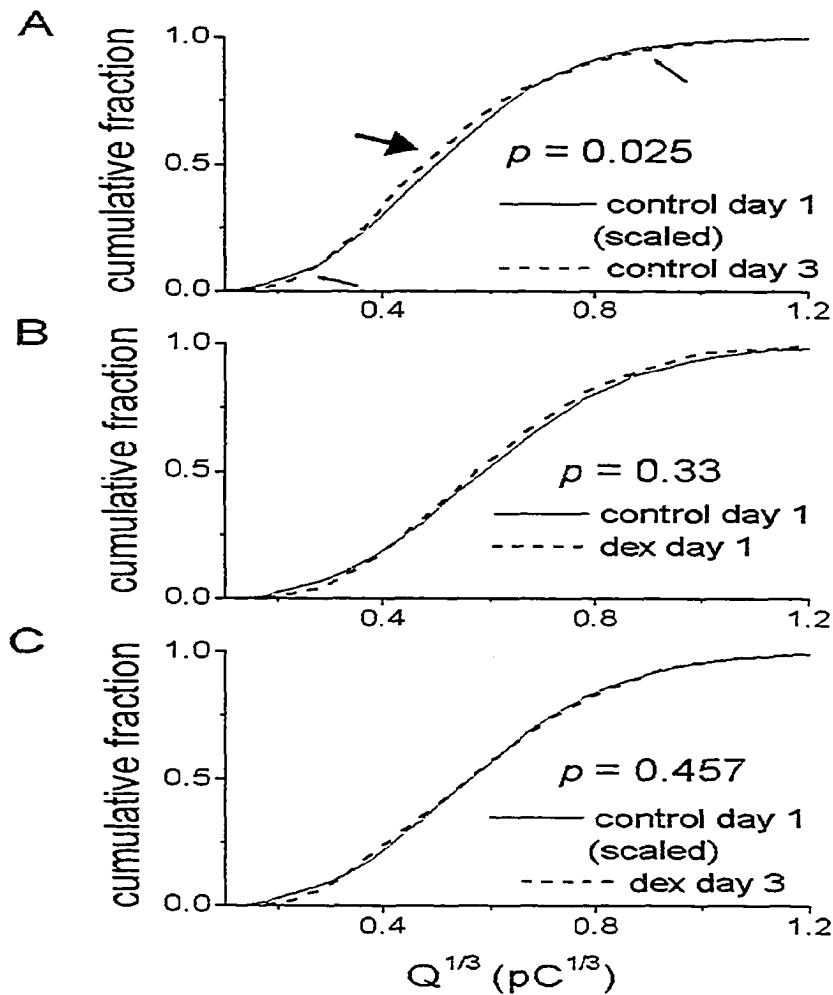


Figure 3-14 Dexamethasone prevented the shift in the proportional release of the granules during rundown. Plots of the cumulative frequency histogram of $Q^{1/3}$ for all amperometric events collected from: control cells cultured for 1 or 3 days (A); cells cultured for 1 day in control condition or in 1 μM dexamethasone (B); cells cultured for 3 days in control condition or in 1 μM dexamethasone (C). For comparison, the Q values in each plot [except for (B)] were matched by scaling the Q value of all amperometric events from control day 1 cells. Note that in (A) there was a shift in the proportional release (denotes by arrows). The thick arrows indicate the region that was critical for the K-S test. Dexamethasone treatment for 1 day did not affect the proportional release of granules (B). In (C), dexamethasone completely prevented the change in proportional release.

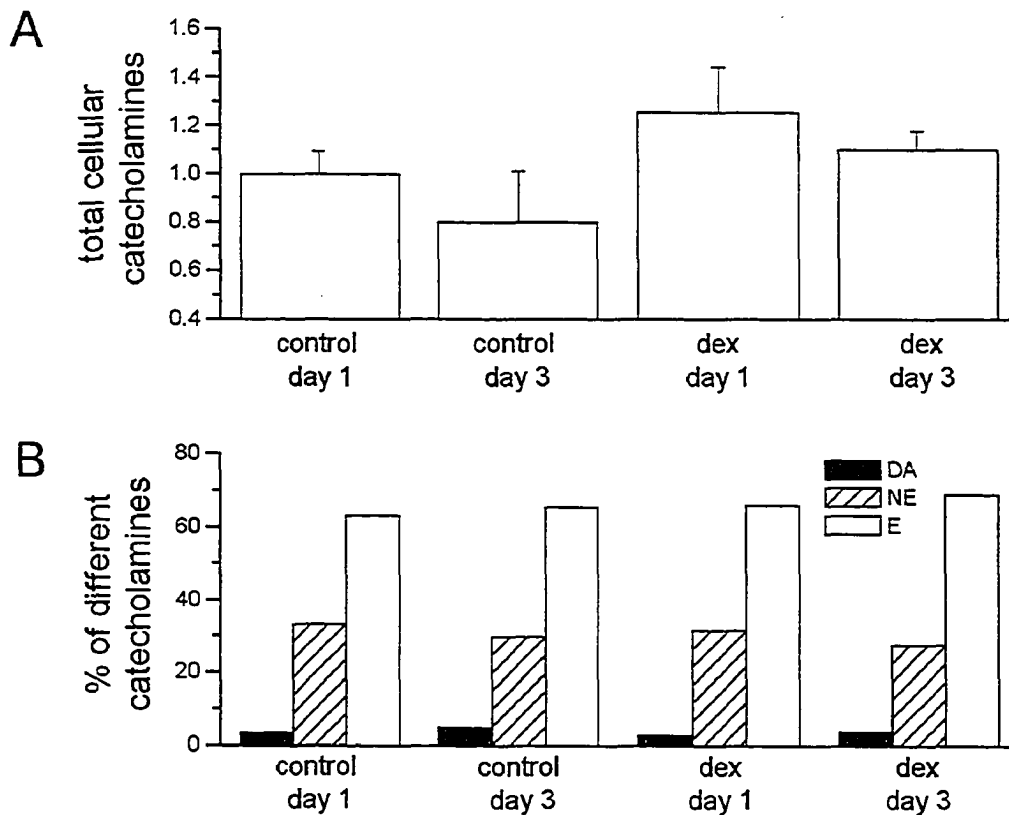


Figure 3-15 Dexamethasone prevented the time-dependent rundown in the cellular catecholamine content without affecting the proportion of the different catecholamines. (A) HPLC measurements of the total cellular catecholamines of rat chromaffin cells under different culture conditions. Each value was the average from three cell culture preparations and was normalized to the values from cells cultured for 1 day. After 3 days of culture, the total cellular catecholamine content was reduced by ~20%. This time-dependent reduction was prevented by dexamethasone (1 μ M). (B) Neither the time of culture nor dexamethasone affected the proportion of DA, NE, and E in the chromaffin cells.

References

- Angleson J. K., Cochilla A. J., Kilic G., Nussinovitch I., and Betz W. J. (1999) Regulation of dense core release from neuroendocrine cells revealed by imaging single exocytic events. *Nature Neuroscience* **2**, 440-446.
- Betito K., Diorio J., Meaney M. J., and Boksa P. (1992) Adrenal phenylethanolamine N-methyltransferase induction in relation to glucocorticoid receptor dynamics - evidence that acute exposure to high cortisol levels is sufficient to induce the enzyme. *Journal of Neurochemistry* **58**, 1853-1862.
- Burgoyne R. D. and Barclay J. W. (2002) Splitting the quantum: regulation of quantal release during vesicle fusion. *Trends in Neurosciences* **25**, 176-178.
- Chow R. H. and von Ruden L. (1995) Electrochemical detection of secretion from single cells, in *Single-Channel Recording* (Sakmann B. and Neher E., eds.), pp. 245-275. Plenum Press, New York.
- Cochilla A. J., Angleson J. K., and Betz W. J. (2000) Differential regulation of granule-to-granule and granule-to-plasma membrane fusion during secretion from rat pituitary lactotrophs. *Journal of Cell Biology* **150**, 839-848.

- Colliver T. L., Hess E. J., Pothos E. N., Sulzer D., and Ewing A. G. (2000a) Quantitative and statistical analysis of the shape of amperometric spikes recorded from two populations of cells. *Journal of Neurochemistry* **74**, 1086-1097.
- Colliver T. L., Pyott S. J., Achalabun M., and Ewing A. G. (2000b) VMAT-mediated changes in quantal size and vesicular volume. *Journal of Neuroscience* **20**, 5276-5282.
- Coupland R. E. (1965) Electron microscopic observations on structure of rat adrenal medulla .I. Ultrastructure and organization of chromaffin cells in normal adrenal medulla. *Journal of Anatomy* **99**, 231-254.
- Coupland R. E. and Hopwood D. (1966) The mechanism of differential staining reaction for adrenaline- and noradrenaline-storing granules in tissues fixed in glutaraldehyde. *Journal of Anatomy* **100**, 227-243.
- Coupland R. E. and Tomlinson A. (1989) The development and maturation of adrenal medullary chromaffin cells of the rat *in vivo*: a descriptive and quantitative study. *International Journal of Developmental Neuroscience* **7**, 419-438.
- Doupe A. J., Landis S. C., and Patterson P. H. (1985) Environmental influences in the development of neural crest derivatives: glucocorticoids, growth-factors, and chromaffin cell plasticity. *Journal of Neuroscience* **5**, 2119-2142.

- Elhamdani A., Brown M. E., Artalejo C. R., and Palfrey H. C. (2000) Enhancement of the dense-core vesicle secretory cycle by glucocorticoid differentiation of PC12 cells: Characteristics of rapid exocytosis and endocytosis. *Journal of Neuroscience* **20**, 2495-2503.
- Elhamdani A., Palfrey H. C., and Artalejo C. R. (2001) Quantal size is dependent on stimulation frequency and calcium entry in calf chromaffin cells. *Neuron* **31**, 819-830.
- Finnegan J. M., Pihel K., Cahill P. S., Huang L., Zerby S. E., Ewing A. G., Kennedy R. T., and Wightman R. M. (1996) Vesicular quantal size measured by amperometry at chromaffin, mast, pheochromocytoma, and pancreatic beta-cells. *Journal of Neurochemistry* **66**, 1914-1923.
- Fisher R. J., Pevsner J., and Burgoyne R. D. (2001) Control of fusion pore dynamics during exocytosis by Munc18. *Science* **291**, 875-878.
- Glavinovic M. I., Vitale M. L., and Trifaro J. M. (1998) Comparison of vesicular volume and quantal size in bovine chromaffin cells. *Neuroscience* **85**, 957-968.
- Gong L. W., Hafez I., de Toledo G. A., and Lindau M. (2003) Secretory vesicles membrane area is regulated in tandem with quantal size in chromaffin cells. *Journal of Neuroscience* **23**, 7917-7921.
- Hodel A. (2001) Effects of glucocorticoids on adrenal chromaffin cells. *Journal of Neuroendocrinology* **13**, 217-221.

- Honma K. I., Honma S., and Hiroshige T. (1984) Feeding-associated corticosterone peak in rats under various feeding cycles. *American Journal of Physiology - Regulatory, Integrative and Comparative Physiology* **246**, R721-R726.
- Hwang O., Kim M. L., and Lee J. D. (1994) Differential induction of gene expression of catecholamine biosynthetic enzymes and preferential increase in norepinephrine by forskolin. *Biochemical Pharmacology* **48**, 1927-1934.
- Kelner K. L. and Pollard H. B. (1985) Glucocorticoid receptors and regulation of phenylethanolamine-N-methyltransferase activity in cultured chromaffin cells. *Journal of Neuroscience* **5**, 2161-2168.
- Koga T. and Takahashi M. (2004) Quantal size of catecholamine release from rat chromaffin cells is regulated by tonic activity of protein kinase A. *Neuroscience Letters* **360**, 145-148.
- Koval L. M., Yavorskaya E. N., and Lukyanetz E. A. (2000) Ultrastructural features of medullary chromaffin cell cultures. *Neuroscience* **96**, 639-649.
- Koval L. M., Yavorskaya E. N., and Lukyanetz E. A. (2001) Electron microscopic evidence for multiple types of secretory vesicles in bovine chromaffin cells. *General and Comparative Endocrinology* **121**, 261-277.

- Kumai T., Asoh K., Tateishi T., Tanaka M., Watanabe M., and Kobayashi S. (1999) Effects of nitric oxide synthase inhibitor on tyrosine hydroxylase mRNA in the adrenal medulla of spontaneously hypertensive and Wistar Kyoto rats. *Nitric Oxide - Biology and Chemistry* **3**, 321-326.
- Kumar G. K., Overholt J. L., Bright G. R., Hui K. Y., Lu H. W., Gratzl M., and Prabhakar N. R. (1998) Release of dopamine and norepinephrine by hypoxia from PC12 cells. *American Journal of Physiology - Cell Physiology* **43**, C1592-C1600.
- Levitt M., Spector S., Sjoerdsma A., and Udenfriend S. (1965) Elucidation of rate-limiting step in norepinephrine biosynthesis in perfused guinea-pig heart. *Journal of Pharmacology and Experimental Therapeutics* **148**, 1-7.
- Machado J. D., Morales A., Gomez J. F., and Borges R. (2001) cAMP modulates exocytotic kinetics and increases quantal size in chromaffin cells. *Molecular Pharmacology* **60**, 514-520.
- Machado J. D., Segura F., Briosio M. A., and Borges R. (2000) Nitric oxide modulates a late step of exocytosis. *Journal of Biological Chemistry* **275**, 20274-20279.
- Mosharov E. V., Gong L. W., Khanna B., Sulzer D., and Lindau M. (2003) Intracellular patch electrochemistry: regulation of cytosolic catecholamines in chromaffin cells. *Journal of Neuroscience* **23**, 5835-5845.

- Nakanishi N., Onozawa S., Matsumoto R., Hasegawa H., and Yamada S. (1995) Cyclic AMP-dependent modulation of vesicular monoamine transport in pheochromocytoma cells. *Journal of Neurochemistry* **64**, 600-607.
- Nordmann J. J. (1984) Combined stereological and biochemical analysis of storage and release of catecholamines in the adrenal medulla of the rat. *Journal of Neurochemistry* **42**, 434-437.
- Pihel K., Schroeder T. J., and Wightman R. M. (1994) Rapid and selective cyclic voltammetric measurements of epinephrine and norepinephrine as a method to measure secretion from single bovine adrenal medullary cells. *Analytical Chemistry* **66**, 4532-4537.
- Plattner H., Artalejo A. R., and Neher E. (1997) Ultrastructural organization of bovine chromaffin cell cortex - analysis by cryofixation and morphometry of aspects pertinent to exocytosis. *Journal of Cell Biology* **139**, 1709-1717.
- Pothos E. N., Larsen K. E., Krantz D. E., Liu Y., Haycock J. W., Setlik W., Gershon M. D., Edwards R. H., and Sulzer D. (2000) Synaptic vesicle transporter expression regulates vesicle phenotype and quantal size. *Journal of Neuroscience* **20**, 7297-7306.
- Pothos E. N., Mosharov E., Liu K. P., Setlik W., Haburcak M., Baldini G., Gershon M. D., Tamir H., and Sulzer D. (2002) Stimulation-dependent regulation of the pH, volume and quantal size of bovine and rodent secretory vesicles. *Journal of Physiology - London* **542**, 453-476.

- Pothos E. N., Przedborski S., Davila V., Schmitz Y., and Sulzer D. (1998) D₂-like dopamine autoreceptor activation reduces quantal size in PC12 cells. *Journal of Neuroscience* **18**, 5575-5585.
- Radomski M. W., Palmer R. M. J., and Moncada S. (1990) Glucocorticoids inhibit the expression of an inducible, but not the constitutive, nitric oxide synthase in vascular endothelial cells. *Proceedings of the National Academy of Sciences of the United States of America* **87**, 10043-10047.
- Raum W. J. (1997) Adrenal medulla, in *Endocrinology: Basic and Clinical Principles* (Conn P. M. and Melmed S., eds.), pp. 377-392. Humana Press, Totowa, NJ.
- Reimer R. J., Fon E. A., and Edwards R. H. (1998) Vesicular neurotransmitter transport and the presynaptic regulation of quantal size. *Current Opinion in Neurobiology* **8**, 405-412.
- Rozansky D. J., Wu H. J., Tang K. C., Parmer R. J., and Oconnor D. T. (1994) Glucocorticoid activation of chromogranin A gene expression. Identification and characterization of a novel glucocorticoid response element. *Journal of Clinical Investigation* **94**, 2357-2368.
- Sargent R. N. (1985) Determination of corticosterone in rat plasma by HPLC. *Journal of Analytical Toxicology* **9**, 20-23.

- Schwarz P. M., RodriguezPascual F., Koesling D., Torres M., and Forstermann U. (1998) Functional coupling of nitric oxide synthase and soluble guanylyl cyclase in controlling catecholamine secretion from bovine chromaffin cells. *Neuroscience* **82**, 255-265.
- Tang K. S., Tse A., and Tse F. W. (2005) Differential regulation of multiple populations of granules in rat adrenal chromaffin cells by culture duration and cyclic AMP. *Journal of Neurochemistry* **92**, 1126-1139.
- Tank A. W., Ham L., and Curella P. (1986) Induction of tyrosine hydroxylase by cyclic AMP and glucocorticoids in a rat pheochromocytoma cell line: effect of the inducing agents alone or in combination on the enzyme levels and rate of synthesis of tyrosine hydroxylase. *Molecular Pharmacology* **30**, 486-496.
- Tischler A. S., Perlman R. L., Nunnemacher G., Morse G. M., Delellis R. A., Wolfe H. J., and Sheard B. E. (1982) Long-term effects of dexamethasone and nerve growth factor on adrenal medullary cells cultured from young adult rats. *Cell and Tissue Research* **225**, 525-542.
- Torres M., Ceballos G., and Rubio R. (1994) Possible role of nitric oxide in catecholamine secretion by chromaffin cells in the presence and absence of cultured endothelial cells. *Journal of Neurochemistry* **63**, 988-996.

- Uchiyama Y., Morita K., Kitayama S., Suemitsu T., Minami N., Miyasako T., and Dohi T. (1994) Possible involvement of nitric oxide in acetylcholine-induced increase of intracellular Ca^{2+} concentration and catecholamine release in bovine adrenal chromaffin cells. *Japanese Journal of Pharmacology* **65**, 73-77.
- Unsworth B. R., Hayman G. T., Carroll A., and Lelkes P. I. (1999) Tissue-specific alternative mRNA splicing of phenylethanolamine N-methyltransferase (PNMT) during development by intron retention. *International Journal of Developmental Neuroscience* **17**, 45-55.
- Wightman R. M., Jankowski J. A., Kennedy R. T., Kawagoe K. T., Schroeder T. J., Leszczyszyn D. J., Near J. A., Diliberto E. J., and Viveros O. H. (1991) Temporally resolved catecholamine spikes correspond to single vesicle release from individual chromaffin cells. *Proceedings of the National Academy of Sciences of the United States of America* **88**, 10754-10758.
- Xu J., Tang K. S., Lu V. B., Weerasinghe C. P., Tse A., and Tse F. W. (2005) Maintenance of quantal size and immediately releasable granules in rat chromaffin cells by glucocorticoid. *American Journal of Physiology-Cell Physiology* doi:10.1152/ajpcell.00514.2004.
- Zerby S. E. and Ewing A. G. (1996) The latency of exocytosis varies with the mechanism of stimulated release in PC12 cells. *Journal of Neurochemistry* **66**, 651-657.

CHAPTER 4

Changes in the Kinetics of Quantal Catecholamine Release with Quantal Size and Elevation of Cyclic AMP

4.1 Introduction

The amount of chemical messenger that is released via the exocytosis of individual vesicles or granules (i.e. quantal size; Q) can be regulated by the synthesis and packaging of chemical messenger (Sulzer and Pothos 2000), as well as the kinetics of fusion pore opening/closure (Burgoyne and Barclay 2002) and the granule matrix dissolution/expansion (Amatore *et al.* 2000). Indeed, many experimental manipulations [e.g. brefeldin A, cysteine string protein, cyclic AMP (cAMP), entry of extracellular Ca^{2+} , munc-18, catecholamine precursor, complexin, protein kinase C, and vesicular volume] resulted in changes in both the quantal size and kinetics (Xu and Tse 1999; Graham and Burgoyne 2000; Elhamdani *et al.* 2001; Fisher *et al.* 2001; Machado *et al.* 2001; Archer *et al.* 2002; Pothos 2002; Sombers *et al.* 2004; Staal *et al.* 2004). However, the precise interpretation of such simultaneous changes is complicated by the fact that the kinetics of quantal release can be significantly influenced by the vesicular size, and hence the quantal size (Alvarez de Toledo *et al.* 1993; Bruns and Jahn 1995; Sombers *et al.* 2004). A classical comparison of amperometric events involved three different cell models: mast cells from beige mice and normal rats, and chromaffin cells from the bovine adrenal medulla (Alvarez de Toledo *et al.* 1993). This comparison suggests that the vesicular radius of dense core granules strongly influences the quantal kinetics. A similar comparison was extended to the small synaptic vesicles and the large dense core granules from Retzius cells of the leech (Bruns and Jahn 1995). Both studies showed that amperometric

events with a larger Q tend to have slower kinetics. A recent study on rat pheochromocytoma (PC12) cells (Sombers *et al.* 2004) has also reported that increasing the value of Q pharmacologically resulted in an increase in the duration of the foot signals (which reflect the leakage of neurotransmitter from an opened, but minimally dilated fusion pore). In contrast, the frequency of events with a foot signal and the fractional release of catecholamines during the foot signal decreased as the quantal size increased (Sombers *et al.* 2004). Overall, the above studies suggest that granules with a larger Q have a longer duration of foot signals, a longer half-width of the main amperometric spikes (which reflects the rapid release from the granule matrix) but a smaller fractional release during the foot signal.

The chromaffin cell is a popular model for the study of quantal catecholamine release from dense core granules. We have shown in Chapter 3 that rat chromaffin cells release granules with a large range of Q (Tang *et al.* 2005). This range of Q arose from the exocytosis of large dense core granules (100 - 700 nm diameter) (Plattner *et al.* 1997; Koval *et al.* 2001) and perhaps also of some small dense core granules (100 - 230 nm in diameter, found in 1 - 5% of the cells) (Kobayashi *et al.* 1978). The relationship between the quantal size and the kinetics of amperometric events in this cell type has not been documented in detail, except for an early study (Wightman *et al.* 1995) that showed a weak correlation for some key parameters (e.g. between the half-width duration and the amplitude or Q) and a very recent study (Amatore *et al.* 2005) that focused mainly on the foot signals. Here, we exploited the natural variations

in the quantal size among individual granules of rat chromaffin cells to examine in detail the correlation between the quantal size and the kinetics of release. An increase in cellular cAMP level has been reported to cause dramatic slowing of the main amperometric spikes in bovine chromaffin cells (Machado *et al.* 2001). However, in Chapter 3, we found that elevation of cAMP in rat chromaffin cells increased the quantal size of every amperometric event by a fixed percentage (35%) (Tang *et al.* 2005). This finding raises the question of whether cAMP directly affects the kinetics of quantal release or indirectly slows the release kinetics via an increase in the quantal size. Here we addressed this issue by examining the effect of cAMP on the kinetics of release in granules with matched values of quantal size.

4.2 Results

4.2.1 Influence of quantal size and cAMP on the foot signals

When rat chromaffin cells were stimulated by bath perfusion with 50 mM KCl, non-overlapping amperometric events of diverse quantal size and kinetics could be observed (Figure 4-1). The amplitude of the events ranged from 2.4 to 650 pA. In some of the events, the main amperometric spike was preceded by a conspicuous foot signal (e.g. Figures 4-1B, C, and E). In this study, the existence of a foot signal for each event was identified with the criteria of the Mini Analysis Program (Synaptosoft), which is the existence of an "inflection" (calculated from the second derivative of the signal) during the rising phase. By definition, the

rising phase of an event is the duration between the beginning and the peak of that event. Procedurally, the beginning of an event was determined by searching backward in time from the peak to the first data point that crosses the calculated baseline (depicted as the circle symbol in Figure 4-1). By definition, the inflection represents the transition between the end of the foot signal (depicted as the square symbol in Figure 4-1) and the onset of the main amperometric spike. Note that although the events shown in Figures 4-1D and E had a similar amplitude and quantal size, the foot signal in Figure 4-1E had a much longer duration. In fact, the foot signal for the large Q event in Figure 4-1D was so short and large that (at least with the time scale of Figure 4-1) the transition to the main amperometric spike was less conspicuous than the foot signal in the event with a much smaller Q shown in Figure 4-1B. The above comparisons suggest that the detection of the foot signal by mathematical criteria is overall more rigorous, because with visual inspection, the existence of an obvious inflection depends on the choice of the time scale.

Because our amperometric events were low passed at 1 kHz, it was uncertain whether the foot duration of ≤ 1 ms could be measured reliably. Therefore, we initially classified an event with a foot signal only when the duration of the foot signal was > 1 ms. With the above criterion, in a group of 60 control cells (cultured for 3 days in defined medium), ~74% of the events ($n = 11$ 225) was found to be associated with a foot signal. The frequency of events with a foot signal at different cube-root of quantal size ($Q^{1/3}$) for this group of control cells was plotted in Figure 4-2A. In this plot, the data set was first sorted with an

ascending value of $Q^{1/3}$, and each point denotes the frequency of events with a foot signal (averaged from 300 amperometric events) and the corresponding mean value of $Q^{1/3}$. Note that the frequency of events with a foot signal increased with the value of $Q^{1/3}$. For the events with mean $Q^{1/3}$ of $\sim 0.3 \text{ pC}^{1/3}$, only $\sim 40\%$ of the events had a foot signal (Figure 4-2A). For the events with mean $Q^{1/3}$ value of $\geq 0.6 \text{ pC}^{1/3}$, the frequency of events with a foot signal increased to $\sim 75\%$ (Figure 4-2A). The distributions of $Q^{1/3}$ for the events with ($n = 8278$) or without ($n = 2947$) a foot signal for the same group of control cells were plotted in Figures 4-2B and C, respectively. Note that the distribution of $Q^{1/3}$ for the events with a foot signal (Figure 4-2B) was skewed to larger values of $Q^{1/3}$ when compared to the distribution of events without a foot signal (Figure 4-2C). The above results show that a foot signal could be detected in the events with small Q , and the vast majority of events with medium and large Q had a foot signal.

In the above analysis, because the criterion of foot duration $> 1 \text{ ms}$ was employed to classify the events with a foot signal, we specifically examined whether changing the criterion between 0 and 3 ms changed any of the trends in Figure 4-2. As expected, when the criterion for minimum duration of the foot signal was increased, there was a small decrease in the frequency of events with a foot signal for each data set (data not shown). However, the magnitude of change was very small and did not alter any of the trends shown in Figure 4-2. Therefore, the criterion of foot duration $> 1 \text{ ms}$ was adopted for all subsequent analysis.

To further examine the correlation between the quantal size and the foot signal, we tested whether the frequency of amperometric events with a foot signal in rat chromaffin cells could be altered when the Q values of granules were increased with pharmacological manipulation of cAMP. In Chapter 3, we have shown that treatment with dibutyryl cyclic-AMP (dBcAMP; 1 mM) for 3 days increased the mean cellular quantal size by ~35% when compared with time-matched controls (Tang *et al.* 2005). Therefore, in this study, we elevated the cAMP level in rat chromaffin cells by incubating the cells with dBcAMP (1 mM) or with forskolin (10 μ M) for 3 days. The comparisons between dBcAMP-treated cells and their time-matched controls were shown in Figures 4-2A - C. The comparisons between the forskolin-treated cells and their corresponding time-matched controls were shown in Figures 4-2D - F. In 60 cells treated with dBcAMP, the frequency of events detected with a foot signal (72% of 10 777 events) was similar to the controls (74%). For the 30 cells treated with forskolin, the foot signal was detected in 58% of the 5466 events collected, similar to that of controls (63% of 6642 events; 30 cells). Figures 4-2A and D show that elevation of cAMP did not affect the general trend of increase in the frequency of events (with a foot signal) with $Q^{1/3}$ value. However, there might be a small reduction in the frequency of events with a foot signal in cells treated with forskolin (Figure 4-2D). Note that cAMP elevation shifted the distributions of the events (with or without a foot signal) toward larger values of $Q^{1/3}$ (Figures 4-2B, C, E, and F). This result is consistent with the finding in Chapter 3 that elevation

of cAMP caused a general increase in the quantal size of every granule in rat chromaffin cells (Tang *et al.* 2005).

Previous amperometric studies (Alvarez de Toledo *et al.* 1993; Sombers *et al.* 2004) have shown that an increase in quantal size was generally associated with an increase in the duration of the foot signals. We found that this trend was also robust in the events with a foot signal in rat chromaffin cells over the entire range of $Q^{1/3}$ (Figures 4-3). A similar trend was also observed when all events (with or without a detectable foot signal) were included in the analysis (data not shown). We arbitrarily selected five different ranges of $Q^{1/3}$ (denoted by the bars in the Figure 4-3) and plotted the distribution of the foot duration from these five groups of events (with matched ranges of $Q^{1/3}$) in Figure 4-4. Note that the distribution of the foot duration at any particular range of $Q^{1/3}$ deviated significantly from Gaussian. For the events with small mean $Q^{1/3}$ ($\leq 0.4 \text{ pC}^{1/3}$), neither dBcAMP (Figures 4-4A and B) nor forskolin (Figures 4-4F and G) affected the distribution of the foot duration. For the events with mean $Q^{1/3} \geq 0.6 \text{ pC}^{1/3}$, both dBcAMP (Figures 4-4C - E) and forskolin (Figures 4-4H - J) shifted the distribution of the foot duration to smaller values. Since the distribution of the foot duration was not Gaussian and therefore could not be compared with simple parametric statistics, we applied the K-S test to compare the distribution of the foot duration between the cAMP-elevated cells and their time-matched controls. The results of the K-S test are summarized in Figure 4-3 as asterisks (***) for significant difference at the level of $p < 0.001$) at the relevant mean value of $Q^{1/3}$. Note that the most significant differences were found at mean values of $Q^{1/3} \geq 0.6$

$\text{pC}^{1/3}$ for the cells treated with dBcAMP (Figure 4-3A) or forskolin (Figure 4-3B). The above result suggests that the main effect of cAMP elevation was a reduction in the mean duration of the foot signal for the events with $Q^{1/3} \geq 0.6 \text{ pC}^{1/3}$. We also found that the cAMP-mediated reduction in the duration of the foot signals at different values of $Q^{1/3}$ was accompanied by a parallel decrease in the time integral (i.e. the charge) of the foot signals (data not shown), suggesting that cAMP elevation did not affect other aspects of the foot signals (e.g. the amplitude or its overall rate of change).

Since the quantal size affects both the frequency and the duration of the foot signals (Figures 4-2 and 4-3), we examined how the fractional release during the foot signal (relative to the entire amperometric event) was influenced by the quantal size. Figure 4-5 shows the mean values of the fractional release during the foot signal over a range of $Q^{1/3}$. For both sets of control data (Figures 4-5A and B), the fractional release during the foot signal decreased by ~2-fold (from > 15% to < 10 %) when the mean value of $Q^{1/3}$ increased from ~0.3 to ~0.6 $\text{pC}^{1/3}$. At mean values of $Q^{1/3} > 0.6 \text{ pC}^{1/3}$, however, the fractional release during the foot signal increased with $Q^{1/3}$. To examine the effect of cAMP elevation on the fractional release during the foot signal, we plotted in Figure 4-6, the distribution of the fractional release during the foot signal from the events selected from five different ranges of $Q^{1/3}$ (denoted by the bars in Figure 4-5). Note that for the events with mean $Q^{1/3} \geq 0.6 \text{ pC}^{1/3}$, elevation of cAMP shifted the distribution of the fractional release during the foot signal to smaller values (Figures 4-6C – E, and H - J). Therefore, the main effect of cAMP elevation was a shift in the

distribution of the fractional release during the foot signal at mean $Q^{1/3} \geq 0.6 \text{ pC}^{1/3}$ (Figure 4-5). Interestingly, at this range of $Q^{1/3}$, elevation of cAMP also significantly shortened the duration of the foot signals (Figure 4-3). Thus, this result is consistent with the possibility that the shortening of the foot duration by cAMP contributed significantly to the reduction in the fractional release during the foot signal.

4.2.2 Influence of quantal size and cAMP on the main amperometric spikes

To examine the influence of quantal size on the kinetics of the main amperometric spikes, we plotted the mean half-width duration of all events (with or without a foot signal) as a function of $Q^{1/3}$ for both sets of control cells (Figures 4-7A and D). Note that when the mean value of $Q^{1/3}$ was $< 0.6 \text{ pC}^{1/3}$, the half-width of the main amperometric spikes increased almost linearly with $Q^{1/3}$ (Figures 4-7A and D). At larger mean $Q^{1/3}$ values, the half-width of the main amperometric spikes stayed near a plateau value of ~6 - 7 ms. A similar trend was observed when the analysis was restricted to events with a foot signal (Figures 4-7B and E). Interestingly, when the analysis included only events without a foot signal, the half-width of the main amperometric spikes increased monotonically with the entire range of $Q^{1/3}$ (Figures 4-7C and F). To further examine whether there was any fundamental difference between the events with a foot signal and those without a foot signal, in Figures 4-8A – E we plotted the distribution of half-width of these events at five selected ranges of $Q^{1/3}$ (denoted by the bars in Figures 4-7B and C). Note that Figures 4-8D and E did not include

the distribution of events without a foot signal because there were too few of such signals with $Q^{1/3} > 0.7 \text{ pC}^{1/3}$. As shown in Figures 4-8A - C, the distribution of events without a foot signal shifted to larger values of half-width as the value of $Q^{1/3}$ increased. For the events with a foot signal (Figures 4-8A - E), the pattern of change in the distribution with increasing $Q^{1/3}$ was very different. When the mean $Q^{1/3}$ increased from 0.3 to 0.6 $\text{pC}^{1/3}$ (Figures 4-8A - C), there was a reduction in the contribution of events with a short half-width (e.g. $< 5 \text{ ms}$) and it was accompanied by a spread of the right-end of the distribution to larger values of half-width. For the events with mean $Q^{1/3}$ between 0.6 and 1.0 $\text{pC}^{1/3}$ (Figures 4-8C - E), the overall change in the distribution of half-width was small. The only measurable trend was that as the mean value of $Q^{1/3}$ became progressively larger than 0.6 $\text{pC}^{1/3}$, there were slightly fewer events with half-width $\sim 10 - 15 \text{ ms}$, and the maximum value of half-width also became larger. This pattern of change allowed the half-width to remain at essentially a plateau value at $Q^{1/3} > 0.6 \text{ pC}^{1/3}$ (Figures 4-7B and E), although the distribution for the half-width clearly had a longer right-skewed tail in Figures 4-8C - E as the value of Q increased.

In Figures 4-7A and D, we examined the effect of cAMP elevation on the half-width of the main amperometric spikes when all events (with or without a foot) were considered. In general, elevation of cAMP did not affect the relationship between the half-width and $Q^{1/3}$. However, at mean $Q^{1/3}$ of $\sim 0.6 \text{ pC}^{1/3}$, the mean half-width was slightly increased in the forskolin-treated cells (Figure 4-7D). When the events with a foot signal were analyzed separately from the events without a foot signal, cAMP elevation did not appear to have any

appreciable effect on the half-width of the events without a foot signal (Figure 4-7C and F). For the events with a foot signal, the cAMP-elevated cells appear to have a slightly longer half-width for events with larger $Q^{1/3}$ ($\geq 0.6 \text{ pC}^{1/3}$). In Figure 4-9, we compared the distributions of half-width (at selected ranges of $Q^{1/3}$) from the events with a foot signal between the cAMP-elevated cells and their time-matched controls. Note that cAMP elevation caused a significant effect only at the distribution with mean $Q^{1/3}$ of $\sim 0.6 \text{ pC}^{1/3}$ (Figures 4-9C and H). At this range of $Q^{1/3}$ both dBcAMP and forskolin reduced the contribution of events with a small half-width (e.g. $< 2.5 \text{ ms}$) and increased the contribution of events with an intermediate half-width (e.g. $5 - 10 \text{ ms}$). The above analysis shows that the main effect of cAMP elevation on the main spike of events with a foot signal was a small increase in the half-width, but this was significant only for the events with mean $Q^{1/3}$ of $\sim 0.6 \text{ pC}^{1/3}$ (summarized in Figures 4-7B and E). On the other hand, as shown in Figure 4-10, elevation of cAMP did not affect the distribution of half-width for the events without a foot signal at any value of $Q^{1/3}$.

4.3 Discussion

4.3.1 *Correlation between the release kinetics and quantal size*

Our results indicate that among rat chromaffin granules, quantal size can strongly affect the kinetics of the foot signals as well as the main amperometric spikes. In our study, $\sim 58 - 74\%$ of the amperometric events had a foot signal. The frequency of events with a foot signal is similar to early studies which

reported the presence of a foot signal in ~80 - 90% of the events (with amplitudes > 20 pA) in bovine chromaffin cells (Chow *et al.* 1992) and PC12 cell (Wang *et al.* 2001). As reported in bovine chromaffin cells (Amatore *et al.* 2005), the values of $Q^{1/3}$ in rat chromaffin cells are larger for the events with a foot than those without one. The $Q^{1/3}$ distribution for the events with a foot signal in rat chromaffin cells (Figures 4-2 B and E) was skewed to higher $Q^{1/3}$ values when compared with the events without a foot signal (Figures 4-2 C and F).

Opposite to the trend reported in PC12 cells (Sombers *et al.* 2004), the foot signals in rat chromaffin cells were more frequently detected as the value of $Q^{1/3}$ was increased (Figures 4-2A and D, but note that the two cell types have different ranges of Q values). However, similar to the trend reported in PC12 cells (Sombers *et al.* 2004), the duration of the foot signals in rat chromaffin cells lengthened with increasing values of $Q^{1/3}$. As shown in Figure 4-3A, the duration of foot signals in the control cells increased by ~2-fold when the mean value of $Q^{1/3}$ was doubled (expected to correspond to ~8-fold increase in Q or vesicular volume). Indeed, an 8-fold increase in vesicular volume was associated with ~2-fold increase in the duration of foot signals in PC12 cells (Sombers *et al.* 2004). Interestingly, when the events with similar $Q^{1/3}$ were examined, the duration of the foot signals distributed over a considerable range (Figure 4-4). There is increasing consensus (Amatore *et al.* 2000; Troyer and Wightman 2002) that the end of the foot signal (or the onset of the rapid dilation of the fusion pore) occurs when the energy associated with the constrained dissolution/expansion of the granule matrix overcomes the edge energy of the pore. This is postulated to

cause a dramatic acceleration in the rate of fusion pore dilation. The variability in the delay between fusion pore opening and rapid dilation among granules with the same Q may be related to variations in the state of the matrix in individual granules. The mechanism contributing to this variation in granule matrix probably includes variations in the density of the matrix and the concentration of other granular contents (including catecholamines and ions). Moreover, changes in the ionic condition and pH inside dense core granules can be triggered by elevation of intracellular Ca^{2+} concentration ($[Ca^{2+}]_i$), probably by opening of vesicular Ca^{2+} -activated cation channels that may pass protons (Han *et al.* 1999), and such changes are known to affect the state of the granule matrix (Amatore *et al.* 2000; Troyer and Wightman 2002). In this study, $[Ca^{2+}]_i$ in rat chromaffin cells was elevated for several minutes by KCl depolarization. Thus, it is possible that individual granules might be exposed to elevated $[Ca^{2+}]_i$ of different magnitudes and duration, thus affecting the state of the granular matrix to different degrees before fusion pore opening.

Previous studies (Alvarez de Toledo *et al.* 1993; Sombers *et al.* 2004) have shown that the fractional release during the foot signal (relative to the release from the entire amperometric event) decreases with increasing vesicular size. Interestingly, this trend was observed in the rat chromaffin cells only for the granules with mean $Q^{1/3}$ between 0.3 and $\sim 0.6 \text{ pC}^{1/3}$ (Figures 4-5A and B). At this range of $Q^{1/3}$, the decrease in the fractional release during the foot signal ($\sim 50\%$ decrease as $Q^{1/3}$ doubled) in rat chromaffin cells was more dramatic than the previous studies [c.f. ~ 10 or 20% decrease when the vesicular radius was

doubled (Alvarez de Toledo *et al.* 1993; Sombers *et al.* 2004)]. However, note that for rat chromaffin granules with mean $Q^{1/3} \geq 0.6 \text{ pC}^{1/3}$, the fractional release during the foot signal tends to increase with increasing $Q^{1/3}$. Since granules in this range of $Q^{1/3}$ were not present in PC12 cells (Sombers *et al.* 2004), this effect could not be compared between two cell types. It is not surprising that the relationship between the fractional release during the foot signal and the quantal size is complex, if the complex interactions that determine the end of the foot signal, are considered. The end of the foot signal is not the onset of fusion pore dilation; instead at this point the rate of fusion pore dilation accelerated dramatically as the energy of granule matrix dissolution/expansion overcame the edge energy of the minimally dilated fusion pore. The critical energy for the above may have a minimum at an intermediate quantal (and hence vesicular) size.

Our results show that the kinetics of the main amperometric spikes were strongly influenced by the quantal size for mean values of $Q^{1/3} < 0.6 \text{ pC}^{1/3}$. As shown in Figures 4-7C and F, for the events without a foot signal, the half-width of the main amperometric spikes increased monotonically with $Q^{1/3}$. Linear regression (not shown) of the initial ascending slopes in Figures 4-7C and F show that as the mean value of $Q^{1/3}$ of events without a foot signal doubled, the half-width increased by ~3-fold (c.f. ~2.5-fold for the events with a foot signal). A slowing of the kinetics of the main amperometric spikes in granules with large vesicular size has been reported previously in other cell types (Alvarez de Toledo *et al.* 1993; Bruns and Jahn 1995). However, the increase in half-width observed

here is steeper than that reported in PC12 cells, where a ~16% increase in the mean cellular value of Q (corresponding to an increase of $Q^{1/3}$ by ~5%) produced by 3,4-dihydroxy-L-phenylalanine (L-DOPA) lengthened the half-width by only 12% (Colliver *et al.* 2000). On the other hand, for the events with a foot signal, an increase in the half-width of the main amperometric spikes was observed only for the events with mean $Q^{1/3} < 0.6 \text{ pC}^{1/3}$ (Figures 4-7B and E). There was no further increase in the half-width at mean values of $Q^{1/3} \geq 0.6 \text{ pC}^{1/3}$ (Figures 4-7B and C). Most interestingly, the effect of cAMP (on reducing the duration of foot signals) was also most prominent among events with mean $Q^{1/3} \geq 0.6 \text{ pC}^{1/3}$, where the half-width stayed at a plateau value.

In the literature, there are at least two examples in which the kinetics of the main amperometric spikes in chromaffin cells did not always increase with quantal size. First, when the mean cellular value of Q in bovine chromaffin cells was increased by 73% (via exposure to L-DOPA), the half-width decreased by 73% (from 35.5 ms to 9.6 ms) (Pothos *et al.* 2002). Secondly, when the value of Q was increased in calf chromaffin cells (from 0.5 to ~1.2 pC by altering voltage-gated Ca^{2+} entry), the overall width of the main amperometric spikes (measured as the sum of the duration of rising and falling phases) was only increased at the middle range of Q (Elhamdani *et al.* 2001). These previous findings, together with our results, suggest that the half-width of the main amperometric spikes for chromaffin granules does not necessarily increase monotonically with quantal size. In contrast, Alvarez de Toledo *et al.* (1993) showed that the half-width of the main amperometric spikes increased monotonically with vesicular size (even for

a very large granule of beige mouse mast cells). This discrepancy among the different cell types may arise, at least in part, from the loading of exogenous serotonin into mast cell granules.

If the half-width of the main amperometric spikes is assumed to be determined mainly by the vesicular radius (Almers *et al.* 1989), theoretically it is possible to have no increase in the half-width as the quantal size gets larger under the following condition. One can assume that in the present study, granules with $Q^{1/3} \geq 0.6$ pC had the same radius, but some of such granules simply contained a higher concentration of releasable catecholamines. However, such a condition is extremely unlikely to be the main mechanism if one considers that the half-width stayed at practically the same value while $Q^{1/3}$ increased from ~ 0.5 to ~ 1.5 pC^{1/3}, which corresponded to ~ 27 -fold difference in concentration. Instead, we speculate that for large Q granules, the most rapid dilation of the fusion pore (which is associated with the most rapid dissolution and probable expansion of granule matrix) occurred at a faster rate such that the fusion pore became much larger (relative to that of granules with smaller Q) within milliseconds at the end of the foot signal. The existence of such a large fusion pore allows the large Q granules to discharge at a much faster rate that is mainly limited only by the rate of granule dissolution. As discussed earlier, our observation that the duration of the foot signals (even when granules of exactly the same large Q were compared) distributed over a considerable range (Figure 4-4) probably reflects the large variability in the state of matrix dissolution among individual granules even before fusion pore opening. This variability may also

affect the maximal rate of matrix dissolution and fusion pore dilation for any particular value of Q . A discussion of how granules with small and large Q can undergo fundamentally different rates of rapid matrix expansion and fusion pore dilation will be presented in Chapter 5.

4.3.2 *Modulation of quantal release kinetics by cAMP*

In Chapter 3, we found that elevation of cellular cAMP indeed increased the mean cellular quantal size in rat chromaffin cells (Tang *et al.* 2005) as reported previously for bovine chromaffin cells (Machado *et al.* 2001). However, we found that the increase in quantal size in rat chromaffin cells was significant only after a much longer period of treatment (3 days instead of 5 - 30 min) with dBcAMP or forskolin. The difference between the two species may be attributed to the observation that cAMP can rapidly enhance voltage-gated Ca^{2+} channels (VGCC) in bovine (but not in rat) chromaffin cells (Artalejo *et al.* 1990; Carbone *et al.* 2001; Cesetti *et al.* 2003) and this enhancement of VGCC has been suggested to be the major mechanism underlying the increase in quantal size of catecholamine release (Elhamdani *et al.* 2001). In rat chromaffin cells, we have shown in Chapter 3 that elevation of cAMP uniformly increased the quantal size of all granules (Tang *et al.* 2005). Consistent with this, here we found that cAMP elevation shifted the distribution of events with (Figures 4-2B and E) or without a foot signal (Figures 4-2C and F) towards larger values of $Q^{1/3}$. Since quantal size can dramatically affect both the duration of the foot signals (Figure 4-3) and the half-width of the main amperometric spikes (Figure 4-7) in rat chromaffin cells, it

is important to determine whether cAMP affects the kinetics of release independently of the increase in quantal size. Therefore, in the current study, the effect of cAMP was compared between cAMP-elevated cells and their time-matched controls at matched values of $Q^{1/3}$. We found that cAMP appeared to act selectively on large Q granules with mean $Q^{1/3} \geq 0.6 \text{ pC}^{1/3}$. The duration of the foot signals for large Q granules was reduced by cAMP elevation (Figure 4-3). Note that the major effect of cAMP was an increase in the fraction of events with a very short foot (e.g. $< 3 \text{ ms}$; Figures 4-4C - E, and H - J). Some of these very short foot signals might become undetectable under our experimental conditions (filtering at 1 kHz). This will explain the slight reduction in the frequency of events with a foot signal in cells treated with dBcAMP or forskolin (Figures 4-2A and D). In addition, the fractional release during the foot signal for large Q granules was also reduced by cAMP (Figure 4-5).

The phenomenon that elevation of cAMP shortened the duration of foot signals is similar to an effect reported for the overexpression of synaptotagmin IV in PC12 cells (Wang *et al.* 2001). The shortening of the foot duration in PC12 cells was attributed to a destabilization of the opened but minimally dilated fusion pore (via exiting the state of the opened small pore by either closure or rapid dilation of the fusion pore) (Wang *et al.* 2001). Most interestingly, the expression of synaptotagmin IV in PC12 cells could be induced (from undetectable levels) after 4 - 8 hr of forskolin treatment (Wang *et al.* 2003). These findings raise the possibility that the shortening of the foot duration by cAMP observed here may be related to a destabilization of the opened small fusion pore (e.g. via increase

in the expression of synaptotagmin IV as reported in PC12 cells). If one considers that the end of the foot signal (or the onset of the rapid dilation of fusion pore) occurs when the energy associated with the constrained dissolution/expansion of granule matrix overcomes the edge energy of the pore, then the destabilization of the fusion pore is equivalent to lowering the critical energy for rapid pore dilation. Such a model (Amatore *et al.* 2000) also predicted that rapid fusion pore dilation is more prominent among granules with larger values of Q. Consistent with this model, we found that the shortening of the foot duration by cAMP was more prominent for the granules with larger values of Q. Another phenomenon that was associated with increased expression of synaptotagmin IV in PC12 cells was an increase in the frequency and the duration of the stand alone foot signals (SAF; i.e. amperometric events with no conspicuous spike component) (Wang *et al.* 2003). However, in the current study as well as in a previous study (Xu and Tse 1999), we found that the frequency of SAF signals in rat chromaffin cells was < 1%. This value was ~50-fold lower than that reported in PC12 cells (Wang *et al.* 2003). Therefore, we could not collect a sufficient number of SAF signals for any statistical comparison of the effects of cAMP.

It has been suggested that granules with little or no matrix (e.g. containing $Q < 20\,000$ catecholamine molecules) never proceed to rapid fusion pore dilation (Amatore *et al.* 2000). Indeed, in the current study, for the events without a foot signal, cAMP elevation also did not affect their release kinetics as there was no change in the half-width of the main amperometric spikes over the entire range of

$Q^{1/3}$ (Figures 4-7C and F). This finding raises the possibility that in these events without a foot signal, the rapid discharge of catecholamines may occur before any significant dilation of fusion pore and thus the stage where cAMP acts most prominently is simply absent. However, the events without a foot signal in the present study had a modal $Q^{1/3}$ value of $0.4 \text{ pC}^{1/3}$, which corresponded to $Q = 0.064 \text{ pC}$ or 200 000 catecholamine molecules, which was 10-fold larger than that predicted from the previous model (Amatore *et al.* 2000). Thus, it is unlikely that the events without a foot signal in the current study arise from granules without fusion pore dilation. Instead, these granules probably had a significantly dissociated matrix even before fusion pore opening. In such granules, the maximum rate of fusion pore dilation is probably lower.

Our analysis of the events with a foot signal also shows that cAMP did not cause any significant increase in the half-width of the main amperometric spikes over a wide range of $Q^{1/3}$ (Figures 4-7B and E). This finding is consistent with the notion that cAMP does not directly cause any slowing of the kinetics of the main amperometric spikes. However, for the events with mean $Q^{1/3}$ of $\sim 0.6 \text{ pC}^{1/3}$, there was a small but significant increase in the half-width of the main amperometric spikes in cAMP-elevated cells (Figures 4-7B and E). We speculate that this phenomenon may be related to the cAMP-mediated reduction in the duration of foot signals. Note that the effect of cAMP on the duration of foot signals (Figure 4-3) was prominent only for the events with mean $Q^{1/3} \geq 0.6 \text{ pC}^{1/3}$. Consistent with the possibility that cAMP reduced the duration of foot signals by reducing the critical energy for rapid fusion pore dilation, the dissolution of the granule matrix

at the end of the foot signal might be the lowest for control cells at mean $Q^{1/3} \simeq 0.6 \text{ pC}^{1/3}$ (the lowest point for the fractional release during the foot signal in Figure 4-5). If cAMP indeed allowed rapid fusion pore dilation to occur with even less dissociation (and release) of catecholamine from granule matrix, the remaining matrix at the end of the foot signal must be less dissociated. It is likely that a less dissociated matrix will require a longer time to undergo subsequent dissolution. This effect may be smaller or negligible for the granules with a very large Q . As discussed above, the rapid matrix expansion in very large Q granules may always cause a larger fusion pore size within milliseconds after the end of the foot signal, thus counteracting the effect of larger undissociated matrix.

The overall findings from the present study extends a concept that was first developed in the mast cells: vesicle fusion (the foot signal) and bulk release (the main amperometric spike) are separate processes (Fernandez-Chacon and Alvarez de Toledo 1995). We found that in rat chromaffin granules, quantal size regulates both the duration of the foot signals and the kinetics of the main amperometric spikes. In contrast, elevation of cAMP mainly modulates the duration of the foot signals, which in turn, caused subtle secondary effects on the kinetics of the main amperometric spikes. This finding provides new insight into how second messengers can modulate the release process via actions on the function of fusion pore.

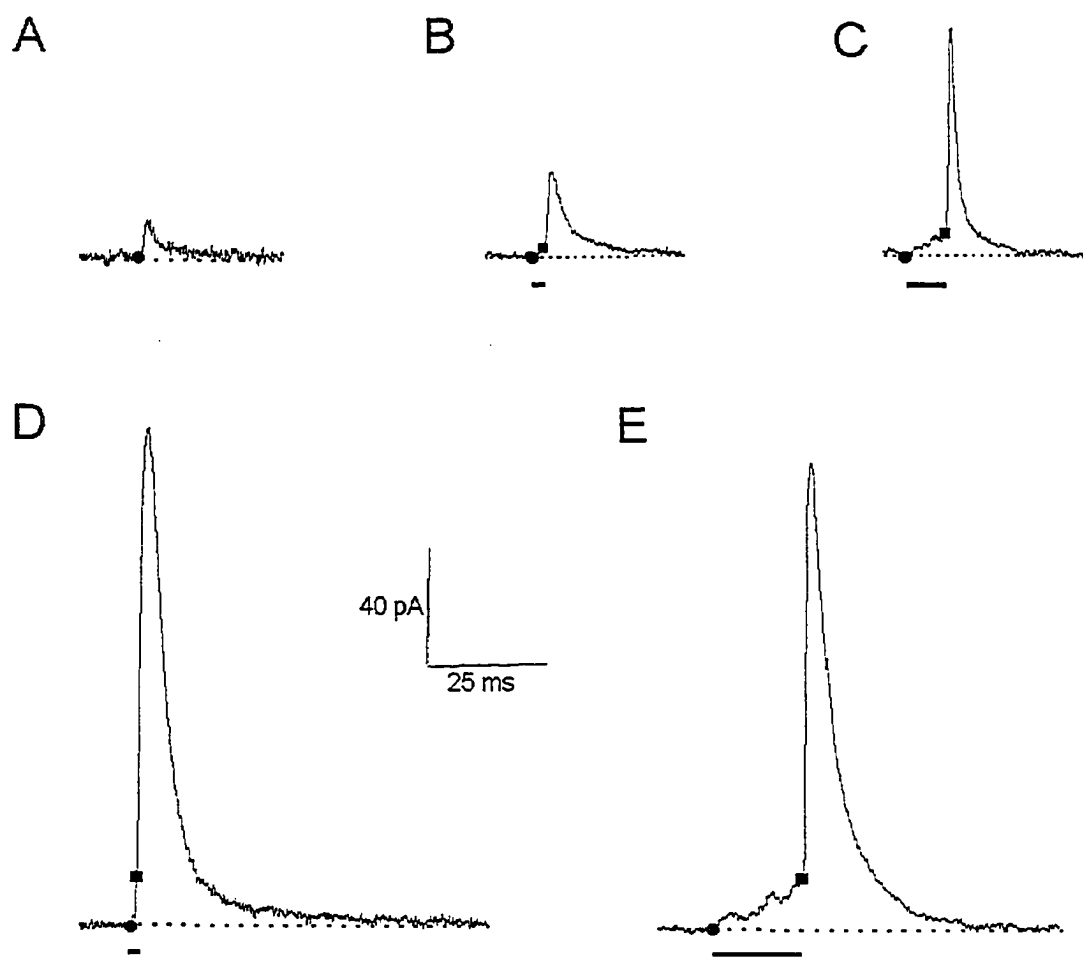


Figure 4-1 A wide variety of amperometric events could be detected in rat chromaffin cells. The circle symbol and the square symbol depict the threshold for detecting an amperometric event and the end of the foot signal, respectively. The duration of the foot signals for the events in B - E is indicated by a bar. The value of Q (in pC) for each signal in A - E was 0.054, 0.181, 0.258, 1.556, and 1.534; the corresponding value of $Q^{1/3}$ (in $\text{pC}^{1/3}$) was 0.378, 0.566, 0.636, 1.159, and 1.153.

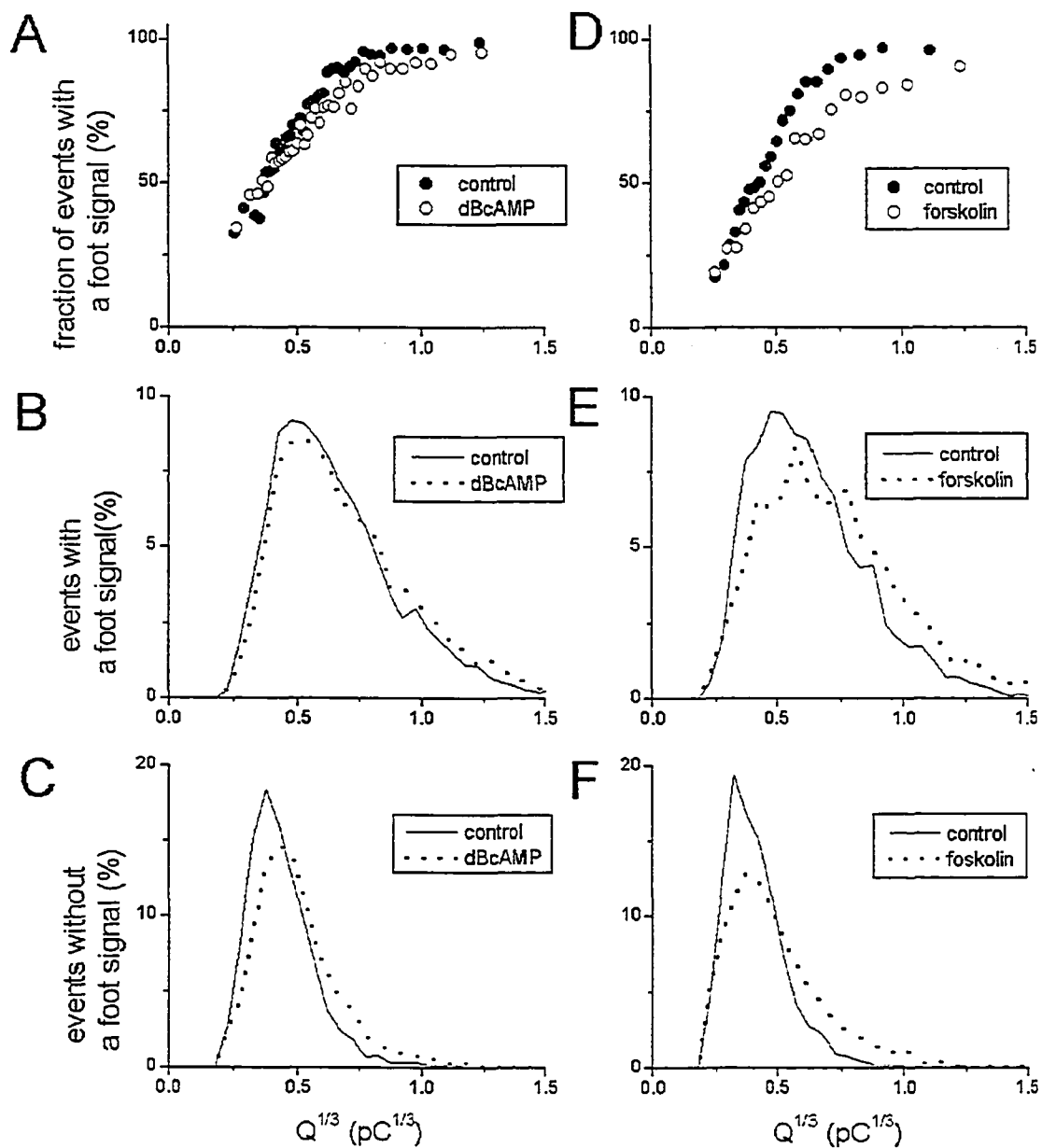


Figure 4-2 Influence of quantal size and cAMP on the frequency of amperometric events with a foot signal. Data from dBcAMP-treated cells and their time-matched controls are shown in A - C. Data from forskolin-treated cells and their time-matched controls are shown in D - F. In this analysis, an event is classified as "with a foot signal" if the end of the foot signal (an inflection) was detected at times > 1 ms after the threshold of the signal. A and D show the percentage of events with a foot signal at different $Q^{1/3}$. Each data set was first sorted according to an ascending value of $Q^{1/3}$. Each point shown was the average calculated from 300 consecutive events after sorting. B and E show the distribution of all events without a foot signal at different values of $Q^{1/3}$ (bin size = $0.05 \text{ pC}^{1/3}$). C and F show the distribution of all events with a foot signal at different values of $Q^{1/3}$ (bin size = $0.05 \text{ pC}^{1/3}$).

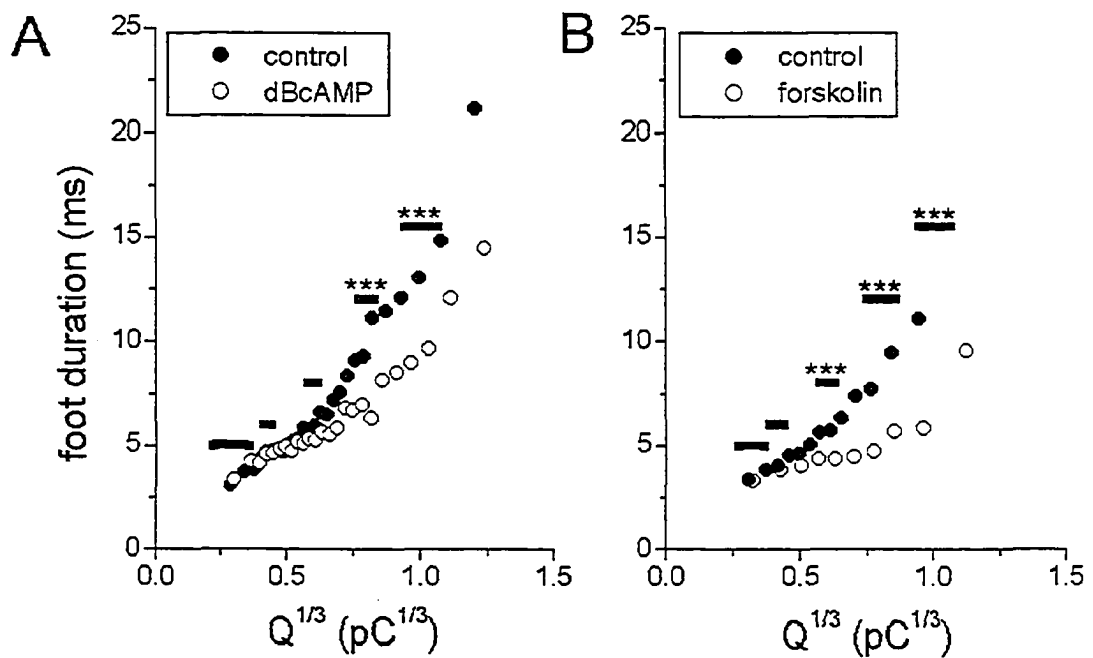


Figure 4-3 Influence of quantal size and cAMP on the duration of foot signals. Plots of foot duration with $Q^{1/3}$. (A) dBcAMP-treated cells and their time-matched controls; (B) forskolin-treated cells and their time-matched controls. Each data set was first sorted according to an ascending order of $Q^{1/3}$. Each point shown was the average calculated from 300 consecutive events. The bars denote the five ranges of $Q^{1/3}$ used for the distributions shown in Figure 4-4.

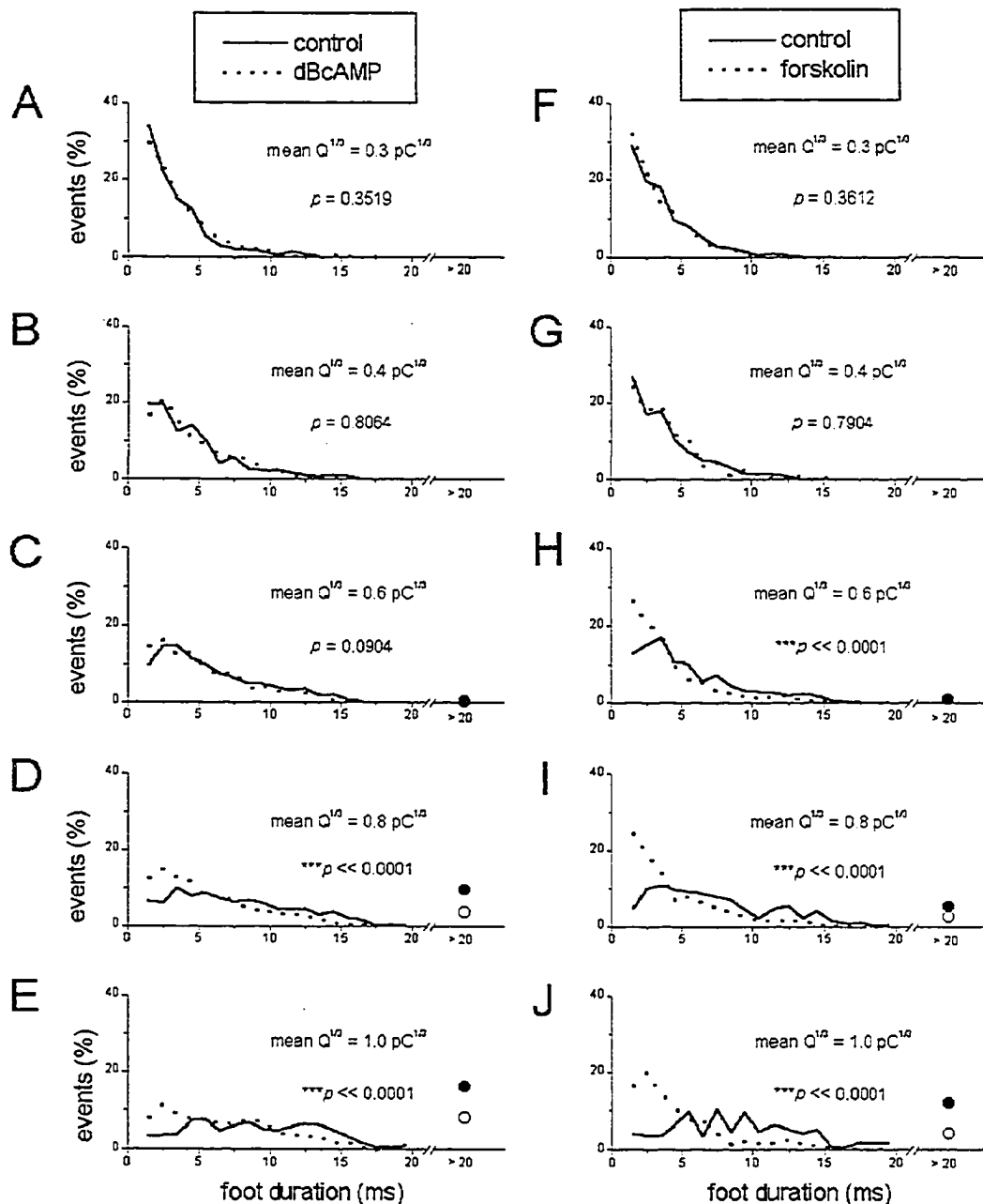


Figure 4-4 Distributions of foot duration from events selected from five different ranges of quantal size. Data from dBcAMP-treated cells and their time-matched controls are shown in A - E. Data from forskolin-treated cells and their time-matched controls are shown in F - J. Each plot was obtained by selecting ~250 - 600 events from a matched range of $Q^{1/3}$ (shown in Figure 4-3). For each plot, the events with a foot duration of < 1 ms were excluded to avoid the inclusion of events without a foot signal, which appeared to have a very short foot simply because of 1 kHz low pass filtering. In C - E, and H - J, the percentage of events with foot duration > 20 ms is represented by a circle symbol: filled circle for the control cells and unfilled circle for the cAMP-elevated cells.

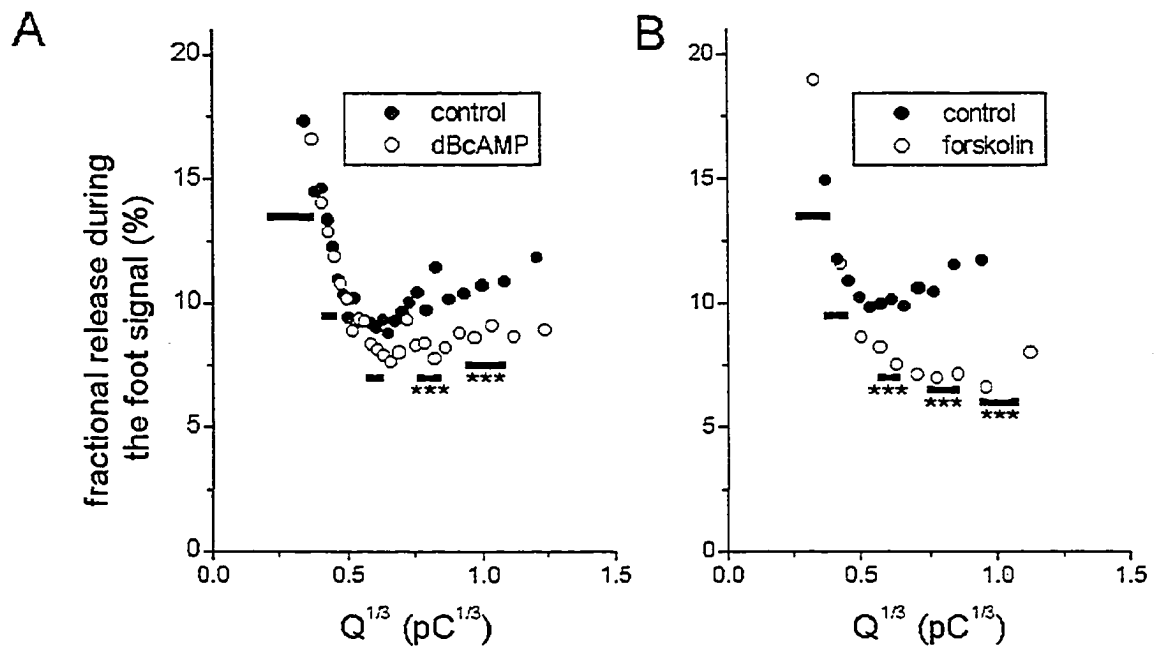


Figure 4-5 Influence of quantal size and cAMP on the fractional release during the foot signal. Plots of amount of catecholamine released during the foot signal relative to the total release during the entire amperometric event at different $Q^{1/3}$. (A) dBcAMP-treated cells and their time-matched controls; (B) forskolin-treated cells and their time-matched controls. Each set of data was sorted and analysed as described in Figure 4-3. Each point shown here was the average calculated from 300 events. The bars denote the five ranges of $Q^{1/3}$ used for the distributions shown in Figure 4-6.

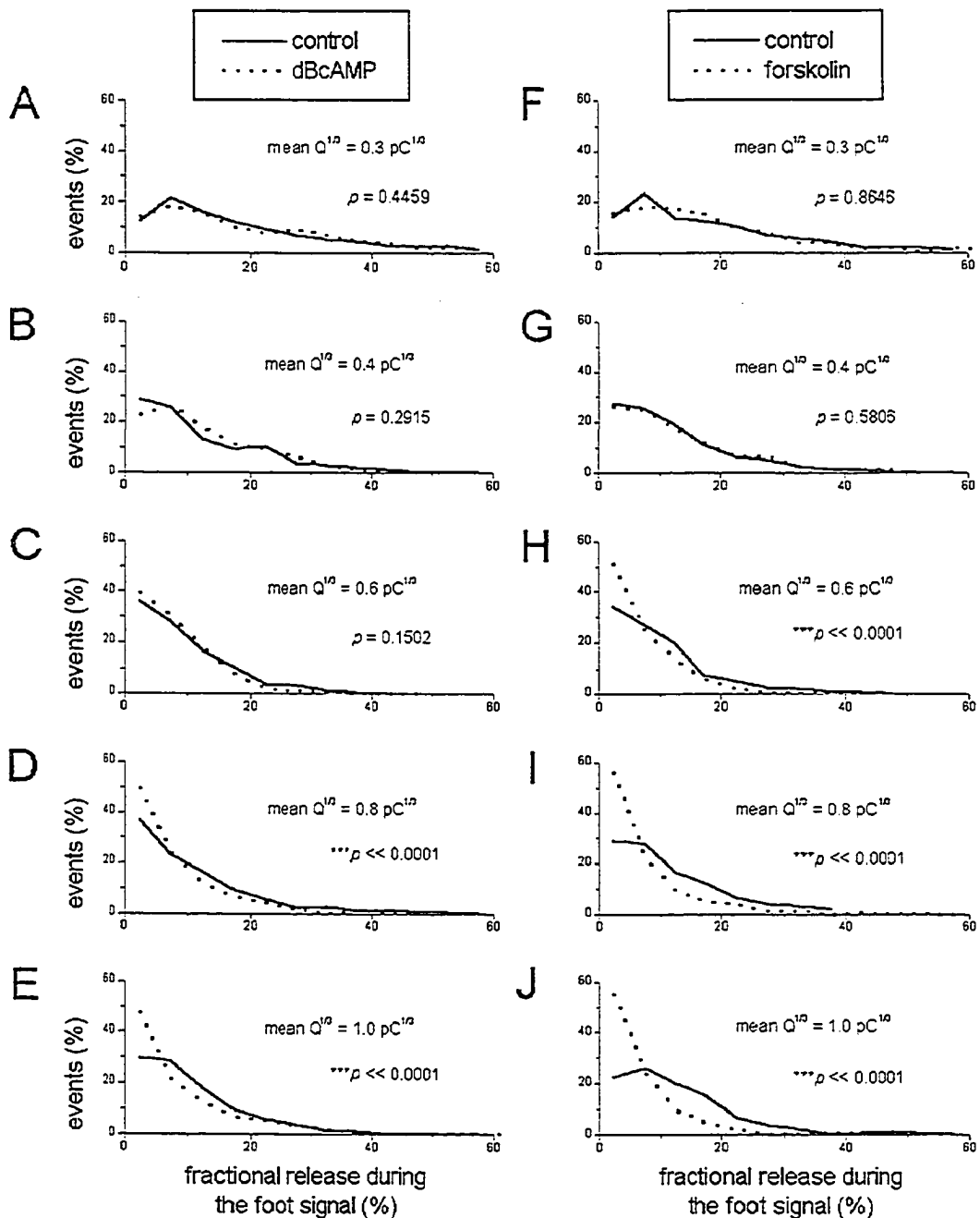


Figure 4-6 Distributions of fractional release during the foot signal from events selected from five different ranges of quantal size. Data from dBcAMP-treated cells and their time-matched controls are shown in A - E. Data from forskolin-treated cells and their time-matched controls are shown in F - J. The range of $Q^{1/3}$ used in each distribution was shown in Figure 4-5.

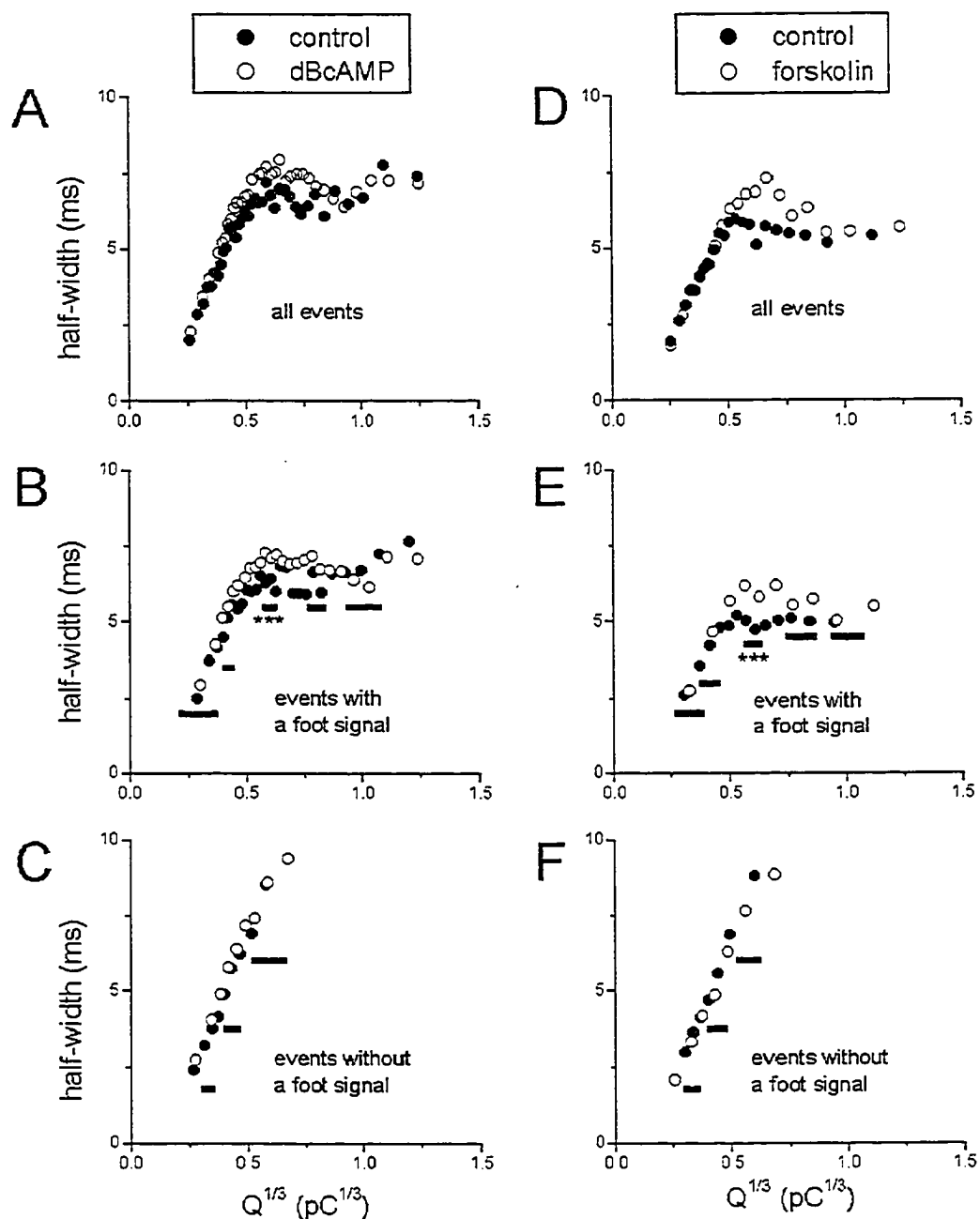


Figure 4-7 Influence of quantal size and cAMP on the half-width of the main amperometric spikes. Data from dBcAMP-treated cells and their time-matched controls are shown in A - C. Data from forskolin-treated cells and their time-matched controls are shown in D - F. The change in half-width with $Q^{1/3}$ were analyzed for all events (A and D); for the events with a foot signal (B and E), for the events without a foot signal (C and F). The classification of events with or without a foot signal used the same criterion as in Figure 4-2. Each set of data was sorted and analyzed as described in Figure 4-3. Each point shown here was the average calculated from 300 events. The bars denote the different ranges of $Q^{1/3}$ used for the distributions shown in Figures 4-8, 4-9, and 4-10.

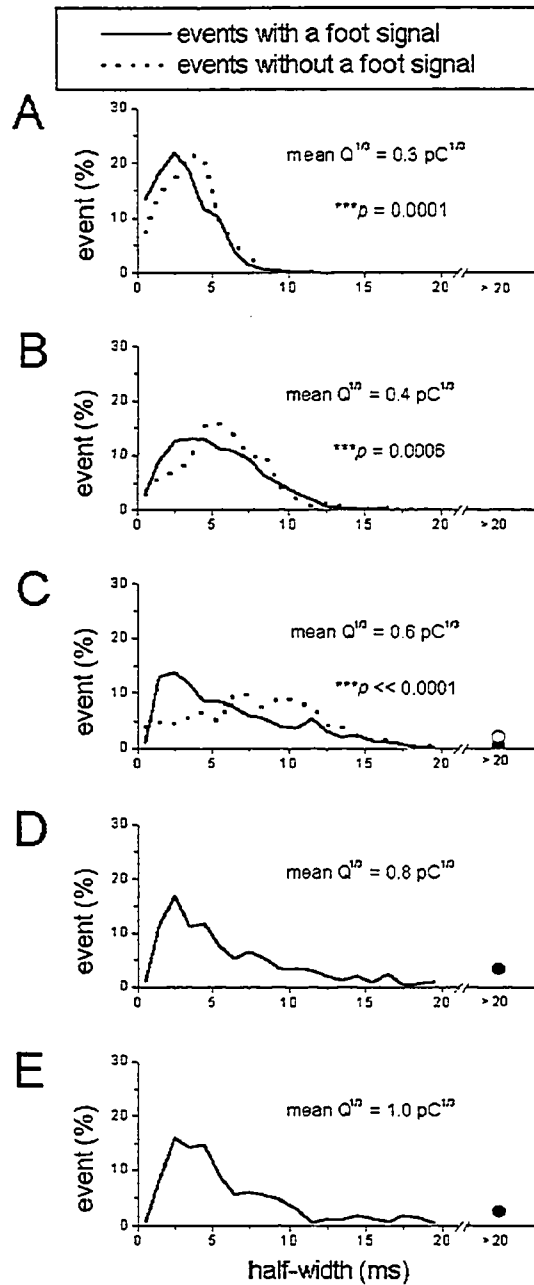


Figure 4-8 Distributions of half-width from events with or without a foot signal selected from different ranges of quantal size. The range of $Q^{1/3}$ used in each of the distributions was shown in Figures 4-7B and C. In C - E, the percentage of events with half-width > 20 ms is represented by a circle symbol: filled circle for the events with a foot signal and unfilled circle for the events without a foot signal.

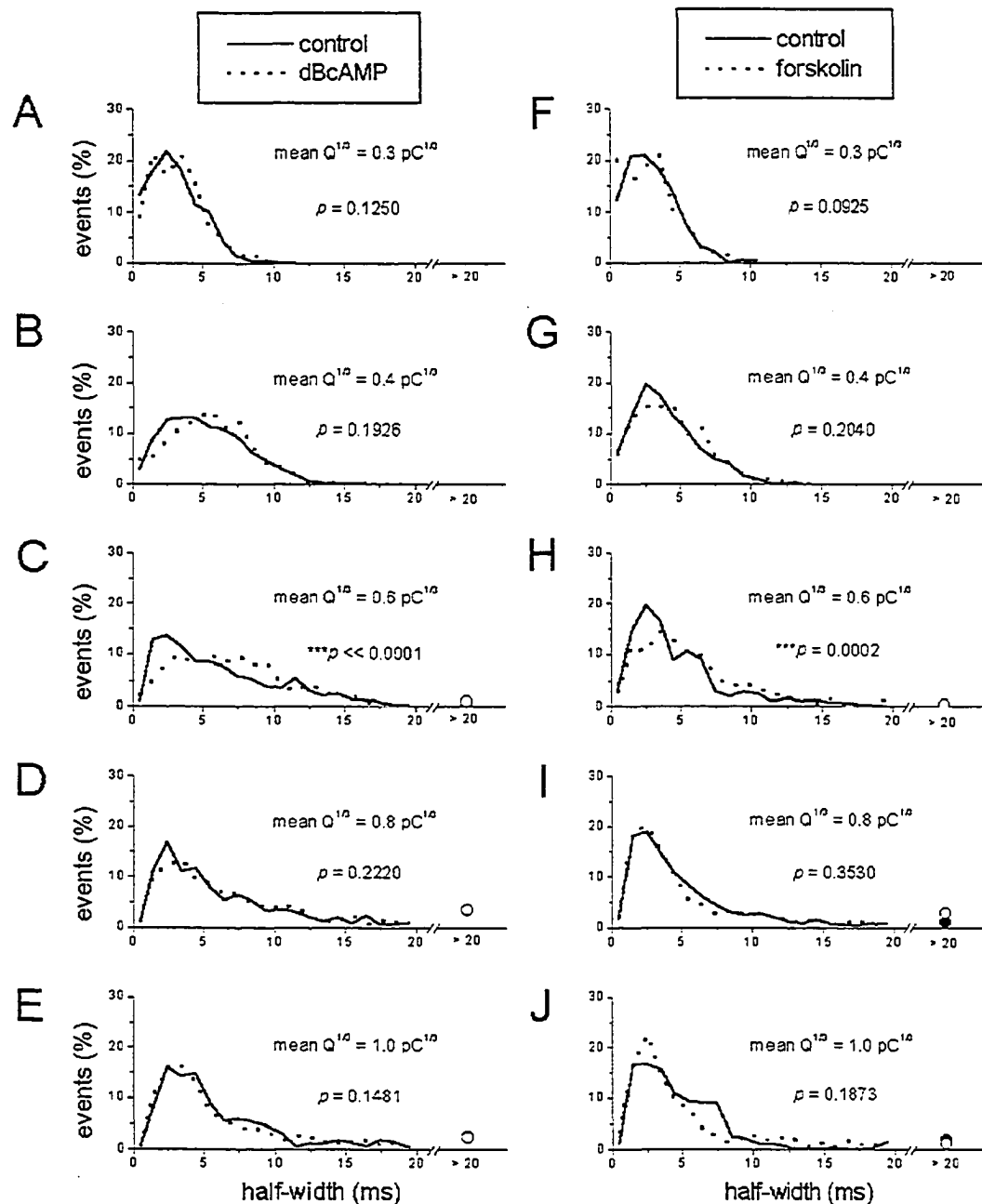


Figure 4-9 Distributions of half-width from events with a foot signal selected from different ranges of quantal size. Data from dBCAMP-treated cells and their time-matched controls are shown in A - E. Data from forskolin-treated cells and their time-matched controls are shown in F - J. The range of $Q^{1/3}$ used in each of the distributions was shown in Figures 4-7B and E. In C - E, and H - J, the percentage of events with half-width > 20 ms is represented by a circle symbol: filled circle for the control cells and unfilled circle for the cAMP-elevated cells.

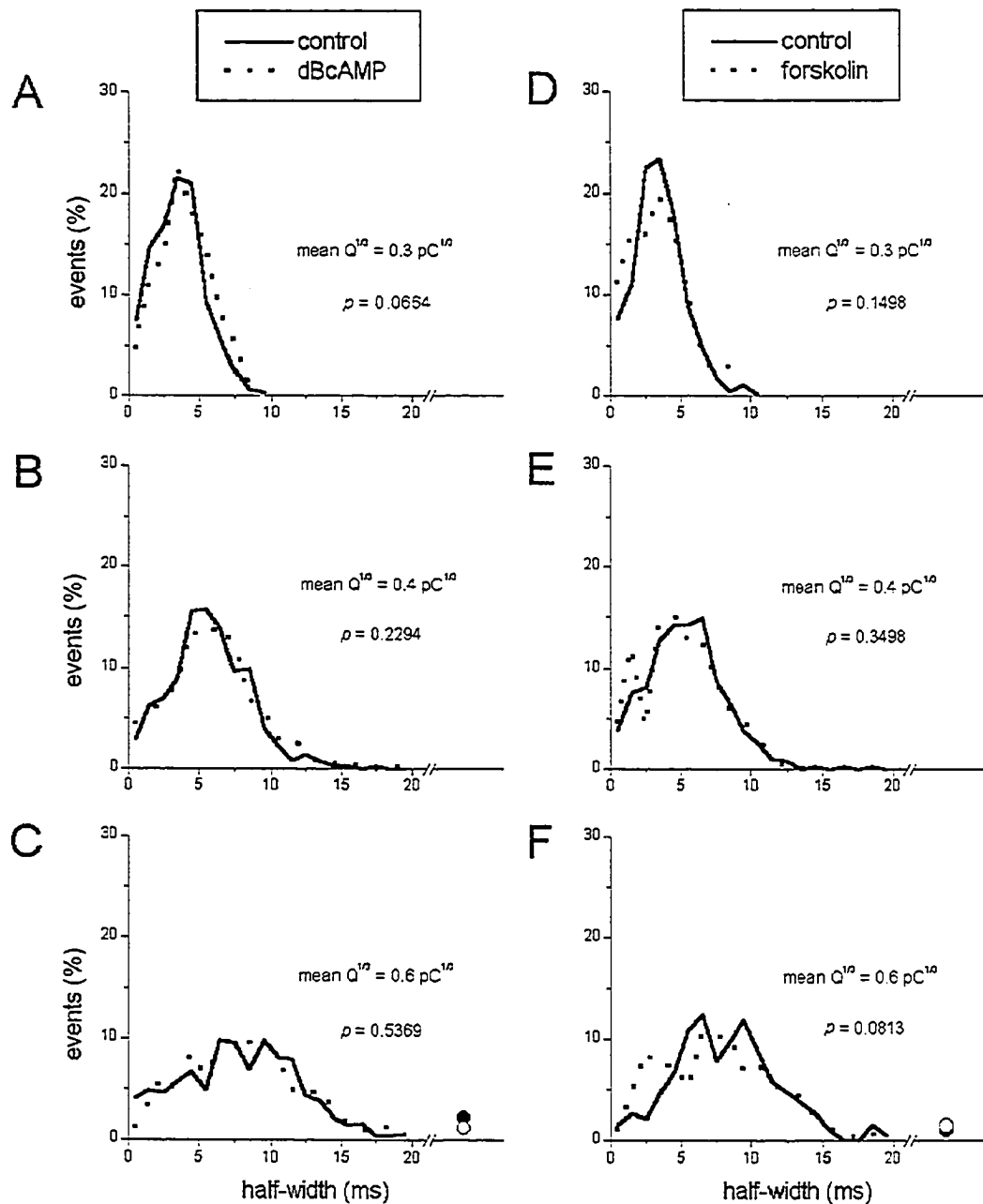


Figure 4-10 Distributions of half-width from events without a foot signal selected from different ranges of quantal size. Data from dBcAMP-treated cells and their time-matched controls are shown in A - C. Data from forskolin-treated cells and their time-matched controls are shown in D - F. The range of $Q^{1/3}$ used in each of the distributions was shown in Figures 4-7C and F. In C and F, the percentage of events with half-width > 20 ms is represented by a circle symbol: filled circle for the control cells and unfilled circle for the cAMP-elevated cells.

References

- Almers W., Breckenridge L. J., and Spruce A. E. (1989) The mechanism of exocytosis during secretion in mast cells, in *Secretion and Its Control* (Oxford G. S. and Armstrong C. M., eds.), pp. 269-282. The Rockefeller University Press, New York.
- Alvarez de Toledo G., Fernandez-Chacon R., and Fernandez J. M. (1993) Release of secretory products during transient vesicle fusion. *Nature* **363**, 554-558.
- Amatore C., Arbault S., Bonifas I., Bouret Y., Erard M., Ewing A. G., and Sombers L. A. (2005) Correlation between vesicle quantal size and fusion pore release in chromaffin cell exocytosis. *Biophysical Journal* **88**, 4411-4420.
- Amatore C., Bouret Y., Travis E. R., and Wightman R. M. (2000) Interplay between membrane dynamics, diffusion and swelling pressure governs individual vesicular exocytotic events during release of adrenaline by chromaffin cells. *Biochimie* **82**, 481-496.
- Archer D. A., Graham M. E., and Burgoyne R. D. (2002) Complexin regulates the closure of the fusion pore during regulated vesicle exocytosis. *Journal of Biological Chemistry* **277**, 18249-18252.

- Artalejo C. R., Ariano M. A., Perlman R. L., and Fox A. P. (1990) Activation of facilitation calcium channels in chromaffin cells by D₁ dopamine receptors through a cAMP/protein kinase A-dependent mechanism. *Nature* **348**, 239-242.
- Bruns D. and Jahn R. (1995) Real-time measurement of transmitter release from single synaptic vesicles. *Nature* **377**, 62-65.
- Burgoyne R. D. and Barclay J. W. (2002) Splitting the quantum: regulation of quantal release during vesicle fusion. *Trends in Neurosciences* **25**, 176-178.
- Carbone E., Carabelli V., Cesetti T., Baldelli P., Hernandez-Guijo J. M., and Giusta L. (2001) G-protein- and cAMP-dependent L-channel gating modulation: a manyfold system to control calcium entry in neurosecretory cells. *Pflugers Archiv - European Journal of Physiology* **442**, 801-813.
- Cesetti T., Hernandez-Guijo J. M., Baldelli P., Carabelli V., and Carbone E. (2003) Opposite action of beta₁- and beta₂-adrenergic receptors on Ca(V)₁ L-channel current in rat adrenal chromaffin cells. *Journal of Neuroscience* **23**, 73-83.
- Chow R. H., von Ruden L., and Neher E. (1992) Delay in vesicle fusion revealed by electrochemical monitoring of single secretory events in adrenal chromaffin cells. *Nature* **356**, 60-63.

- Colliver T. L., Pyott S. J., Achalabun M., and Ewing A. G. (2000) VMAT-mediated changes in quantal size and vesicular volume. *Journal of Neuroscience* **20**, 5276-5282.
- Elhamdani A., Palfrey H. C., and Artalejo C. R. (2001) Quantal size is dependent on stimulation frequency and calcium entry in calf chromaffin cells. *Neuron* **31**, 819-830.
- Fernandez-Chacon R. and Alvarez de Toledo G. (1995) Cytosolic calcium facilitates release of secretory products after exocytotic vesicle fusion. *FEBS Letters* **363**, 221-225.
- Fisher R. J., Pevsner J., and Burgoyne R. D. (2001) Control of fusion pore dynamics during exocytosis by Munc18. *Science* **291**, 875-878.
- Graham M. E. and Burgoyne R. D. (2000) Comparison of cysteine string protein (Csp) and mutant alpha-SNAP overexpression reveals a role for Csp in late steps of membrane fusion in dense-core granule exocytosis in adrenal chromaffin cells. *Journal of Neuroscience* **20**, 1281-1289.
- Han W., Li D., Stout A. K., Takimoto K., and Levitan E. S. (1999) Ca²⁺-induced deprotonation of peptide hormones inside secretory vesicles in preparation for release. *Journal of Neuroscience* **19**, 900-905.

- Kobayashi S., Serizawa Y., Fujita T., and Coupland R. E. (1978) SGC (small granule chromaffin) cells in mouse adrenal medulla: light and electron microscopic identification using semi-thin and ultra-thin sections. *Endocrinologia Japonica* **25**, 467-476.
- Koval L. M., Yavorskaya E. N., and Lukyanetz E. A. (2001) Electron microscopic evidence for multiple types of secretory vesicles in bovine chromaffin cells. *General and Comparative Endocrinology* **121**, 261-277.
- Machado J. D., Morales A., Gomez J. F., and Borges R. (2001) cAMP modulates exocytotic kinetics and increases quantal size in chromaffin cells. *Molecular Pharmacology* **60**, 514-520.
- Plattner H., Artalejo A. R., and Neher E. (1997) Ultrastructural organization of bovine chromaffin cell cortex - analysis by cryofixation and morphometry of aspects pertinent to exocytosis. *Journal of Cell Biology* **139**, 1709-1717.
- Pothos E. N. (2002) Regulation of dopamine quantal size in midbrain and hippocampal neurons. *Behavioural Brain Research* **130**, 203-207.
- Pothos E. N., Mosharov E., Liu K. P., Setlik W., Haburcak M., Baldini G., Gershon M. D., Tamir H., and Sulzer D. (2002) Stimulation-dependent regulation of the pH, volume and quantal size of bovine and rodent secretory vesicles. *Journal of Physiology - London* **542**, 453-476.

- Somers L. A., Hancher H. J., Colliver T. L., Wittenberg N., Cans A., Arbault S., Amatore C., and Ewing A. G. (2004) The effects of vesicular volume on secretion through the fusion pore in exocytotic release from PC12 cells. *Journal of Neuroscience* **24**, 303-309.
- Staal R. G. W., Mosharov E. V., and Sulzer D. (2004) Dopamine neurons release transmitter via a flickering fusion pore. *Nature Neuroscience* **7**, 341-346.
- Sulzer D. and Pothos E. N. (2000) Regulation of quantal size by presynaptic mechanisms. *Reviews in the Neurosciences* **11**, 159-212.
- Tang K. S., Tse A., and Tse F. W. (2005) Differential regulation of multiple populations of granules in rat adrenal chromaffin cells by culture duration and cyclic AMP. *Journal of Neurochemistry* **92**, 1126-1139.
- Troyer K. P. and Wightman R. M. (2002) Temporal separation of vesicle release from vesicle fusion during exocytosis. *Journal of Biological Chemistry* **277**, 29101-29107.
- Wang C. T., Grishanin R., Earles C. A., Chang P. Y., Martin T. F. J., Chapman E. R., and Jackson M. B. (2001) Synaptotagmin modulation of fusion pore kinetics in regulated exocytosis of dense-core vesicles. *Science* **294**, 1111-1115.
- Wang C. T., Lu J. C., Bai J. H., Chang P. Y., Martin T. F. J., Chapman E. R., and Jackson M. B. (2003) Different domains of synaptotagmin control the choice between kiss-and-run and full fusion. *Nature* **424**, 943-947.

- Wightman R. M., Schroeder T. J., Finnegan J. M., Ciolkowski E. L., and Pihel K. (1995) Time course of release of catecholamines from individual vesicles during exocytosis at adrenal medullary cells. *Biophysical Journal* **68**, 383-390.
- Xu J. and Tse F. W. (1999) Brefeldin A increases the quantal size and alters the kinetics of catecholamine release from rat adrenal chromaffin cells. *Journal of Biological Chemistry* **274**, 19095-19102.

CHAPTER 5

General Discussion

In this thesis, carbon fiber amperometry was employed to measure the amount of catecholamine released from individual granules (i.e. the quantal size, Q) of rat chromaffin cells. Using this technique, in Chapter 3, the regulation of multiple populations of granules with different quantal size by culture duration, glucocorticoids, and elevation of cyclic AMP (cAMP) was examined. In Chapter 4, the regulation of the kinetics of catecholamine release from individual granules by quantal size and elevation of cAMP was studied. This chapter will review the two preceding chapters. It will then address general issues on these chapters.

5.1 Summary

5.1.1 Chapter 3

The distribution of cube-root of quantal size ($Q^{1/3}$) of amperometric events could be reasonably described by the summation of at least three Gaussian distributions (Figure 3-6), suggesting that rat chromaffin cells contained at least three distinct populations of granules releasing a small, medium, or large amount of catecholamines. After two extra days of culture in serum-free defined medium, the total cellular catecholamine content was reduced to ~75% of that in the cells cultured for 1 day (Figure 3-12A). This rundown occurred in parallel with a decrease in the mean cellular quantal size (by ~15 - 40%) (Figures 3-2 and 3-13B) and was mainly associated with a decrease in the proportional release from large Q granules and a corresponding increase in the proportional release from medium Q granules (Figure 3-9C).

Glucocorticoids were reported to regulate catecholamine synthesis (Hodel 2001) and storage (Rozansky *et al.* 1994). However, it is not clear whether the quantal size in mature rat chromaffin cells is affected by glucocorticoids. The rundown in mean cellular quantal size during the short-term cell culture can be due to a loss of the paracrine action of glucocorticoids which in turn leads to a reduction in catecholamine synthesis. The synthetic glucocorticoid dexamethasone did not affect the mean cellular quantal size (Figure 3-13) or the proportional release of different populations of granules (Figure 3-14B) in rat chromaffin cells cultured for 1 day. Interestingly, the rundown in the total cellular catecholamine content (Figure 3-15A), the mean cellular quantal size (Figure 3-13B), as well as the shift in the proportional release of different populations of granules (Figures 3-14A and C) after 3 days of culture could be prevented by dexamethasone. The rundown phenomenon and the effect of dexamethasone are summarized in Figure 5-1. Since chromaffin cells *in vivo* are exposed to high concentrations of glucocorticoids (Raum 1997; Hodel 2001), the above findings suggest that the paracrine action of glucocorticoids maintains the mean catecholamine content in chromaffin cell granules.

In contrast, when cells were cultured with dibutyryl-cAMP (dBcAMP) for 3 days, their mean cellular quantal size increased by ~35% (relative to time-matched controls) (Figure 3-2). This increase in quantal size was not associated with any shift in the proportional release of different populations of granules (Figure 3-9C). Instead, cAMP uniformly increased the average amount of catecholamines released from all populations of granules (Figure 3-10). The

effect of cAMP is summarized in Figure 5-2. These data raise the possibility that distinct populations of granules in rat chromaffin cells can be differentially regulated by culture duration, glucocorticoids, and cAMP.

5.1.2 Chapter 4

The quantal size of individual granules is known to affect kinetics of release (Alvarez de Toledo *et al.* 1993; Bruns and Jahn 1995; Sombers *et al.* 2004). The natural variation in quantal size among individual rat chromaffin granules was exploited to examine the influence of the quantal size on release kinetics. The frequency of events with a foot signal (Figures 4-2A and B), as well as the duration of foot signals, increased with quantal size (Figure 4-3).

Among events without a foot signal, the kinetics of the main amperometric spikes (estimated from the half-width duration) slowed down as quantal size increased (Figures 4-7C and F). If the fusion pore size is fixed and all catecholamines are free for diffusion, the time constant (τ) of release is expected to be proportional to the vesicular size (Almers *et al.* 1989). If the release of catecholamines is modeled as the simple diffusion via a fixed fusion pore, the log-log plot of the half-width duration vs. vesicular radius or $Q^{1/3}$ should have a third-power relationship [the dashed lines of Figure 4D of Alvarez de Toledo (1993)]. In that study, however, the actual data had a half-width duration that was shorter (1.5-power of the vesicular radius) than predicted by the simple diffusion. Similarly, our log-log plot of half-width duration vs. $Q^{1/3}$ (data not shown) also had the same slope in comparison to Alvarez de Toledo (1993). Therefore, the faster

release of catecholamines by simple diffusion only partially accounted for the kinetics of release from small size granules (hence the small Q granules) (Figure 5-3).

A similar trend of the increase in the half-width duration with $Q^{1/3}$ was also observed in events with a foot signal, but only at mean $Q^{1/3} \leq 0.6 \text{ pC}^{1/3}$ (Figures 4-7B and E). At larger mean $Q^{1/3}$, the increase in the half-width duration reached a plateau, indicating that the kinetics of the main amperometric spikes in large Q events with a foot signal is faster than that predicted by their quantal size.

Both mimicking and elevation of cAMP (by dBcAMP and forskolin, respectively) increased the quantal size of all events with (Figures 4-2B and C) or without (Figures 4-2E and F) a foot signal. To determine whether cAMP affected the kinetics of release independent of its action on the quantal size, the effect of cAMP was compared among events with matched values of quantal size. The major effect of cAMP was on events with mean $Q^{1/3} \geq 0.6 \text{ pC}^{1/3}$, where both the duration of foot signals (Figure 4-3) and the fractional release during the foot signal (Figure 4-5) were reduced. This effect is consistent with the possibility that cAMP destabilized an opened but undilated (or minimally dilated) fusion pore [e.g. via increase in synaptotagmin IV expression as demonstrated by Wang *et al.* (2001; 2003) in rat pheochromocytoma (PC12) cells] to allow dramatically accelerated fusion pore dilation to occur when the granule matrix had undergone less dissolution and expansion. For the majority of the events, particularly those without a foot signal, the kinetics of the main amperometric spikes were not significantly affected by cAMP (Figure 4-7). Overall, these results suggest that in

rat chromaffin cells, the release from granules with large Q can be accelerated by a cAMP-sensitive mechanism that involves interactions among matrix dissolution, expansion, and fusion pore dilation.

5.2 Interpretation of multiple populations of granules with different quantal size

The quantal size of catecholamine-containing granules can be regulated by multiple factors (reviewed in Section 1.3). The multiple populations of granules that were drawn in Figures 5-1 and 5-2 were based on the assumption that the quantal size directly reflects the vesicular size. This assumption is only true if the concentration of catecholamines among the granules is uniform. Indeed, the concentration of catecholamines had been shown to be relatively constant among chromaffin granules (Gong *et al.* 2003). However, the quantal size can also be regulated by the kinetics of fusion pore opening/closure (reviewed by Burgoyne and Barclay 2002). For example, an increase in voltage-gated Ca^{2+} entry could increase the quantal size via regulation of the fusion pore, to allow more complete release of individual bovine chromaffin granules (Elhamdani *et al.* 2001). Thus, the multiple populations of granules with different quantal size as demonstrated in Chapter 3 could also arise from the regulation of fusion pore kinetics.

A recent study has suggested that events with a foot signal came from the exocytosis of granules that had undergone prefusion of two smaller granules

(Amatore *et al.* 2005). The distribution of $Q^{1/3}$ for events without a foot signal had a modal value of ~ 0.4 pC $^{1/3}$ (Figures 4-2C and F), which was similar to the peak of the first Gaussian distribution in Figure 3-6. In addition, the proportional release of small Q granules ($\sim 32\%$) was also quite similar to the proportional release of events without a foot signal ($\sim 26 - 42\%$). It is tempting to speculate that the population of small Q granules could arise from events without a foot signal, whereas the populations of medium and large Q granules (second and third Gaussian distributions, respectively in Figure 3-6) could arise from the events with a foot signal (Figures 4-2B and E). However, the distribution of $Q^{1/3}$ for events without a foot signal (Figures 4-2C and F) was too skewed to be described by a single Gaussian distribution ($p \ll 0.0001$ in the K-S test).

On the other hand, considering that the distribution of $Q^{1/3}$ among events without a foot signal was indeed skewed (Figures 4-2C and F), if prefusion of such granules occurred, the resultant granules were also expected to have a skewed $Q^{1/3}$ distribution, albeit at a larger value (as shown in Figures 4-2B and E). However, the mean cellular quantal size for the events with a foot signal was $\sim 4\times$ larger than the events without a foot signal. The distribution of $Q^{1/3}$ after prefusion of only two events without a foot signal could not account for the $Q^{1/3}$ distribution of events with a foot signal ($p \ll 0.0001$ in the K-S test). Therefore, if the events with a foot signal indeed arose from the prefusion of multiple granules, then the majority of the prefusion typically involved four granules.

Another possible explanation for the existence of multiple populations of granules with different quantal size is the presence of different pools of granules

of different age. The newly synthesized granules were reported to be released earlier than the older granules (Duncan *et al.* 2003). It is possible that the newly synthesized granules store less catecholamines and hence have a smaller quantal size. Thus, the population of small Q granules in rat chromaffin cells might be the newly synthesized granules, whereas the populations of medium and large Q granules might be the older granules. However, our preliminary analysis on the population of newly synthesized granules [by plotting the distribution of $Q^{1/3}$ for the first 30% of the amperometric events from every cell (data not shown) which is equivalent to the proportional release of small Q granules] suggest that the pool of newly synthesized granules could not account for the population of small Q granules ($p \ll 0.0001$ in the K-S test).

The small dense core granules were found in 1 - 5% of the total population of chromaffin cells (Kobayashi *et al.* 1978). Consistent with this finding, there was only a small percentage of chromaffin cells (~5%) with small mean cellular $Q^{1/3}$ (range: 0.36 - 0.49 $pC^{1/3}$) (Figure 3-7). Also note that the distribution for rat chromaffin cells with small mean cellular $Q^{1/3}$ could almost be covered by the first Gaussian distribution (Figure 3-8A). Kobayashi *et al.* (1978) proposed that the small dense core granules might contain dopamine (DA). As discussed in Section 3.3.1, the PC12 cells (mean $Q^{1/3}$ of ~0.4 $pC^{1/3}$) are also DA-secreting (Finnegan *et al.* 1996; Elhamdani *et al.* 2000). All these findings are consistent with the idea that the rat chromaffin cells with the predominantly population of small Q granules (Figure 3-8A) could be predominantly DA-secreting cells with small dense core granules.

5.3 Implications of multiple populations of granules with different quantal size on the kinetics of quantal catecholamine release

In Chapter 4, we found that cAMP selectively shortened the foot duration of the large Q granules, but not for the small Q granules (Figure 4-3). Consistent with this, the fractional release during the foot signal for the large Q granules was also reduced by cAMP (Figure 4-5). As discussed in Section 4.3.2, the shortening of the foot duration by cAMP might be related to a destabilization of the opened but undilated, or minimally dilated fusion pore. This suggests that although cAMP increased the quantal size of every granule (Tang *et al.* 2005), it selectively lowered the critical energy for fusion pore dilation only in the large Q granules. Thus, although the quantal size of multiple populations of granules was uniformly regulated by cAMP, the kinetics of release from each population of granules were differentially regulated.

The fractional release during the foot signal was minimum for mean cellular $Q^{1/3}$ of $\sim 0.6 \text{ pC}^{1/3}$. As discussed in Section 4.3.1, the medium Q granules may have a minimum critical energy for fusion pore dilation. Our overall findings above suggest that the multiple populations of granules with different quantal size might be different fundamentally. This idea is further supported by a recent finding that showed a deficiency of chromogranin A led to an increase in the size of transgenic mouse chromaffin granules (Kim *et al.* 2005). Thus, the large Q granules in rat chromaffin cells may have a granule matrix that lacks of chromogranin A. As reviewed in Section 1.1.5, there are three different isoforms

of chromogranin (Weiss *et al.* 1996). It is possible that the granule matrix of the large Q granules is composed of different isoforms of chromogranin. Further studies are needed to address this issue.

For the events with a foot signal, an increase in the half-width duration of the main amperometric spikes with increasing quantal size was only observed for mean cellular $Q^{1/3} < 0.6 \text{ pC}^{1/3}$ (Figures 4-7B and E). The half-width duration reached the plateau at mean cellular $Q^{1/3} \geq 0.6 \text{ pC}^{1/3}$. There are three possible mechanisms to explain why there was no further increase in the half-width duration for the large Q granules. The first possible mechanism is an increase in catecholamine concentration for the large Q granules. However, as discussed in Section 4.3.1, this is unlikely to be the main mechanism because the concentration will increase by ~27-fold if the $Q^{1/3}$ increases from ~0.5 to ~1.5 $\text{pC}^{1/3}$, which is essentially the plateau range of the half-width duration.

The second possible mechanism is an increase in the rate of granule matrix dissolution or expansion for the large Q granules. According to the model in Figure 5-4, if one assumes the granule matrix expansion is the main force for the fusion pore dilation and the vesicular membrane area cannot be increased, then if the granule matrix expands to the same percentage, the fusion pore of the large Q granules will dilate to a larger size than that of the small Q granules. However, if one assumes that the rate of granule matrix expansion is constant, this condition alone may not account for the faster kinetics of release from the large Q granules. Therefore, in order to have faster discharge, the rate of expansion should be higher for the large Q granules. Another possible

mechanism is simply an increase in the rate of fusion pore dilation that is independent of the changes in dissolution or expansion of the granule matrix.

5.4 Significance

1. This is the first report to demonstrate that there are multiple populations of granules with different quantal size in rat chromaffin cells.
2. The rundown of mean cellular quantal size during the short-term cell culture was mainly due to the shift in the proportional release of large Q granules to medium Q granules.
3. The maintenance of mean cellular quantal size by glucocorticoids was due to the prevention of the shift in the proportional release of different populations of granules.
4. The increase in mean cellular quantal size by elevation of cAMP was due to uniform increase in quantal size of every granule.
5. This thesis attempted to study the release kinetics of multiple populations of granules with different quantal size.

6. The present work also demonstrated for the first time that the kinetics of the main amperometric spikes for the large Q granules were faster than predicted.

7. The major effect of cAMP was mainly to shorten the duration of foot signals.

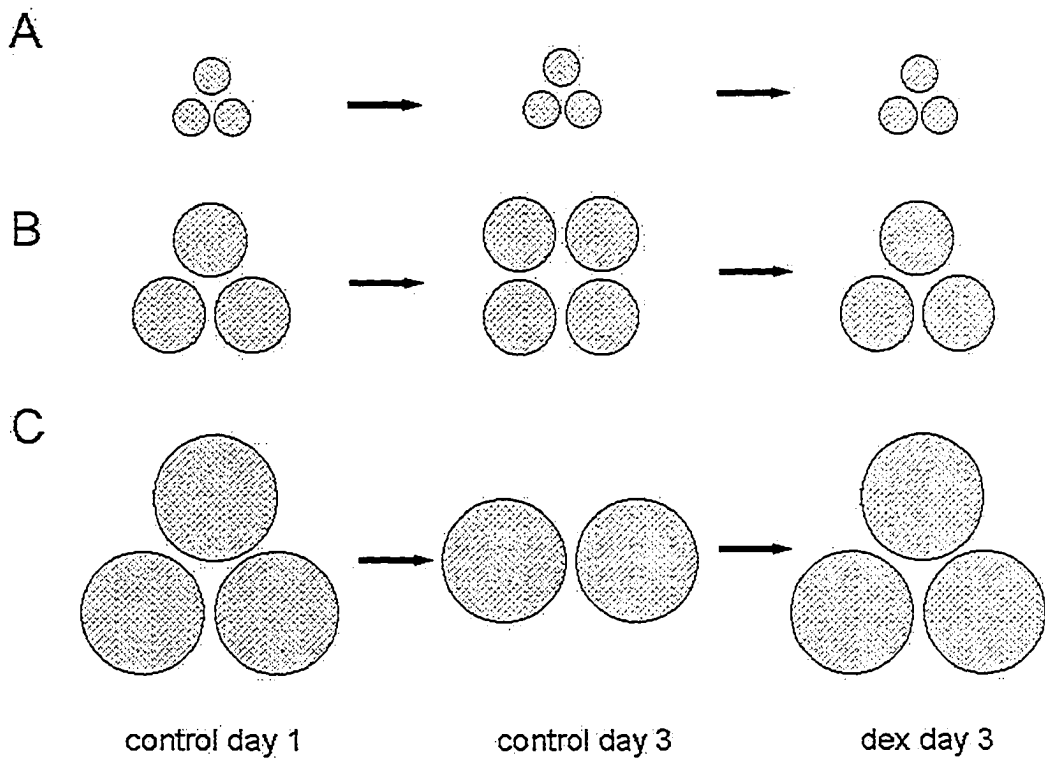


Figure 5-1 Diagram illustrating the differential regulation of multiple populations of granules with different quantal size by culture duration and dexamethasone. Small (A), medium (B), and large (C) Q granules of chromaffin cells that were cultured for 1 day or 3 days in control conditions, or in dexamethasone ($1 \mu\text{M}$) for 3 days. The shift in the proportional release of each population of granules after 3 days of culture is indicated by the change in the number of granules. Note that the number of granules after 3 days of treatment with dexamethasone is similar to control cells cultured for 1 day.

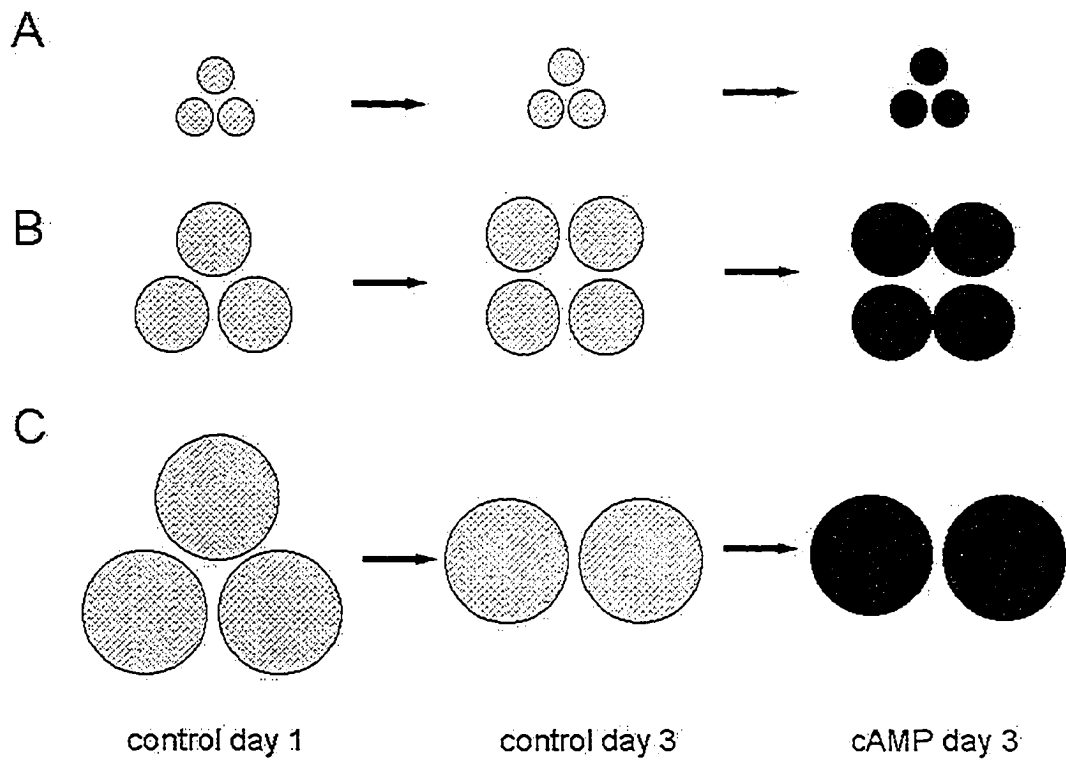
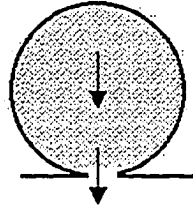


Figure 5-2 Diagram illustrating the differential regulation of multiple populations of granules with different quantal size by culture duration and cAMP. Small (A), medium (B), and large Q granules (C) of chromaffin cells that were cultured for 1 day, 3 days, or with cAMP for 3 days. The shift in the proportional release of each population of granules is indicated by the change in the number of granules. The uniform increase in quantal size of all granules by cAMP is indicated by the darker granules. Also note that the number of granules is similar for control cells and cAMP-treated cells cultured for 3 days.

A



B

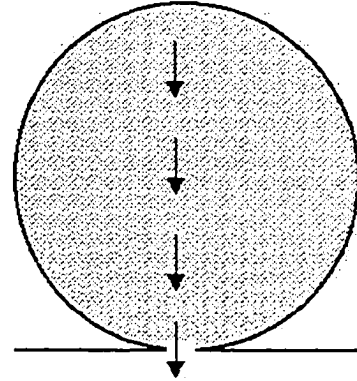


Figure 5-3 The release of catecholamines by free diffusion. The release from the small Q granule (A) is faster than the large Q granule (B) if both granules have the same fusion pore size.

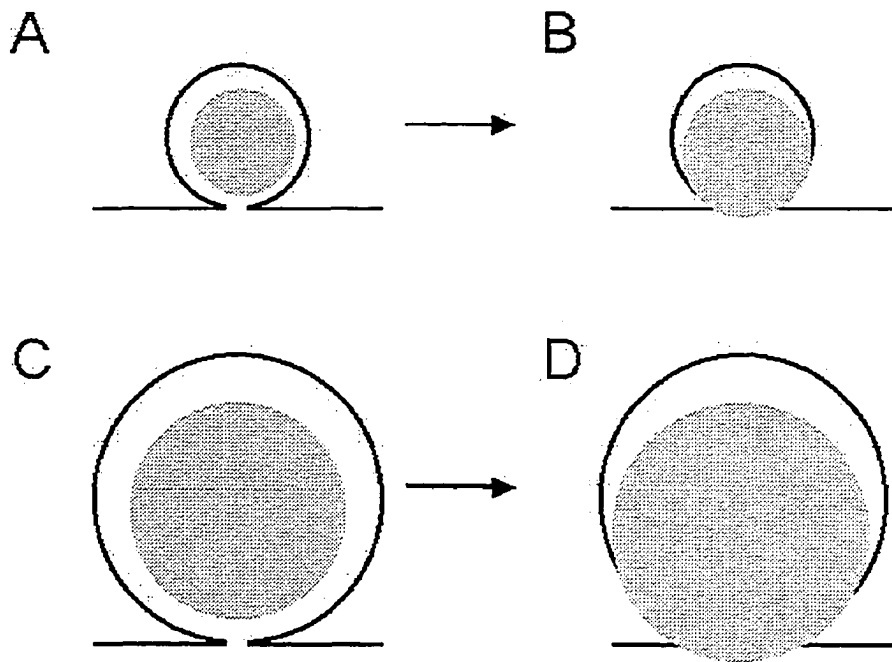


Figure 5.4 Expansion of granule matrix. The granule matrix is represented by the filled circle in small Q granules (A and B) and large Q granules (C and D). The granule matrix volumes in A and C are expanded by the same proportion into B and D, respectively. If the vesicular membrane area cannot be increased, then any excess surface area of the granule matrix must be accommodated by enlargement of the fusion pore. Therefore, the large Q granule (D) has a larger fusion pore in comparison to the small Q granule (B).

References

- Almers W., Breckenridge L. J., and Spruce A. E. (1989) The mechanism of exocytosis during secretion in mast cells, in *Secretion and Its Control* (Oxford G. S. and Armstrong C. M., eds.), pp. 269-282. The Rockefeller University Press, New York.
- Alvarez de Toledo G., Fernandez-Chacon R., and Fernandez J. M. (1993) Release of secretory products during transient vesicle fusion. *Nature* **363**, 554-558.
- Amatore C., Arbault S., Bonifas I., Bouret Y., Erard M., Ewing A. G., and Sombers L. A. (2005) Correlation between vesicle quantal size and fusion pore release in chromaffin cell exocytosis. *Biophysical Journal* **88**, 4411-4420.
- Amatore C., Bouret Y., Travis E. R., and Wightman R. M. (2000) Interplay between membrane dynamics, diffusion and swelling pressure governs individual vesicular exocytotic events during release of adrenaline by chromaffin cells. *Biochimie* **82**, 481-496.
- Bruns D. and Jahn R. (1995) Real-time measurement of transmitter release from single synaptic vesicles. *Nature* **377**, 62-65.

- Burgoyne R. D. and Barclay J. W. (2002) Splitting the quantum: regulation of quantal release during vesicle fusion. *Trends in Neurosciences* **25**, 176-178.
- Duncan R. R., Greaves J., Wiegand U. K., Matskovich I., Bodammer G., Apps D. K., Shipston M. J., and Chow R. H. (2003) Functional and spatial segregation of secretory vesicle pools according to vesicle age. *Nature* **422**, 176-180.
- Elhamdani A., Brown M. E., Artalejo C. R., and Palfrey H. C. (2000) Enhancement of the dense-core vesicle secretory cycle by glucocorticoid differentiation of PC12 cells: Characteristics of rapid exocytosis and endocytosis. *Journal of Neuroscience* **20**, 2495-2503.
- Elhamdani A., Palfrey H. C., and Artalejo C. R. (2001) Quantal size is dependent on stimulation frequency and calcium entry in calf chromaffin cells. *Neuron* **31**, 819-830.
- Finnegan J. M., Pihel K., Cahill P. S., Huang L., Zerby S. E., Ewing A. G., Kennedy R. T., and Wightman R. M. (1996) Vesicular quantal size measured by amperometry at chromaffin, mast, pheochromocytoma, and pancreatic beta-cells. *Journal of Neurochemistry* **66**, 1914-1923.
- Gong L. W., Hafez I., de Toledo G. A., and Lindau M. (2003) Secretory vesicles membrane area is regulated in tandem with quantal size in chromaffin cells. *Journal of Neuroscience* **23**, 7917-7921.

- Hodel A. (2001) Effects of glucocorticoids on adrenal chromaffin cells. *Journal of Neuroendocrinology* **13**, 217-221.
- Kim T., Zhang C. F., Sun Z. Q., Wu H. L., and Loh Y. P. (2005) Chromogranin A deficiency in transgenic mice leads to aberrant chromaffin granule biogenesis. *Journal of Neuroscience* **25**, 6958-6961.
- Kobayashi S., Serizawa Y., Fujita T., and Coupland R. E. (1978) SGC (small granule chromaffin) cells in mouse adrenal medulla: light and electron microscopic identification using semi-thin and ultra-thin sections. *Endocrinologia Japonica* **25**, 467-476.
- Raum W. J. (1997) Adrenal medulla, in *Endocrinology: Basic and Clinical Principles* (Conn P. M. and Melmed S., eds.), pp. 377-392. Humana Press, Totowa, NJ.
- Rozansky D. J., Wu H. J., Tang K. C., Parmer R. J., and Oconnor D. T. (1994) Glucocorticoid activation of chromogranin A gene expression. Identification and characterization of a novel glucocorticoid response element. *Journal of Clinical Investigation* **94**, 2357-2368.
- Somers L. A., Hancher H. J., Colliver T. L., Wittenberg N., Cans A., Arbault S., Amatore C., and Ewing A. G. (2004) The effects of vesicular volume on secretion through the fusion pore in exocytotic release from PC12 cells. *Journal of Neuroscience* **24**, 303-309.

- Tang K. S., Tse A., and Tse F. W. (2005) Differential regulation of multiple populations of granules in rat adrenal chromaffin cells by culture duration and cyclic AMP. *Journal of Neurochemistry* **92**, 1126-1139.
- Wang C. T., Grishanin R., Earles C. A., Chang P. Y., Martin T. F. J., Chapman E. R., and Jackson M. B. (2001) Synaptotagmin modulation of fusion pore kinetics in regulated exocytosis of dense-core vesicles. *Science* **294**, 1111-1115.
- Wang C. T., Lu J. C., Bai J. H., Chang P. Y., Martin T. F. J., Chapman E. R., and Jackson M. B. (2003) Different domains of synaptotagmin control the choice between kiss-and-run and full fusion. *Nature* **424**, 943-947.
- Weiss C., Cahill A. L., Laslop A., Fischer-Colbrie R., Perlman R. L., and Winkler H. (1996) Differences in the composition of chromaffin granules in adrenaline and noradrenaline containing cells of bovine adrenal medulla. *Neuroscience Letters* **211**, 29-32.